Introduction and Overview (Preskills Notes)

8-27-2024

Physics of Information: Turing
von Neumann

Notions: What is a computation ?
What is computable

Formulation of Computer Science that is Device Independent

1937 Turing Machine:

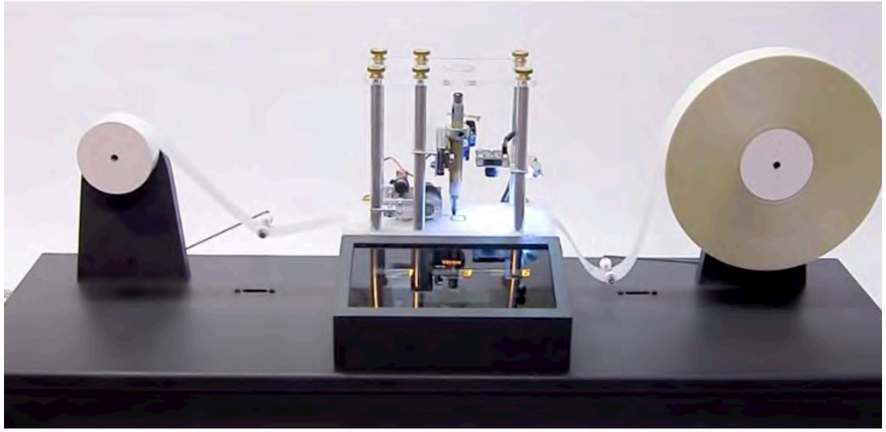

https://www.youtube.com/watch?v=E3keLeMwfHY

Wikipedia:

A Turing Machine (TM) is a mathematical model of computation describing an abstract machine that manipulates symbols on a strip of paper according to a table of rules.

The TM operates on an infinite tape divided into cells, each of which can hold a symbol drawn from a finite set.

At each step the head reads the symbol in the cell. Then, based on the symbol and the TM's present state, the machine writes a symbol in the cell, and moves the head one step to the left or the right, or halts the computation.

https://en.wikipedia.org/wiki/Turing_machine

Church – Turing Thesis:

Everything that is computable can be computed on a Turing Machine with at most polynomial overhead.

8-27-2024

Introduction and Overview (Preskills Notes)

Wikipedia:

A Turing Machine (TM) is a mathematical model of computation describing an abstract machine that manipulates symbols on a strip of paper according to a table of rules.

The TM operates on an infinite tape divided into cells, each of which can hold a symbol drawn from a finite set.

At each step the head reads the symbol in the cell. Then, based on the symbol and the TM's present state, the machine writes a symbol in the cell, and moves the head one step to the left or the right, or halts the computation.

Church – Turing Thesis:

Everything that is computable can be computed on a Turing Machine with at most polynomial overhead.

Landaur: **Information is Physical !**

Example: **Erasure = Dissipation**

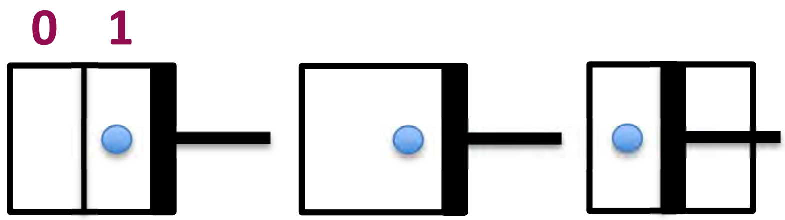

Entropy: $\Delta S_{gas} = -k \ln 2$

Work: $W = kT \ln 2 = 0.96 \times 10^{-23} \frac{J}{K} \cdot 300K$

$\sim 3 \times 10^{-21} J \sim 0.02 eV$

Is there a way around it ?

Reversible Computation !

But we need a different gate set !

Introduction and Overview (Preskills Notes)

8-27-2024

NAND Gate:

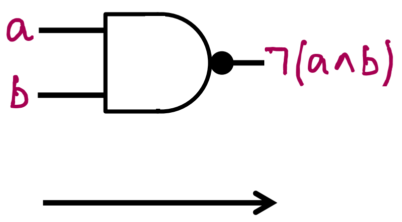

irreversible

Toffoli Gate:

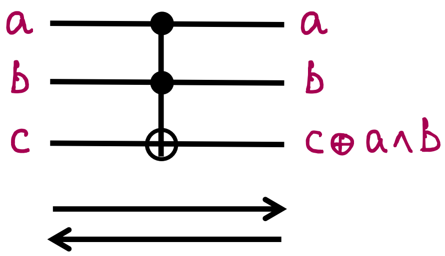

reversible

Maxwells Demon:

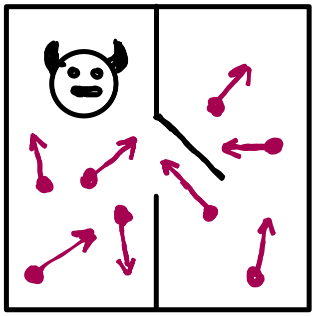

Information is Physical!

Quantum Information

Carl Caves: Quantum States are states of knowledge

Physics is Information!

End 8-29-2024

New properties of QM

Measurement:

$$[A,B] \neq 0 \Rightarrow \Delta A \Delta B \geq \frac{\hbar}{2} |\langle [A,B] \rangle|$$

Acquire Info ➡ Disturb system

Randomness:

Outcome fundamentally unpredictable

"Collapse" of wavefunction

Cannot determine state of a single quantum if initially unknown } Cannot Copy No cloning theorem

Entanglement:

Non-local correlations

pure state, entangled

$$|\psi\rangle = \frac{1}{\sqrt{2}}\left(|00\rangle + |11\rangle\right)$$

$$\rho = \frac{1}{2}\left(|00\rangle\langle 00| + |11\rangle\langle 11|\right)$$

mixed state, not entangled

8-27-2024

Introduction and Overview (Preskills Notes)

New properties of QM

Measurement:

$$[A,B] \neq 0 \Rightarrow \Delta A \Delta B \geq \frac{\hbar}{2} |\langle [A,B] \rangle|$$

Acquire Info ⇨ Disturb system

Randomness:

Outcome fundamentally unpredictable

"Collapse" of wavefunction

Cannot determine state of a single quantum if initially unknown } Cannot Copy
No cloning theorem

Entanglement:

pure state, entangled

$$|\psi\rangle = \frac{1}{\sqrt{2}} \left(|00\rangle + |11\rangle \right)$$

Non-local correlations

$$\rho = \frac{1}{2} \left(|00\rangle\langle 00| + |11\rangle\langle 11| \right)$$

mixed state,
not entangled

Quantum Computing

Does QM impact Computation?

Peter Shor (1994): YES ! ⇨ Quantum Fourier Transform

⇩

Factoring !

DFT on N bits	$O[(2^N)^2]$	steps
FFT on "	$O[N2^N]$	"
QFT on "	$O[N \log N]$	"

8-27-2024

Introduction and Overview (Preskills Notes)

Quantum Computing

Does QM impact Computation?

Peter Shor (1994): YES ! ➡ Quantum Fourier Transform

⬇

Factoring !

DFT on N bits	$\mathcal{O}[(2^N)^2]$	steps
FFT on "	$\mathcal{O}[N 2^N]$	"
QFT on "	$\mathcal{O}[N \log N]$	"

Efficient Factoring

Factoring $n = p \times q$ ➡ RSA encryption

large integer ↑ ↑ large prime numbers

- easy to verify solution $\log n$ steps
- very hard to solve $\mathcal{O}[n]$ steps

⬇

Exponential in # of digits

QFT ➡ Solvable

Preskill Ch. 1, p. 5-6 $T \propto e^{1.9(\log n)^{1/3}} e^{(\log \log n)^{2/3}}$

Best Classical Algorithm

Introduction and Overview (Preskills Notes)

8-27-2024

Quantum Computing

Does QM impact Computation?

Peter Shor (1994): YES ! → **Quantum Fourier Transform**

↓

Factoring !

DFT on N **bits**	$\mathcal{O}[(2^N)^2]$	**steps**
FFT on "	$\mathcal{O}[N2^N]$	"
QFT on "	$\mathcal{O}[N \log N]$	"

Efficient Factoring

Factoring $n = p \times q$ → **RSA encryption**

large integer ↑ n; ↑ p, q: large prime numbers

- **easy to verify solution** $\log n$ **steps**
- **very hard to solve** $\mathcal{O}[n]$ **steps**

↓

Exponential in # of digits

QFT → Solvable

Preskill Ch. 1, p. 5-6 $T \propto e^{1.9 (\log n)^{1/3}} e^{(\log \log n)^{2/3}}$

(1998) 130 digits in 1 month

↓

400 digits in 10^{10} years

↓

(2022) 24 yrs = 16 Moores Law doublings

2^{16} = 65,536 → 400 digits ~ 150kYrs

Introduction and Overview (Preskills Notes)

8-27-2024

Quantum Computing

Does QM impact Computation?

Peter Shor (1994): YES ! ⇨ Quantum Fourier Transform

⇩

Factoring !

DFT on N bits	$\mathcal{O}[(2^N)^2]$	steps
FFT on "	$\mathcal{O}[N 2^N]$	"
QFT on "	$\mathcal{O}[N \log N]$	"

Efficient Factoring

Factoring $n = p \times q$ ⇨ **RSA encryption**

large integer → n; p, q ← large prime numbers

- easy to verify solution $\log n$ steps
- very hard to solve $\mathcal{O}[n]$ steps

⇩

Exponential in # of digits

QFT ⇨ Solvable

Preskill Ch. 1, p. 5-6 $T \propto e^{1.9 (\log n)^{1/3}} e^{(\log \log n)^{2/3}}$

(1998) 130 digits/month

⇩

400 digits/ 10^{10} years

Polynomial in # of digits

Shors algorithm: $\mathcal{O}[(\log n)^3]$ ←

130 digits/mo. ⇨ **400 digits/3 yrs if Quantum**

8-27-2024

Introduction and Overview (Preskills Notes)

Efficient Factoring

Factoring $n = p \times q$ → RSA encryption

large integer ↑ ↑ large prime numbers

- easy to verify solution $\log n$ steps
- very hard to solve $O[n]$ steps

Exponential in # of digits

QFT → Solvable

Preskill Ch. 1, p. 5-6 $T \propto e^{1.9(\log n)^{1/3}} e^{(\log \log n)^{2/3}}$

(1998) 130 digits/month

400 digits/ 10^{10} years

Polynomial in # of digits

Shors algorithm: $O[(\log n)^3]$

130 digits/mo. → 400 digits/3 yrs if Quantum

Quantum Complexity

Benioff, Feynman → Simulating QM is hard

Simulating Physics with computers (1982)

qubit

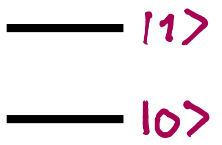

$|\psi\rangle = a|0\rangle + b|1\rangle$

N qubits → $\underbrace{|01101011\ldots010\rangle} = |x\rangle \in \mathcal{E}$

N bit integer = X : logical basis state

2^N - dimensional Hilbert Space

General State: $\boxed{|\psi\rangle = \frac{1}{2^{N/2}} \sum_{x=0}^{2^N-1} a_x |x\rangle}$

Introduction and Overview (Preskills Notes)

8-29-2024

Quantum Complexity

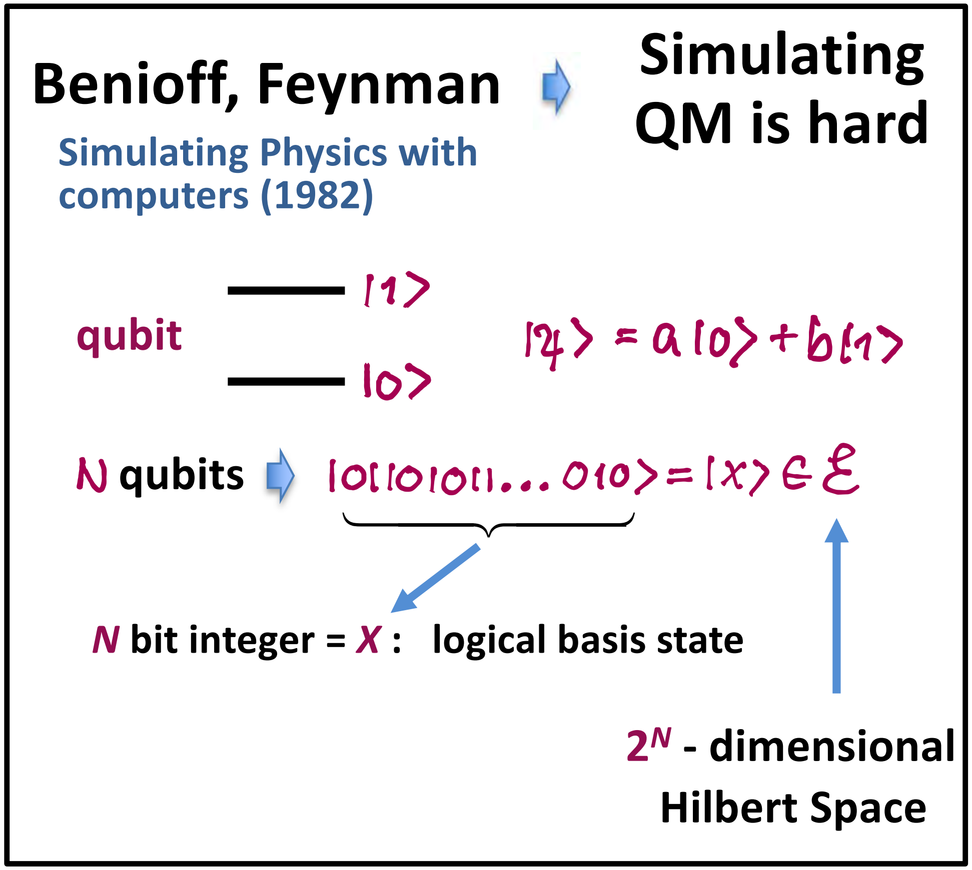

Benioff, Feynman ➡ **Simulating QM is hard**

Simulating Physics with computers (1982)

qubit

$|1\rangle$

$|0\rangle$

$|\psi\rangle = a|0\rangle + b|1\rangle$

N qubits ➡ $\underbrace{|01101011\ldots010\rangle}= |x\rangle \in \mathcal{E}$

N bit integer = *X* : logical basis state

2^N - dimensional Hilbert Space

General State:

$$\boxed{|\psi\rangle = \frac{1}{2^{N/2}} \sum_{x=0}^{2^N-1} a_x |x\rangle}$$

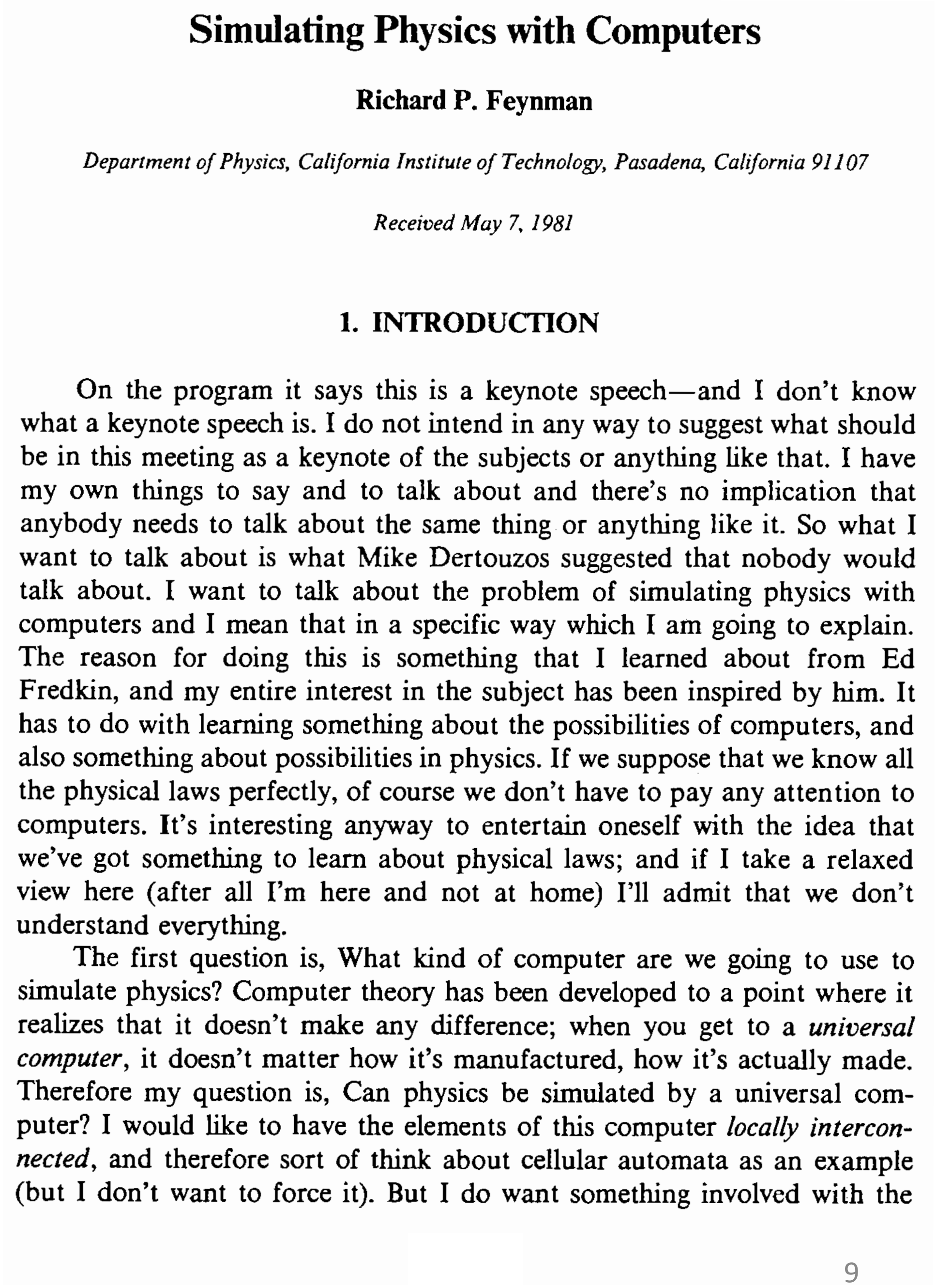

Simulating Physics with Computers

Richard P. Feynman

Department of Physics, California Institute of Technology, Pasadena, California 91107

Received May 7, 1981

1. INTRODUCTION

On the program it says this is a keynote speech—and I don't know what a keynote speech is. I do not intend in any way to suggest what should be in this meeting as a keynote of the subjects or anything like that. I have my own things to say and to talk about and there's no implication that anybody needs to talk about the same thing or anything like it. So what I want to talk about is what Mike Dertouzos suggested that nobody would talk about. I want to talk about the problem of simulating physics with computers and I mean that in a specific way which I am going to explain. The reason for doing this is something that I learned about from Ed Fredkin, and my entire interest in the subject has been inspired by him. It has to do with learning something about the possibilities of computers, and also something about possibilities in physics. If we suppose that we know all the physical laws perfectly, of course we don't have to pay any attention to computers. It's interesting anyway to entertain oneself with the idea that we've got something to learn about physical laws; and if I take a relaxed view here (after all I'm here and not at home) I'll admit that we don't understand everything.

The first question is, What kind of computer are we going to use to simulate physics? Computer theory has been developed to a point where it realizes that it doesn't make any difference; when you get to a *universal computer*, it doesn't matter how it's manufactured, how it's actually made. Therefore my question is, Can physics be simulated by a universal computer? I would like to have the elements of this computer *locally interconnected*, and therefore sort of think about cellular automata as an example (but I don't want to force it). But I do want something involved with the

8-29-2024

Introduction and Overview (Preskills Notes)

Quantum Complexity

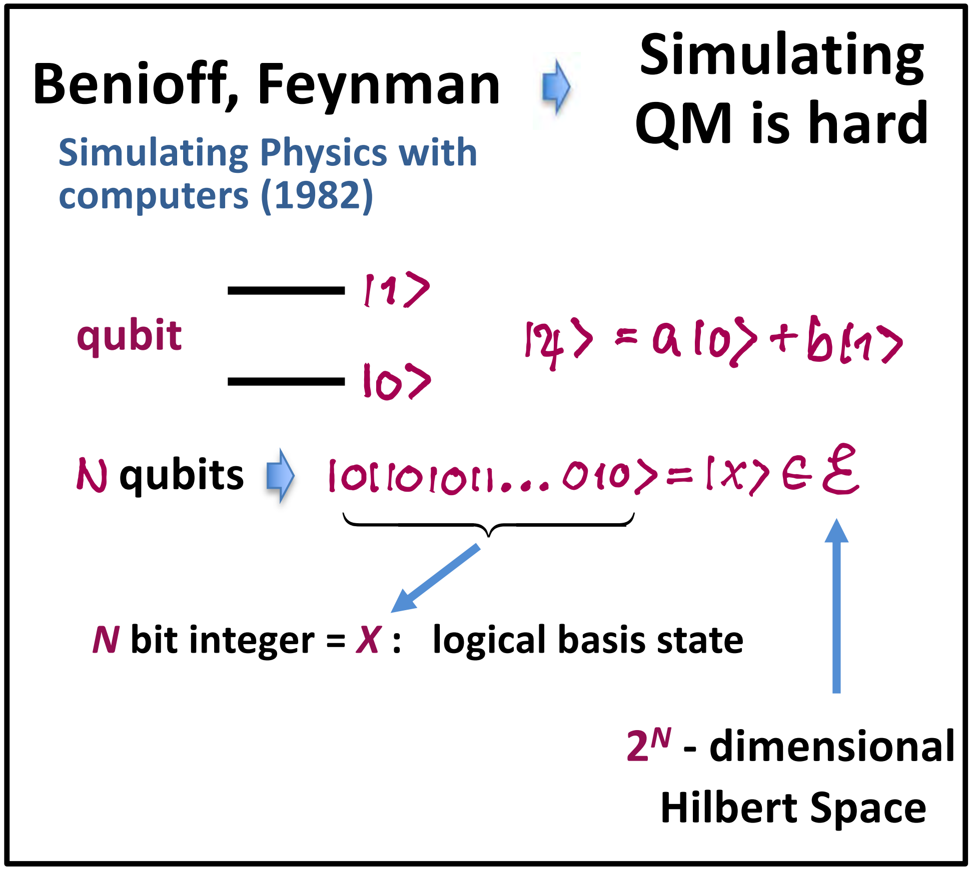

Benioff, Feynman ➡ **Simulating QM is hard**

Simulating Physics with computers (1982)

qubit

$|1\rangle$

$|0\rangle$

$|\psi\rangle = a|0\rangle + b|1\rangle$

N qubits ➡ $|\underbrace{01101011\ldots010}_{}\rangle = |x\rangle \in \mathcal{E}$

N bit integer = *X* : logical basis state

2^N - dimensional Hilbert Space

General State:

$$\boxed{|\psi\rangle = \frac{1}{2^{N/2}} \sum_{x=0}^{2^{N-1}} a_x |x\rangle}$$

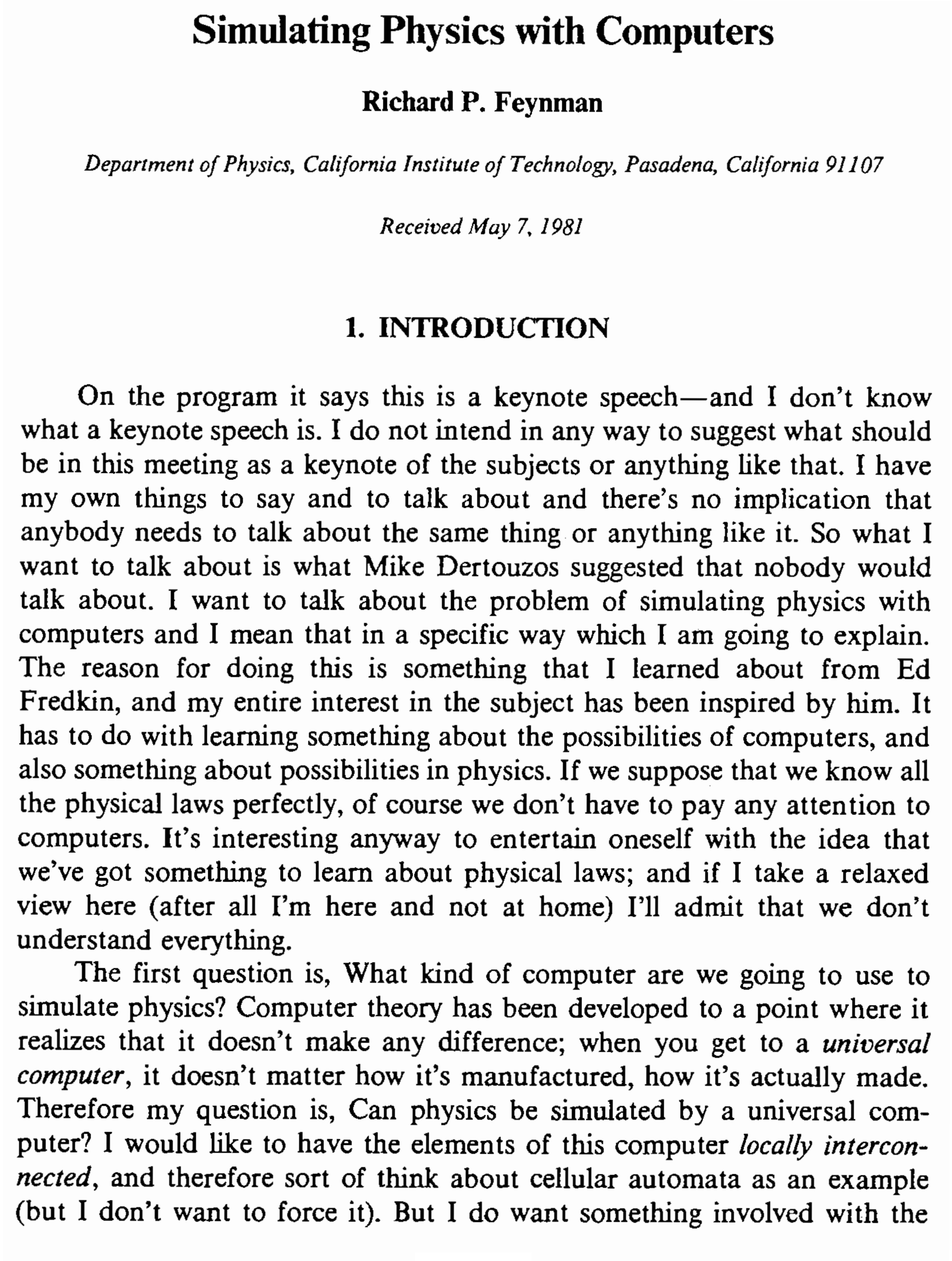

Simulating Physics with Computers

Richard P. Feynman

Department of Physics, California Institute of Technology, Pasadena, California 91107

Received May 7, 1981

1. INTRODUCTION

On the program it says this is a keynote speech—and I don't know what a keynote speech is. I do not intend in any way to suggest what should be in this meeting as a keynote of the subjects or anything like that. I have my own things to say and to talk about and there's no implication that anybody needs to talk about the same thing or anything like it. So what I want to talk about is what Mike Dertouzos suggested that nobody would talk about. I want to talk about the problem of simulating physics with computers and I mean that in a specific way which I am going to explain. The reason for doing this is something that I learned about from Ed Fredkin, and my entire interest in the subject has been inspired by him. It has to do with learning something about the possibilities of computers, and also something about possibilities in physics. If we suppose that we know all the physical laws perfectly, of course we don't have to pay any attention to computers. It's interesting anyway to entertain oneself with the idea that we've got something to learn about physical laws; and if I take a relaxed view here (after all I'm here and not at home) I'll admit that we don't understand everything.

The first question is, What kind of computer are we going to use to simulate physics? Computer theory has been developed to a point where it realizes that it doesn't make any difference; when you get to a *universal computer*, it doesn't matter how it's manufactured, how it's actually made. Therefore my question is, Can physics be simulated by a universal computer? I would like to have the elements of this computer *locally interconnected*, and therefore sort of think about cellular automata as an example (but I don't want to force it). But I do want something involved with the

Introduction and Overview (Preskills Notes)

8-29-2024

- Is it possible for a classical computer to efficiently simulate QM ?
- Use probabilistic local algorithm (the most general kind)

John Bell

Bell's Theorem:

No local probabilistic theory can reproduce all of QM

Non-Local Correlations

Key to Quantum Information

Thought experiment:

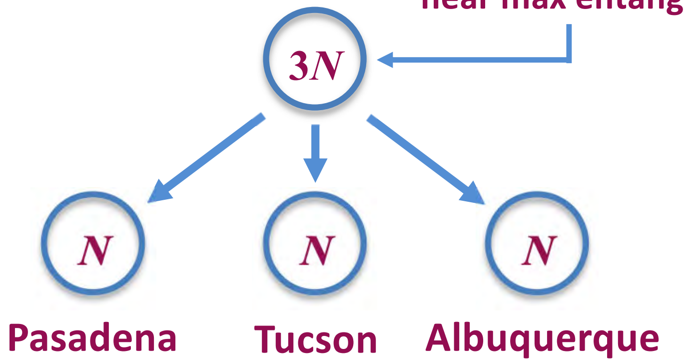

Generic Pure State in 2^{3N} dimensional space near max entangled

Local state close to random $\rho \sim \frac{1}{2^N} \mathbb{I}$

Shannon Info $S = -\sum_{i=1}^{2^N} \overset{\frac{1}{2^N}}{p_i} \text{Log}\, p_i$

Von Neuman Info $S = -\text{Tr}[\rho \,\text{Log}\, \rho]$

$$\left.\begin{matrix} S = -\sum_{i=1}^{2^N} p_i \text{Log}\, p_i \\ S = -\text{Tr}[\rho\, \text{Log}\, \rho] \end{matrix}\right\} \sim N - 2^{-(N+1)}$$

max value of S

entropy

Almost all info in *N* - body state in Non-Local correlations

Introduction and Overview (Preskills Notes)

8-29-2024

Non-Local Correlations

Key to Quantum Information

Thought experiment:

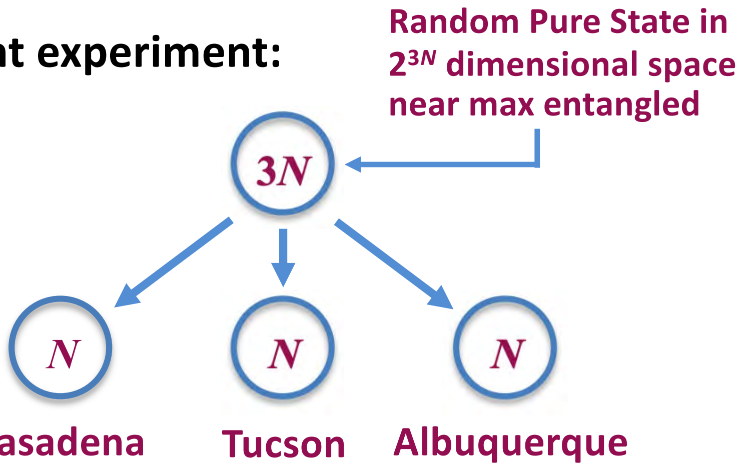

Random Pure State in 2^{3N} dimensional space near max entangled

Pasadena Tucson Albuquerque

Local state close to random $\rho \sim \frac{1}{2^N} \mathbb{I}$

Shannon Info $S = -\sum_{i=1}^{2^N} p_i \operatorname{Log} p_i$ with $p_i = \frac{1}{2^N}$

Von Neuman Info $S = -\operatorname{Tr}[\rho \operatorname{Log} \rho]$

max value of S: $\sim N - 2^{-(N+1)}$

entropy

Almost all info in N - body state in Non-Local correlations

OK – Plausible QM can do more

Where does the QC's power come from?

Visualization of Computation

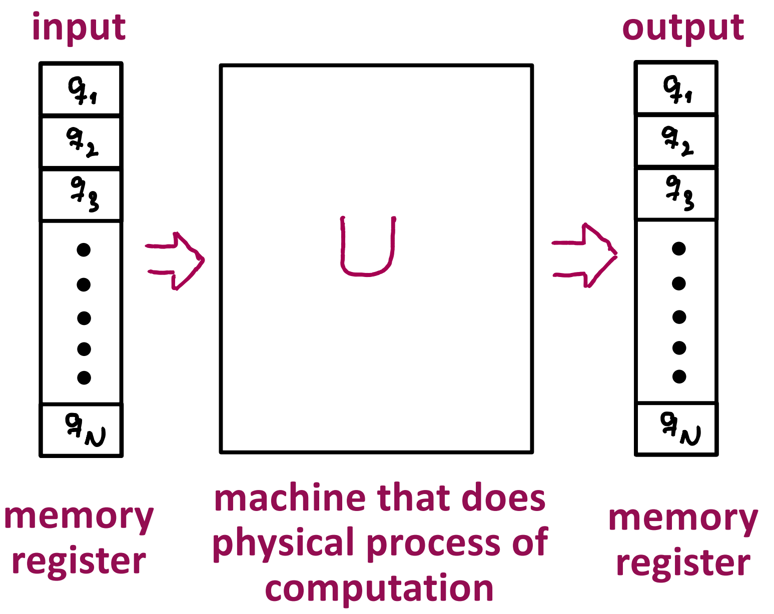

memory register

machine that does physical process of computation

memory register

Classical: Register is in one of the logical states $\underbrace{x = q_1 q_2 q_3 \ldots q_N}_{\text{binary \#}}$

Reversible transformation $U: x \rightarrow y$

8-29-2024

Introduction and Overview (Preskills Notes)

OK – Plausible QM can do more

Where does the QC’s power come from?

Visualization of Computation

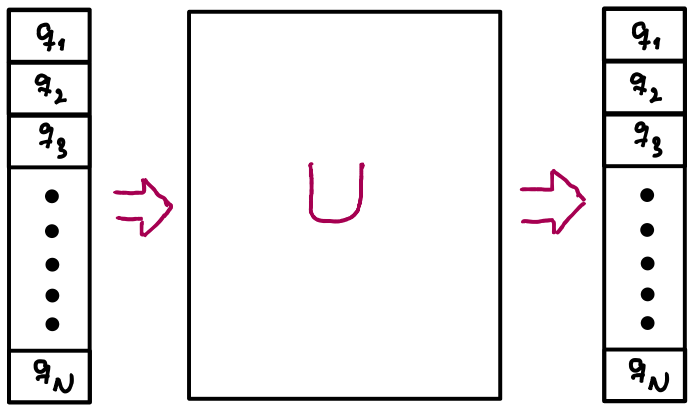

input

output

memory register

machine that does physical process of computation

memory register

Classical: Register is in one of the logical states $\underbrace{x = q_1 q_2 q_3 \ldots q_N}_{\text{binary \#}}$

Reversible transformation $U: x \to y$

Quantum: Register can be in any coherent superposition of logical states $|x\rangle$

Unitary transformation $U: |x\rangle \to |y\rangle$

Maps basis to basis $U: \{|x\rangle\} \to \{|y\rangle\}$

Quantum Parallelism

$$|\psi_{in}\rangle \to \sum_x a_x |x\rangle \to$$

$$\to |\psi_{out}\rangle = U|\psi_{in}\rangle = \sum_x a_x |y\rangle = \sum_x b_x |x\rangle$$

Machine processes 2^N inputs “in parallel” !

Beware: measurement collapses Q. Register into a single basis state at random

We get one random result out of 2^N

Introduction and Overview (Preskills Notes)

8-29-2024

Quantum: Register can be in any coherent superposition of logical states $|x\rangle$

Unitary transformation $U: |x\rangle \rightarrow |y\rangle$

Maps basis to basis $U: \{|x\rangle\} \rightarrow \{|y\rangle\}$

Quantum Parallelism

$$|\psi_{in}\rangle \rightarrow \sum_x a_x |x\rangle \rightarrow$$

Quantum Sampling Problem

$$\rightarrow |\psi_{out}\rangle = U|\psi_{in}\rangle = \sum_x a_x |y\rangle = \sum_x b_x |x\rangle$$

Machine processes 2^N inputs "in parallel" !

Beware: measurement collapses Q. Register into a single basis state at random

We get one random result out of 2^N

Quantum Algorithms look for global properties of functions – symmetry, periodicity, etc.

- ∗ Classical -> requires many function evaluations
- ∗ Quantum -> design U so measurement gives answer with high probability
- ∗ ∃ classes of problems (sampling problems) which are classically hard but quantum "easy"

Google "Quantum Supremacy"

Expert insight into current research

News & views

Quantum information

Quantum computing takes flight

William D. Oliver

A programmable quantum computer has been reported to outperform the most powerful conventional computers in a specific task – a milestone in computing comparable in importance to the Wright brothers' first flights. See p.505

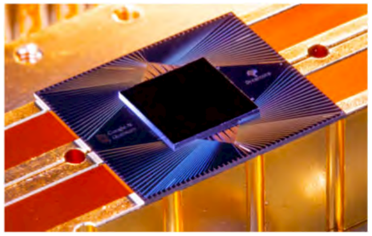

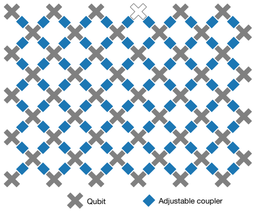

Introduction and Overview (Preskills Notes)

9-03-2024

<u>Quantum Algorithms</u> look for global properties of functions – symmetry, periodicity, etc.

- ✱ Classical ⇨ requires many function evaluations
- ✱ Quantum ⇨ design U so measurement gives answer with high probability
- ✱ ∃ classes of problems (sampling problems) which are classically hard but quantum "easy"

Google "Quantum Supremacy"

Expert insight into current research

News & views

Quantum information

Quantum computing takes flight

William D. Oliver

A programmable quantum computer has been reported to outperform the most powerful conventional computers in a specific task – a milestone in computing comparable in importance to the Wright brothers' first flights. See p.505

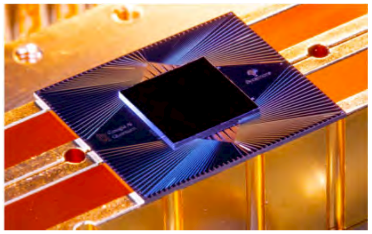

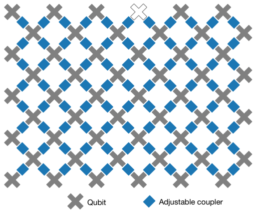

Boson Sampling

An example from Optics/Photonics

Setup

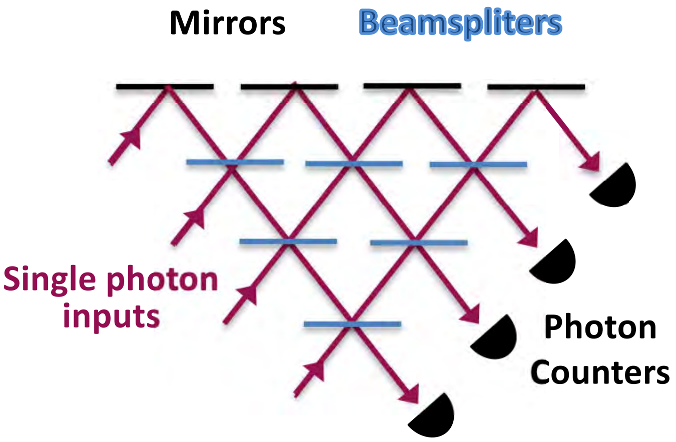

Beware: Boson behavior at Beamsplitters hard to predict photon statistics across outputs.

Exponential in #'s of Beamsplitters

9-03-2024

Introduction and Overview (Preskills Notes)

Quantum Algorithms look for global properties of functions – symmetry, periodicity, etc.

- ✱ Classical ⇨ requires many function evaluations
- ✱ Quantum ⇨ design U so measurement gives answer with high probability
- ✱ ∃ classes of problems (sampling problems) which are classically hard but quantum "easy"

Google "Quantum Supremacy"

Expert insight into current research

News & views

Quantum information

Quantum computing takes flight

William D. Oliver

A programmable quantum computer has been reported to outperform the most powerful conventional computers in a specific task – a milestone in computing comparable in importance to the Wright brothers' first flights. See p.505

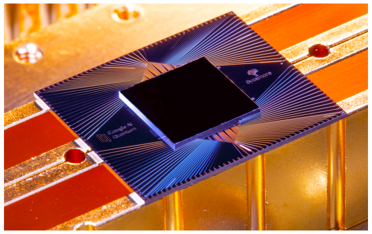

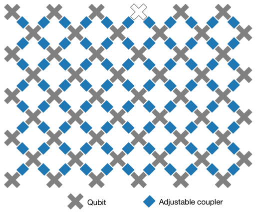

Boson Sampling

An example from Optics/Photonics

Setup

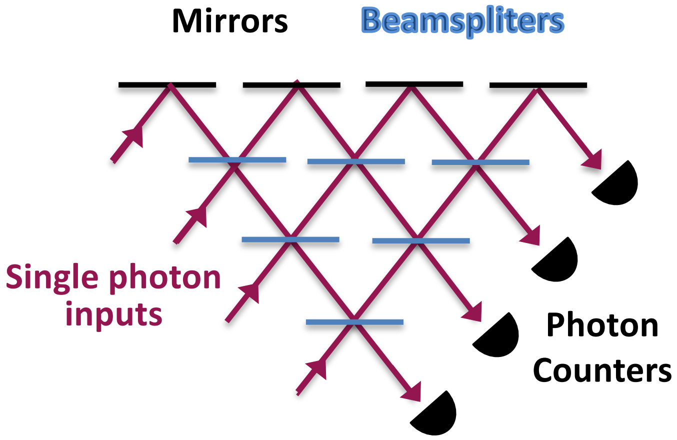

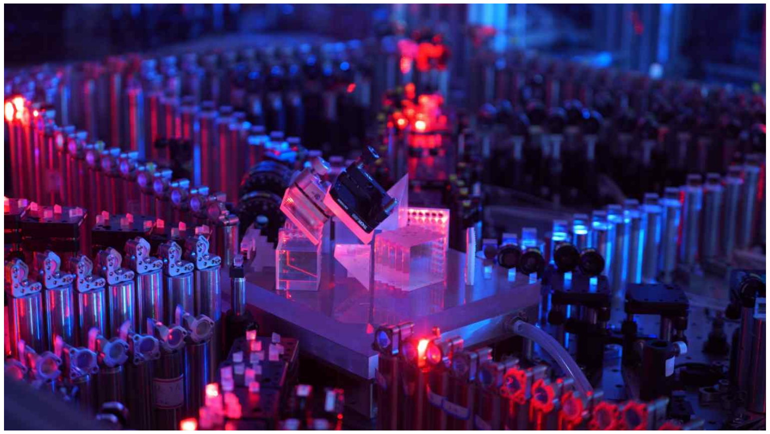

An optical quantum computer developed by a team of Chinese researchers including those from the University of Science and Technology of China. (courtesy of Han-Sen Zhong of the research group)

Introduction and Overview (Preskills Notes)

9-03-2024

Quantum Algorithms look for global properties of functions – symmetry, periodicity, etc.

- Classical → requires many function evaluations
- Quantum → design U so measurement gives answer with high probability
- ∃ classes of problems (sampling problems) which are classically hard but quantum "easy"

Google "Quantum Supremacy"

Expert insight into current research

News & views

Quantum information

Quantum computing takes flight

William D. Oliver

A programmable quantum computer has been reported to outperform the most powerful conventional computers in a specific task – a milestone in computing comparable in importance to the Wright brothers' first flights. See p.505

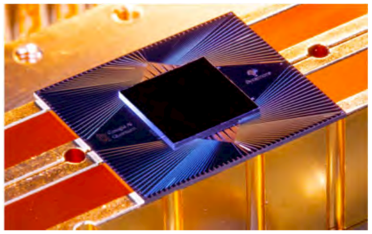

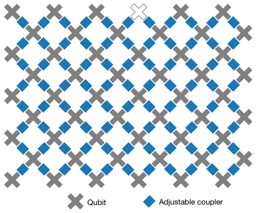

Boson Sampling

An example from Optics/Photonics

Setup

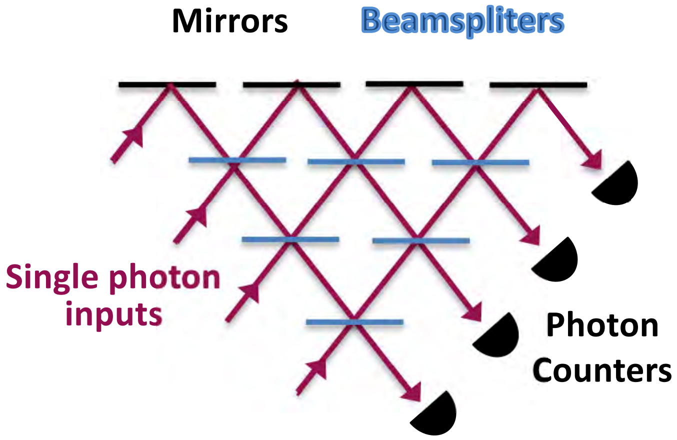

Imagine aligning that thing…!

Introduction and Overview (Preskills Notes)

9-03-2024

Back to Universal Computation

Visualization of Computation

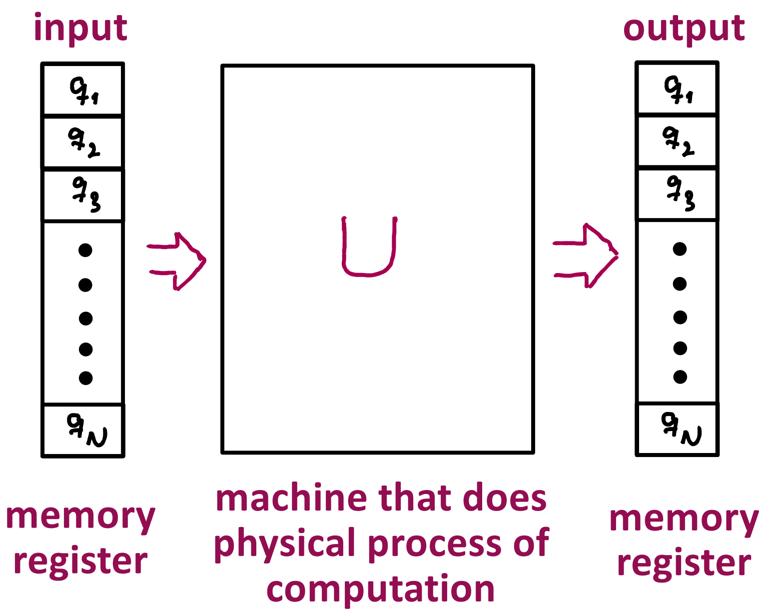
input

output

memory register

machine that does physical process of computation

memory register

Classical: Register is in one of the logical states $\underbrace{x = q_1 q_2 q_3 \ldots q_N}_{\text{binary \#}}$

Reversible transformation $U: x \to y$

What might be inside the machine ?

Wave interference w/classical fields ?

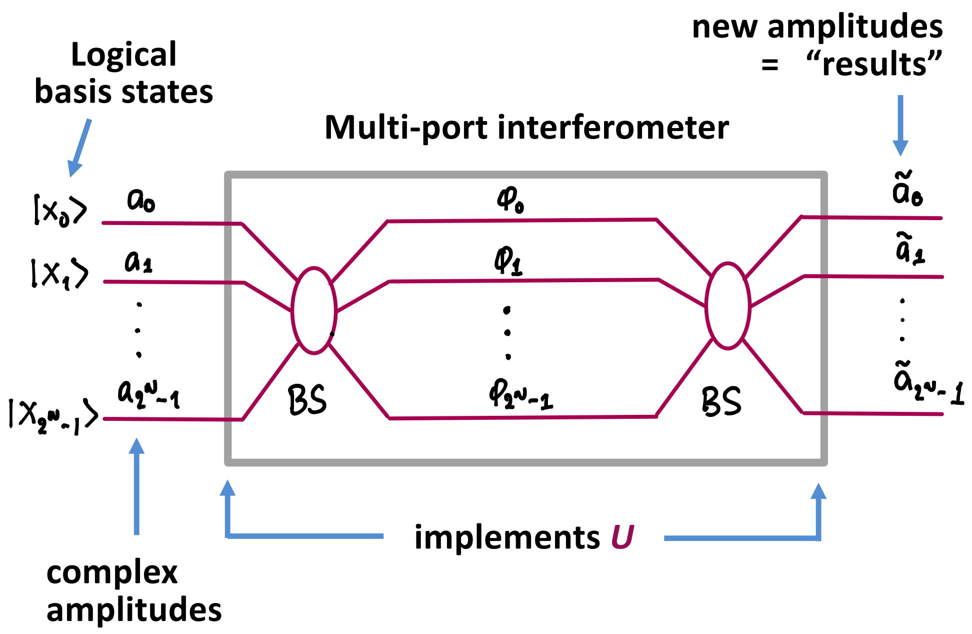
Logical basis states

new amplitudes = "results"

Multi-port interferometer

implements *U*

complex amplitudes

Note: *N* - qubit register ➡ 2^N "paths"

Beware of Resource Scaling !

Introduction and Overview (Preskills Notes)

9-03-2024

Quantum Advantage

David Deutsch: Toy problem that shows Quantum Advantage

Oracle

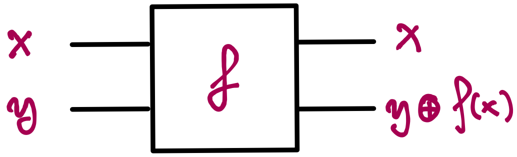

(Black Box)

Is the function

constant $f(0) = f(1)$

balanced $f(0) \neq f(1)$

Classical Box: Need 2 queries $f(0)$ & $f(1)$

Introduction and Overview (Preskills Notes)

Quantum Advantage

David Deutsch: Toy problem that shows Quantum Advantage

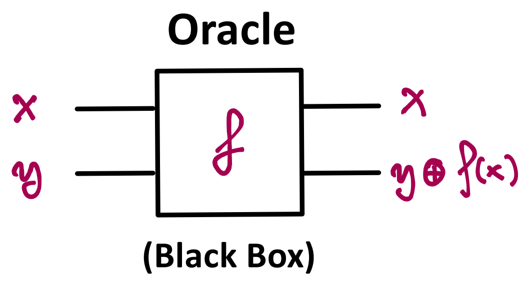

Is the function

constant $f(0) = f(1)$

balanced $f(0) \neq f(1)$

Quantum Box: In 3 steps can show that

(1) $U_f : |x\rangle|y\rangle \rightarrow |x\rangle|y \oplus f(x)\rangle$

(2) $U_f : |x\rangle\frac{1}{\sqrt{2}}(|0\rangle - |1\rangle) \rightarrow |x\rangle\frac{1}{\sqrt{2}}(|f(x)\rangle - |1 \otimes f(x)\rangle)$

$$= |x\rangle\frac{1}{\sqrt{2}}(-1)^{f(x)}(|0\rangle - |1\rangle)$$

(3) $U_f : \frac{1}{\sqrt{2}}(|0\rangle + |1\rangle)\frac{1}{\sqrt{2}}(|0\rangle - |1\rangle)$

$$\rightarrow \frac{1}{2}\left((-1)^{f(0)}|0\rangle + (-1)^{f(1)}|1\rangle\right)(|0\rangle - |1\rangle)$$

9-03-2024

Introduction and Overview (Preskills Notes)

Quantum Advantage

David Deutsch: Toy problem that shows Quantum Advantage

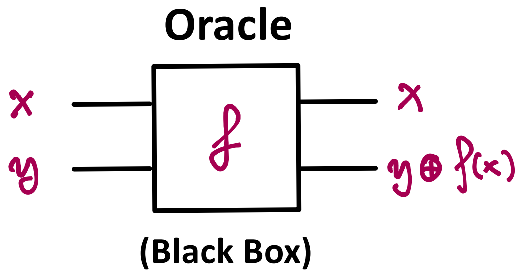

Is the function

constant $f(0) = f(1)$

balanced $f(0) \neq f(1)$

Quantum Box: In 3 steps can show that

(1) $U_f : |x\rangle|y\rangle \to |x\rangle|y \oplus f(x)\rangle$

(2) $U_f : |x\rangle\frac{1}{\sqrt{2}}(|0\rangle - |1\rangle) \to |x\rangle\frac{1}{\sqrt{2}}(|f(x)\rangle - |1 \oplus f(x)\rangle)$

$$= |x\rangle\frac{1}{\sqrt{2}}(-1)^{f(x)}(|0\rangle - |1\rangle)$$

(3) $U_f : \frac{1}{\sqrt{2}}(|0\rangle + |1\rangle)\frac{1}{\sqrt{2}}(|0\rangle - |1\rangle)$

$$\to \frac{1}{2}\left((-1)^{f(0)}|0\rangle + (-1)^{f(1)}|1\rangle\right)(|0\rangle - |1\rangle)$$

Quantum Advantage

David Deutsch: Toy problem that shows Quantum Advantage

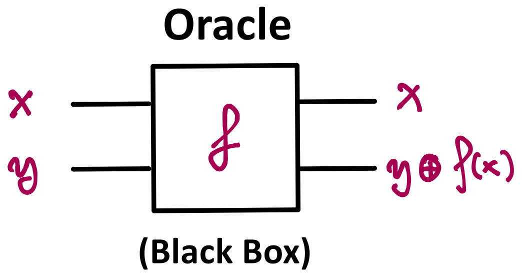

Is the function

constant $f(0) = f(1)$

balanced $f(0) \neq f(1)$

Quantum Computation:

Input $|x\rangle|y\rangle = \frac{1}{\sqrt{2}}(|0\rangle + |1\rangle)\frac{1}{\sqrt{2}}(|0\rangle - |1\rangle)$

$$\xrightarrow{U_f} \left[(-1)^{f(1)}|0\rangle + (-1)^{f(0)}|1\rangle\right]\frac{1}{\sqrt{2}}(|0\rangle - |1\rangle)$$

Measure 1st qubit in basis $|\pm\rangle = \frac{1}{\sqrt{2}}(|0\rangle \pm |1\rangle)$

$\to$ $|+\rangle$ if constant, $|-\rangle$ if balanced

Quantum Speedup: can solve w/1 query

Introduction and Overview (Preskills Notes)

9-03-2024

Quantum Advantage

David Deutsch: Toy problem that shows Quantum Advantage

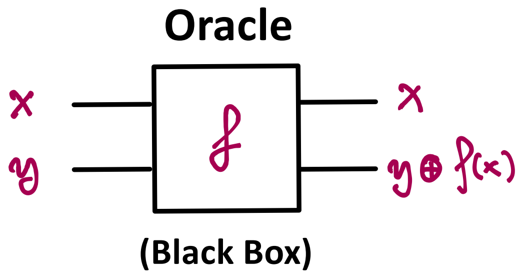

Is the function

constant $f(0) = f(1)$

balanced $f(0) \neq f(1)$

Quantum Computation:

Input $|x\rangle|y\rangle = \frac{1}{\sqrt{2}}(|0\rangle+|1\rangle)\frac{1}{\sqrt{2}}(|0\rangle-|1\rangle)$

$$\xrightarrow{U_f} \left[(-1)^{f(1)}|0\rangle+(-1)^{f(0)}|1\rangle\right]\frac{1}{\sqrt{2}}(|0\rangle-|1\rangle)$$

Measure 1st qubit in basis $|\pm\rangle = \frac{1}{\sqrt{2}}(|0\rangle \pm |1\rangle)$

$\rightarrow$ $|+\rangle$ if constant, $|-\rangle$ if balanced

Quantum Speedup: can solve w/1 query

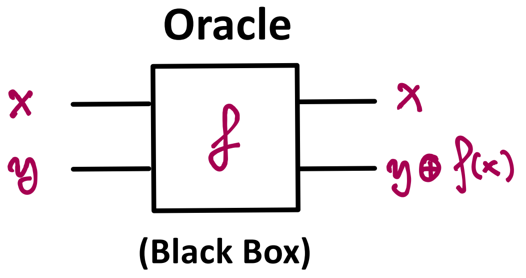

Quantum Advantage

David Deutsch: Toy problem that shows Quantum Advantage

Is the function

constant $f(0) = f(1)$

balanced $f(0) \neq f(1)$

Quantum Computation:

Input $|x\rangle|y\rangle = \frac{1}{\sqrt{2}}(|0\rangle+|1\rangle)\frac{1}{\sqrt{2}}(|0\rangle-|1\rangle)$

$$\xrightarrow{U_f} \left[(-1)^{f(1)}|0\rangle+(-1)^{f(0)}|1\rangle\right]\frac{1}{\sqrt{2}}(|0\rangle-|1\rangle)$$

Measure 1st qubit in basis $|\pm\rangle = \frac{1}{\sqrt{2}}(|0\rangle \pm |1\rangle)$

$\rightarrow$ $|+\rangle$ if constant, $|-\rangle$ if balanced

Quantum Speedup: can solve w/1 query

9-03-2024

Introduction and Overview (Preskills Notes)

Quantum Advantage

David Deutsch: Toy problem that shows Quantum Advantage

Oracle

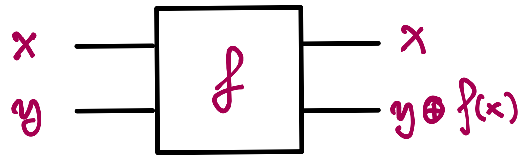

(Black Box)

Is the function

constant $f(0) = f(1)$

balanced $f(0) \neq f(1)$

Quantum Computation:

Input $|x\rangle|y\rangle = \frac{1}{\sqrt{2}}(|0\rangle+|1\rangle)\frac{1}{\sqrt{2}}(|0\rangle-|1\rangle)$

$$\xrightarrow{U_f} \left[(-1)^{f(1)}|0\rangle+(-1)^{f(0)}|1\rangle\right]\frac{1}{\sqrt{2}}(|0\rangle-|1\rangle)$$

Measure 1st qubit in basis $|\pm\rangle = \frac{1}{\sqrt{2}}(|0\rangle \pm |1\rangle)$

$\rightarrow |+\rangle$ if constant, $|-\rangle$ if balanced

Quantum Speedup: can solve w/1 query

Key aspect of Deutsch's algorithm:

We are looking for a global property of the function *f*

N bit binary number

Generally: $U_f: |x\rangle|0\rangle \rightarrow |x\rangle|f(x)\rangle$

Input $|\psi_{in}\rangle = \left[\frac{1}{\sqrt{2}}(|0\rangle+|1\rangle)\right]^{\otimes N}|0\rangle$

$$= \frac{1}{2^{N/2}}\sum_{x=0}^{2^N-1}|x\rangle|0\rangle$$

compute once

Output $|\psi_{out}\rangle = \frac{1}{2^{N/2}}\sum_{x=0}^{2^N-1}|x\rangle|f(x)\rangle$

Global properties encoded in state, trick is to extract desired information

Introduction and Overview (Preskills Notes)

9-03-2024

Quantum Advantage

David Deutsch: Toy problem that shows Quantum Advantage

Oracle

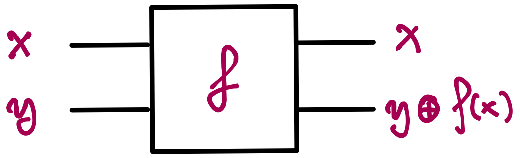

(Black Box)

Is the function

constant $f(0) = f(1)$

balanced $f(0) \neq f(1)$

Quantum Computation:

Input $|x\rangle|y\rangle = \frac{1}{\sqrt{2}}(|0\rangle+|1\rangle)\frac{1}{\sqrt{2}}(|0\rangle-|1\rangle)$

$$\xrightarrow{U_f} \left[(-1)^{f(1)}|0\rangle+(-1)^{f(0)}|1\rangle\right]\frac{1}{\sqrt{2}}(|0\rangle-|1\rangle)$$

Measure 1st qubit in basis $|\pm\rangle = \frac{1}{\sqrt{2}}(|0\rangle \pm |1\rangle)$

→ $|+\rangle$ if constant, $|-\rangle$ if balanced

Quantum Speedup: can solve w/1 query

Key aspect of Deutsch's algorithm:

We are looking for a global property of the function *f*

N bit binary number

Generally: $U_f: |x\rangle|0\rangle \rightarrow |x\rangle|f(x)\rangle$

Input $|\psi_{in}\rangle = \left[\frac{1}{\sqrt{2}}(|0\rangle+|1\rangle)\right]^{\otimes N}|0\rangle$

$$= \frac{1}{2^{N/2}}\sum_{x=0}^{2^N-1}|x\rangle|0\rangle$$

compute once

Output $|\psi_{out}\rangle = \frac{1}{2^{N/2}}\sum_{x=0}^{2^N-1}|x\rangle|f(x)\rangle$

Peter Shor: Period finding, QFT, Factoring

Introduction and Overview (Preskills Notes)

9-03-2024

Key aspect of Deutsch's algorithm:

We are looking for a global property of the function *f*

N bit binary number

Generally: $U_f : |x\rangle|0\rangle \rightarrow |x\rangle|f(x)\rangle$

Input $|\psi_{in}\rangle = \left[\frac{1}{\sqrt{2}}(|0\rangle + |1\rangle)\right]^{\otimes N} |0\rangle$

$$= \frac{1}{2^{N/2}} \sum_{x=0}^{2^N-1} |x\rangle|0\rangle$$

compute once

Output $|\psi_{out}\rangle = \frac{1}{2^{N/2}} \sum_{x=0}^{2^N-1} |x\rangle|f(x)\rangle$

Peter Shor: **Period finding, QFT, Factoring**

Next: Will this work with real-world Quantum Hardware ?

Faulty gates, decoherence !

Introduction and Overview (Preskills Notes)

9-03-2024

Quantum Error Correction

Fundamental Problem

Quantum States are fragile, especially when entangled

Classical Computation ? **Dissipation helps**

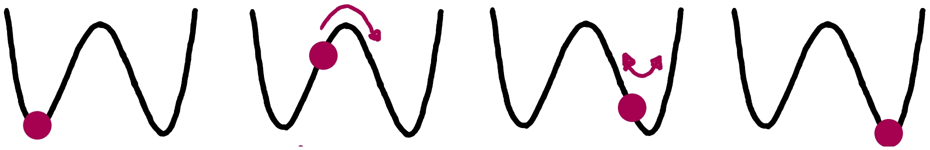

No dissipation ⇨ **Errors build up**

Quantum Computation ⇨

- ∗ Cannot tolerate dissipation
- ∗ Destroys superposition and entanglement

What to do ? **Error Correction !**

Classical Error Correction:

Simple example: **Redundancy protects against bit flips**

Encode:

$0 \rightarrow (000)$

$1 \rightarrow (111)$

Errors:

$(000) \rightarrow (100)$

$(111) \rightarrow (011)$

correct by majority vote

Introduction and Overview (Preskills Notes)

9-03-2024

Quantum Computation ➡

- ∗ Cannot tolerate dissipation
- ∗ Destroys superposition and entanglement

What to do ? Error Correction !

Classical Error Correction:

Simple example: Redundancy protects against bit flips

Encode:
$0 \to (000)$
$1 \to (111)$

Errors:
$(000) \to (100)$
$(111) \to (011)$

correct by majority vote

Von Neumann:

- ∗ A classical computer w/faulty components can work, given enough redundancy
- ∗ Classical error correction is well developed and highly sophisticated…

∗ Quantum Errors

1) Bit Flip $|0\rangle \to |1\rangle$, $|1\rangle \to |0\rangle$, phase flip $|0\rangle \to |0\rangle$, $|1\rangle \to -|1\rangle$

2) Small errors $a|0\rangle + b|1\rangle$ a, b can change by ε
errors accumulate

3) Measurement disturbs ➡ collapse of quantum states

4) No cloning ➡ Cannot protect by making copies

9-03-2024

Introduction and Overview (Preskills Notes)

Von Neumann:

- ∗ A classical computer w/faulty components can work, given enough redundancy
- ∗ Classical error correction is well developed and highly sophisticated…

∗ Quantum Errors

1) Bit Flip $|0\rangle \to |1\rangle$, $|1\rangle \to |0\rangle$, phase flip $|0\rangle \to |0\rangle$, $|1\rangle \to -|1\rangle$

2) Small errors $a|0\rangle + b|1\rangle$ a, b can change by ε errors accumulate

3) Measurement disturbs ⇨ collapse of quantum states

4) No cloning ⇨ Cannot protect by making copies

Example: Peter Shor's code for bit flip error when P(error) << 1

Encode: $|0\rangle \to |\bar{0}\rangle \equiv |000\rangle$ (3 bit code)

$|1\rangle \to |\bar{1}\rangle \equiv |111\rangle$

⇩

$$a|0\rangle + b|1\rangle \to a|000\rangle + b|111\rangle$$

Single-qubit measurement ⇨ collapse of state, destroys info, no majority voting !

Collective 2-qubit measurement:

- for $|x,y,z\rangle$ measure $y \oplus z$, $x \oplus z$ (never measure individual bits)
- if $|000\rangle$, $|111\rangle$ these observables $= 0$
- if one bit-flip, at least one observable $= 1$
- easy to check that $(y \oplus z, x \oplus z) =$ binary address of qubit flip

$|000\rangle \to |010\rangle$ $(1,0) =$ 2nd bit

9-03-2024

Introduction and Overview (Preskills Notes)

Example: Peter Shor's code for bit flip error when $P(\text{error}) << 1$

Encode:

$|0\rangle \to |\bar{0}\rangle \equiv |000\rangle$

$|1\rangle \to |\bar{1}\rangle \equiv |111\rangle$

(3 bit code)

$a|0\rangle + b|1\rangle \to a|000\rangle + b|111\rangle$

Single-qubit measurement ➡ collapse of state, destroys info, no majority voting !

Collective 2-qubit measurement:

- for $|x,y,z\rangle$ measure $y \oplus z$, $x \oplus z$ (never measure individual bits)
- if $|000\rangle$, $|111\rangle$ these observables $= 0$
- if one bit-flip, at least one observable $= 1$
- easy to check that $(y \oplus z, x \oplus z) =$ binary address of qubit flip

$|000\rangle \to |010\rangle$ $(1,0) =$ 2nd bit

Small errors:

$|000\rangle \to |000\rangle + \varepsilon|001\rangle$

$|111\rangle \to |111\rangle + \varepsilon|110\rangle$

Quantum mechanics to the rescue !

- mostly no error detected
  - ➡ collapse into $|000\rangle$ resp. $|111\rangle$
- sometime error detected
  - ➡ collapse into $|001\rangle$ resp. $|110\rangle$
  - ➡ full bit flip, correct as such

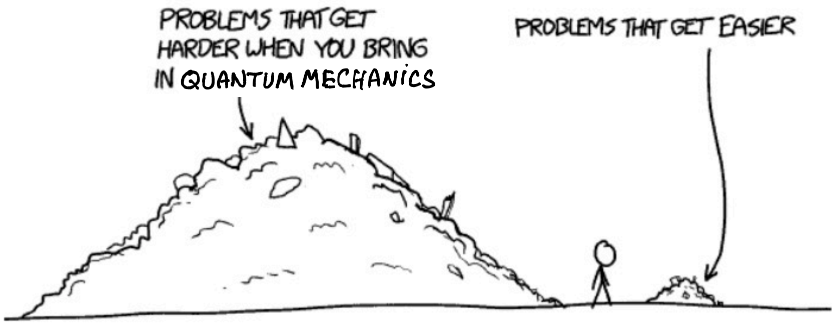

Source: xkcd.com

Introduction and Overview (Preskills Notes)

Example: Peter Shor's code for bit flip error when P(error) << 1

Encode: $|0\rangle \to |\bar{0}\rangle \equiv |000\rangle$

$|1\rangle \to |\bar{1}\rangle \equiv |111\rangle$ (3 bit code)

$$a|0\rangle + b|1\rangle \to a|000\rangle + b|111\rangle$$

Single-qubit measurement ⇨ collapse of state, destroys info, no majority voting !

Collective 2-qubit measurement:

- for $|x,y,z\rangle$ measure $y \oplus z$, $x \oplus z$ (never measure individual bits)
- if $|000\rangle$, $|111\rangle$ these observables $=0$
- if one bit-flip, at least one observable $=1$
- easy to check that $(y\oplus z, x\oplus z) =$ binary address of qubit flip

$|000\rangle \to |010\rangle$ $(1,0) =$ 2nd bit

Small errors: $|000\rangle \to |000\rangle + \varepsilon|001\rangle$

$|111\rangle \to |111\rangle + \varepsilon|110\rangle$

Quantum mechanics to the rescue !

- mostly no error detected
  - ⇨ collapse into $|000\rangle$ resp. $|111\rangle$
- sometime error detected
  - ⇨ collapse into $|001\rangle$ resp. $|110\rangle$
  - ⇨ full bit flip, correct as such

How to implement ?

Quantum circuit + single qubit measurement

Quantum Gates – work on superpositions, and entangled states

Introduction and Overview (Preskills Notes)

9-05-2024

Controlled-NOT (CNOT)

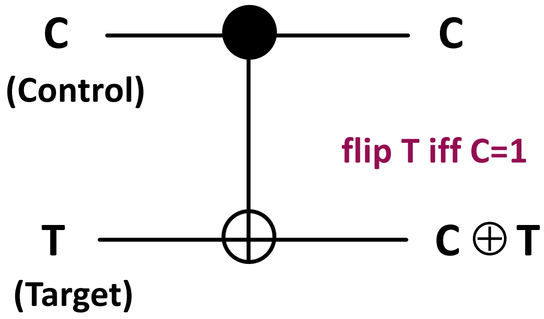

Truth Table

C	T	C ⊕ T
0	0	0
0	1	1
1	0	1
1	1	0

Circuit maps logical basis states as

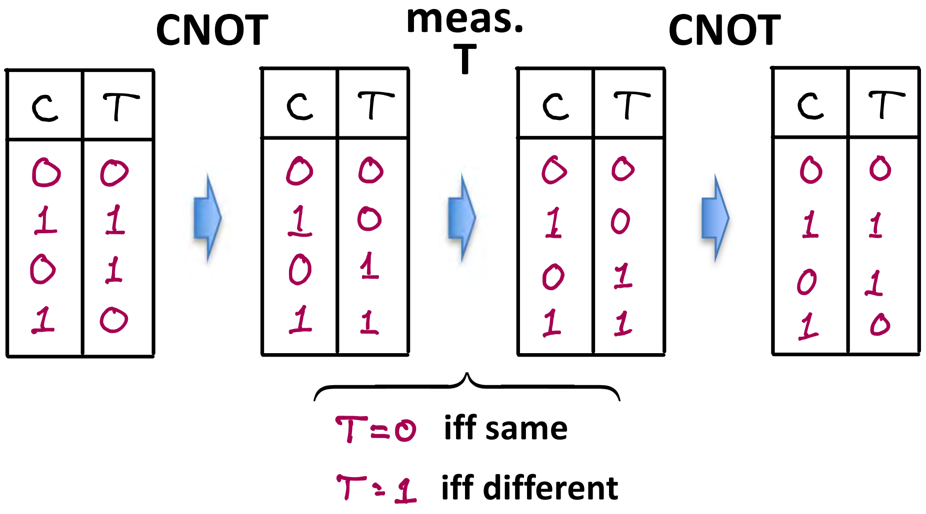

C	T
0	0
1	1
0	1
1	0

C	T
0	0
1	0
0	1
1	1

C	T
0	0
1	0
0	1
1	1

C	T
0	0
1	1
0	1
1	0

T=0 iff same

T=1 iff different

Quantum Circuit for joint measurement

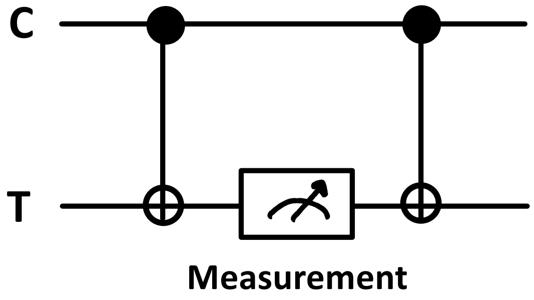

Measurement in $\{|0\rangle, |1\rangle\}$ basis

yields $C \oplus T$

Full circuit to obtain Error Syndrome

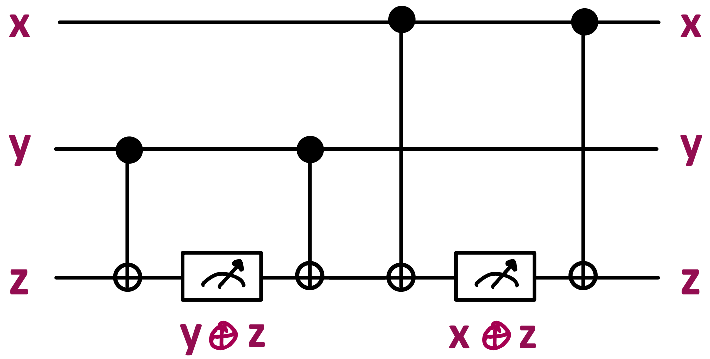

* iff qubit flip, binary address = $(y \oplus z, x \oplus z)$

Introduction and Overview (Preskills Notes)

9-05-2024

Circuit maps logical basis states as

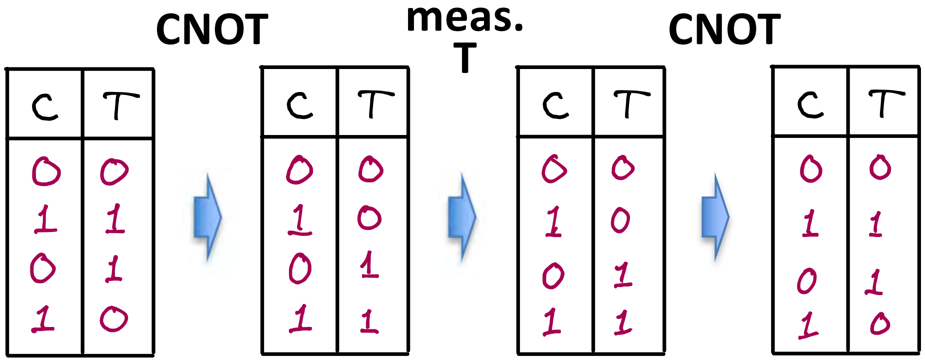

C	T
0	0
1	1
0	1
1	0

C	T
0	0
1	0
0	1
1	1

C	T
0	0
1	0
0	1
1	1

C	T
0	0
1	1
0	1
1	0

T=0 iff same

T=1 iff different

Full circuit to obtain Error Syndrome

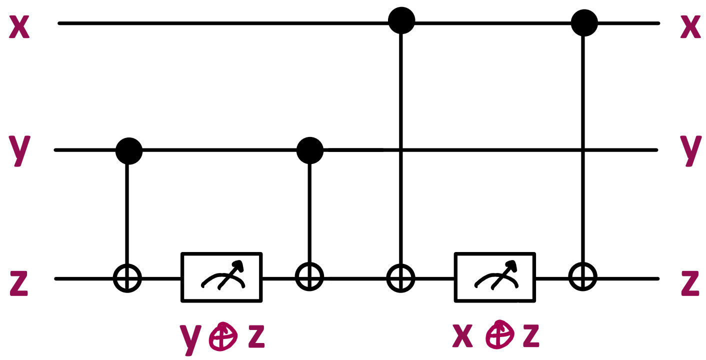

- * iif qubit flip, binary address = $(y \oplus z, x \oplus z)$

Quantum Phase Error

$|0\rangle \to |0\rangle$

$|1\rangle \to -|1\rangle$

Encoding

$$|0\rangle \to |\bar{0}\rangle = \frac{1}{2^{3/2}} \overset{x'}{(|0\rangle+|1\rangle)} \overset{y'}{(|0\rangle+|1\rangle)} \overset{z'}{(|0\rangle+|1\rangle)}$$

$$|1\rangle \to |\bar{1}\rangle = \frac{1}{2^{3/2}} (|0\rangle-|1\rangle)(|0\rangle-|1\rangle)(|0\rangle-|1\rangle)$$

Relabel

$$\frac{1}{\sqrt{2}}(|0\rangle+|1\rangle) = |0'\rangle$$

$$\frac{1}{\sqrt{2}}(|0\rangle-|1\rangle) = |1'\rangle$$

Measure in basis $\{|0'\rangle, |1'\rangle\} \to y'\oplus z', x'\oplus z'$

Error Syndrome

- * Iff phase error, binary address $= (y'\oplus z', x'\oplus z')$
- * Analogous to bit-flip code, just in different basis

Introduction and Overview (Preskills Notes)

9-05-2024

Quantum Phase Error

$|0\rangle \to |0\rangle$

$|1\rangle \to -|1\rangle$

Encoding

$$|0\rangle \to |\bar{0}\rangle = \frac{1}{2^{3/2}}\overset{x'}{(|0\rangle+|1\rangle)}\overset{y'}{(|0\rangle+|1\rangle)}\overset{z'}{(|0\rangle+|1\rangle)}$$

$$|1\rangle \to |\bar{1}\rangle = \frac{1}{2^{3/2}}(|0\rangle-|1\rangle)(|0\rangle-|1\rangle)(|0\rangle-|1\rangle)$$

Relabel

$$\frac{1}{\sqrt{2}}(|0\rangle+|1\rangle) = |0'\rangle$$

$$\frac{1}{\sqrt{2}}(|0\rangle-|1\rangle) = |1'\rangle$$

Measure in basis

$$\{|0'\rangle, |1'\rangle\} \to y'\oplus z',\ x'\oplus z'$$

Error Syndrome

- Iff phase error, binary address $= (y'\oplus z', x'\oplus z')$
- Analogous to bit-flip code, just in different basis

Shor's 9-bit code

- Combines flip/phase error correction
- Corrects one flip or phase error

General principle of error correction

- Encode *p* logical qubits in *n* physical qubits.
- Valid Logical States form 2^p–dimensional subspace $\mathcal{E}_p$ (code space) in *n*-qubit (2^n–dimensional) Hilbert space $\mathcal{E}_N$
- Errors displace system into orthogonal (distinguishable) subspaces.

9-05-2024

Introduction and Overview (Preskills Notes)

Shor’s 9-bit code

- ✱ Combines flip/phase error correction
- ✱ Corrects one flip or phase error

General principle of error correction

- ✱ Encode *p* logical qubits in *n* physical qubits.
- ✱ Valid Logical States form 2^p–dimensional subspace $\mathcal{E}_p$ (code space) in n-qubit (2^n–dimensional) Hilbert space $\mathcal{E}_N$
- ✱ Errors displace system into orthogonal (distinguishable) subspaces.

Geometric illustration

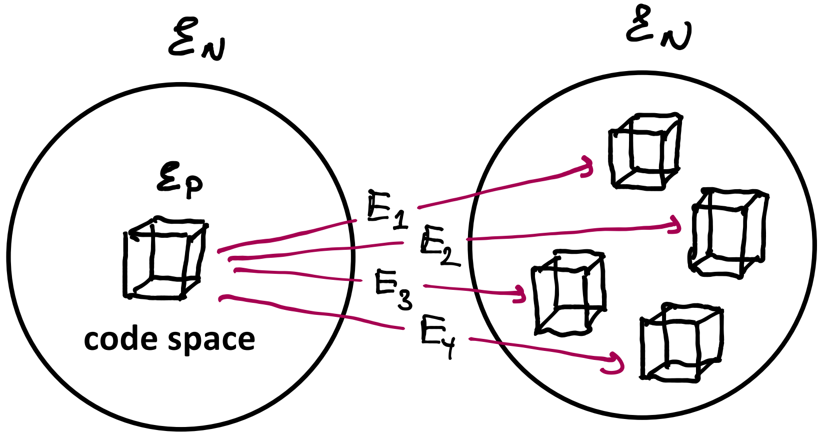

What about non-Unitary errors ?

e. g., decay

$|0\rangle \to |0\rangle$

$|1\rangle \to |0\rangle$

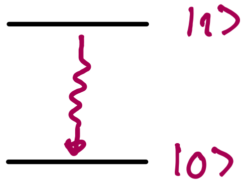

Problem: Errors not displaced into orthogonal subspaces

Solution: ”Quantum jump codes”, monitors the environment

Other kinds of errors ?

Introduction and Overview (Preskills Notes)

9-05-2024

Geometric illustration

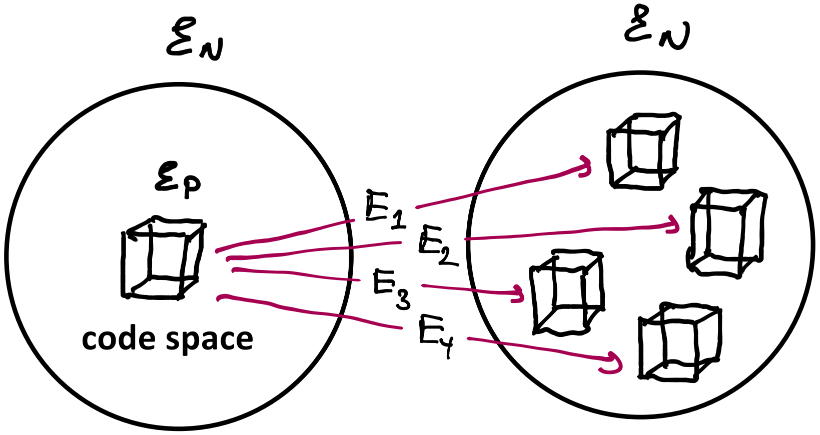

What about non-Unitary errors?

e. g., decay

$|0\rangle \rightarrow |0\rangle$

$|1\rangle \rightarrow |0\rangle$

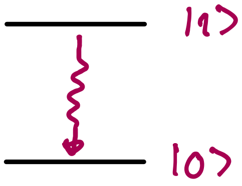

Problem: Errors not displaced into orthogonal subspaces

Solution: ”Quantum jump codes”, monitors the environment

Other kinds of errors?

9-05-2024

Introduction and Overview (Preskills Notes)

Catnip for Theoretical Physicists & Computer Scientists

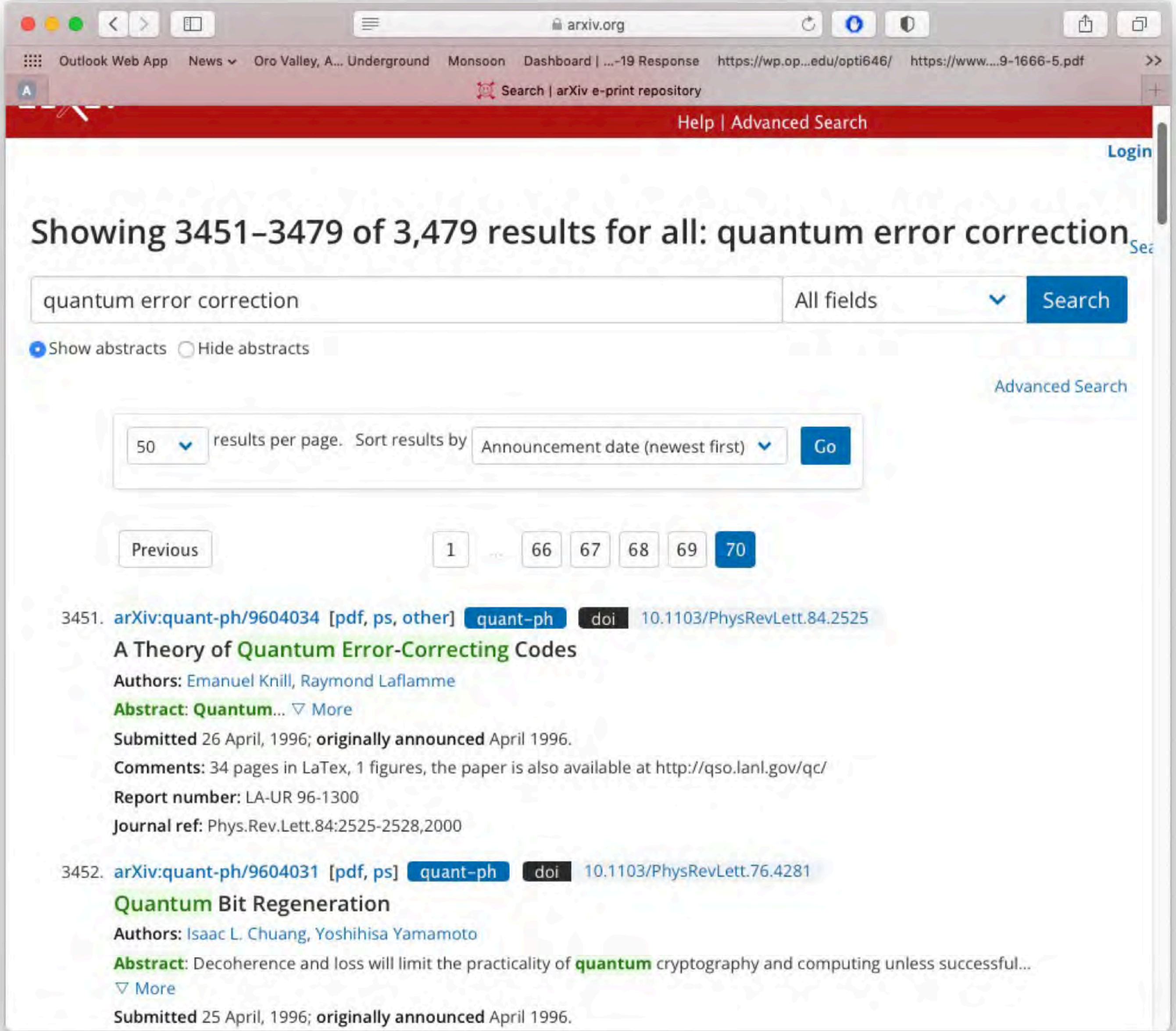

Showing 3451–3479 of 3,479 results for all: quantum error correction

quantum error correction | All fields | Search

● Show abstracts ○ Hide abstracts

Advanced Search

50 results per page. Sort results by Announcement date (newest first) Go

Previous 1 … 66 67 68 69 70

3451. arXiv:quant-ph/9604034 [pdf, ps, other] quant-ph doi 10.1103/PhysRevLett.84.2525

A Theory of Quantum Error-Correcting Codes

Authors: Emanuel Knill, Raymond Laflamme

Abstract: Quantum... ▽ More

Submitted 26 April, 1996; **originally announced** April 1996.

Comments: 34 pages in LaTex, 1 figures, the paper is also available at http://qso.lanl.gov/qc/

Report number: LA-UR 96-1300

Journal ref: Phys.Rev.Lett.84:2525-2528,2000

3452. arXiv:quant-ph/9604031 [pdf, ps] quant-ph doi 10.1103/PhysRevLett.76.4281

Quantum Bit Regeneration

Authors: Isaac L. Chuang, Yoshihisa Yamamoto

Abstract: Decoherence and loss will limit the practicality of quantum cryptography and computing unless successful... ▽ More

Submitted 25 April, 1996; **originally announced** April 1996.

9-05-2024

Introduction and Overview (Preskills Notes)

Catnip for Theoretical Physicists & Computer Scientists

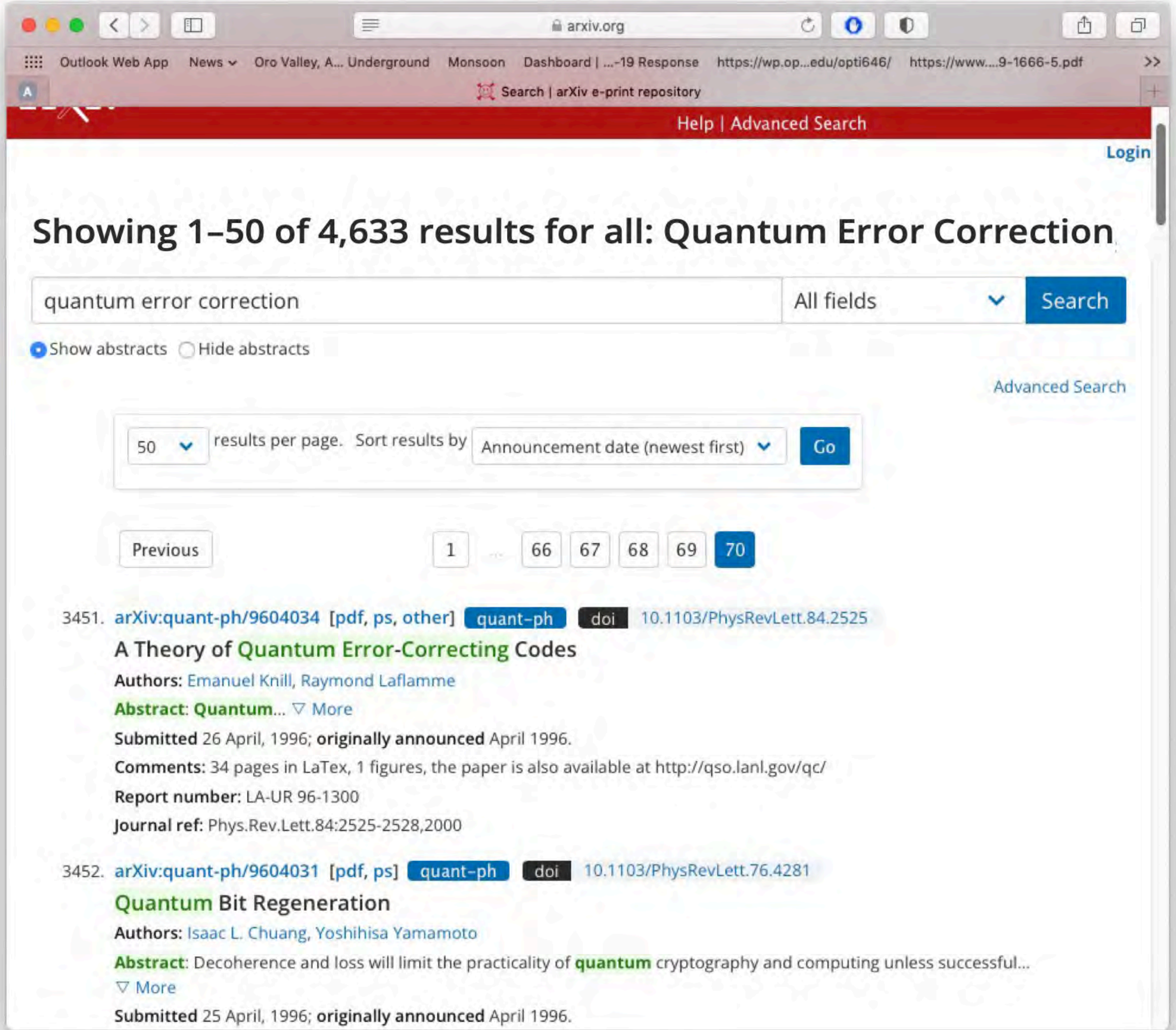

Showing 1–50 of 4,633 results for all: Quantum Error Correction

quantum error correction | All fields | Search

● Show abstracts ○ Hide abstracts

50 results per page. Sort results by Announcement date (newest first) Go

3451. arXiv:quant-ph/9604034 [pdf, ps, other] quant-ph doi 10.1103/PhysRevLett.84.2525

A Theory of Quantum Error-Correcting Codes

Authors: Emanuel Knill, Raymond Laflamme

Abstract: Quantum... ▽ More

Submitted 26 April, 1996; **originally announced** April 1996.

Comments: 34 pages in LaTex, 1 figures, the paper is also available at http://qso.lanl.gov/qc/

Report number: LA-UR 96-1300

Journal ref: Phys.Rev.Lett.84:2525-2528,2000

3452. arXiv:quant-ph/9604031 [pdf, ps] quant-ph doi 10.1103/PhysRevLett.76.4281

Quantum Bit Regeneration

Authors: Isaac L. Chuang, Yoshihisa Yamamoto

Abstract: Decoherence and loss will limit the practicality of quantum cryptography and computing unless successful... ▽ More

Submitted 25 April, 1996; **originally announced** April 1996.

Introduction and Overview (Preskills Notes)

9-05-2024

Quantum Hardware

Physical Implementation is
Extremely demanding !

Requirements

1. Storage: Quantum memory.
2. Gates: We put computation U_f together from 1 and 2-qubit operations.
3. Readout: Method to measure qubits.
4. Isolation: No coupling to environment to avoid decoherence & errors
5. Precision: Gates, readouts must be highly accurate

Inherent Contradictions

2. Gates vs **4. Isolation**

↑ coupling between qubits

↑ no coupling to environment

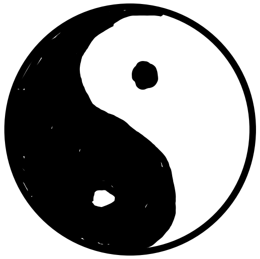

To build a Quantum Computer:

Choose, find or invent a system with acceptable tradeoffs.

6. Error Correction must not create more errors than it corrects.

↓

7. <u>Thresholds</u> for Error Correction and Fault Tolerance

9-05-2024

Introduction and Overview (Preskills Notes)

Inherent Contradictions

2. Gates vs **4. Isolation**

coupling between qubits

no coupling to environment

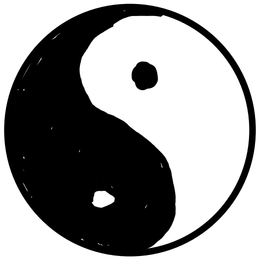

To build a Quantum Computer:

Choose, find or invent a system with acceptable tradeoffs.

6. Error Correction must not create more errors than it corrects.

7. <u>Thresholds</u> for Error Correction and Fault Tolerance

Ion Trap Quantum Computing

First to demonstrate a Quantum Gate

- Qubit is encoded in the electronic ground state of an atomic ion

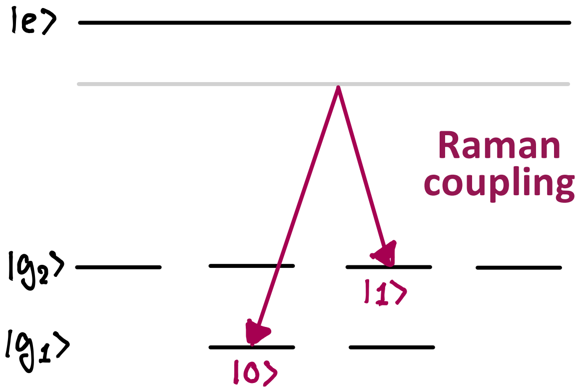

- Early design with a few ions in large trap

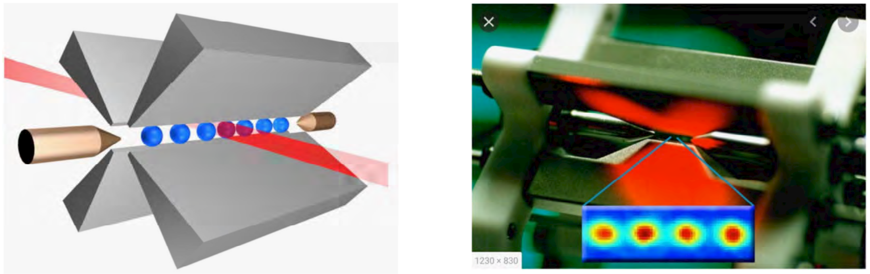

9-05-2024

Introduction and Overview (Preskills Notes)

Ion Trap Quantum Computing

First to demonstrate a Quantum Gate

- Qubit is encoded in the electronic ground state of an atomic ion

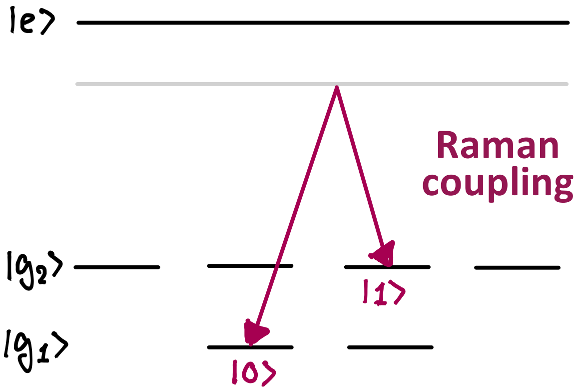

- Early design with a few ions in large trap

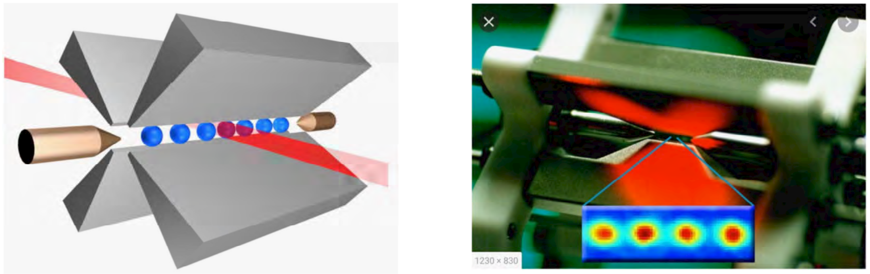

Requirements

1. Storage: 10s-100s coherence time
2. Gates: Use collective vibrations as "quantum bus"
3. Readout: Fluorescence

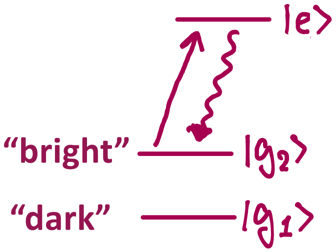

Cirac & Zoller: 5 laser pulses

CNOT gate between any 2 ions in linear array

Wineland: 3 laser pulses enough for CNOT

Use this example serves as conceptual template

Introduction and Overview (Preskills Notes)

9-05-2024

Ion Trap Quantum Computing

First to demonstrate a Quantum Gate

- **Qubit is encoded in the electronic ground state of an atomic ion**

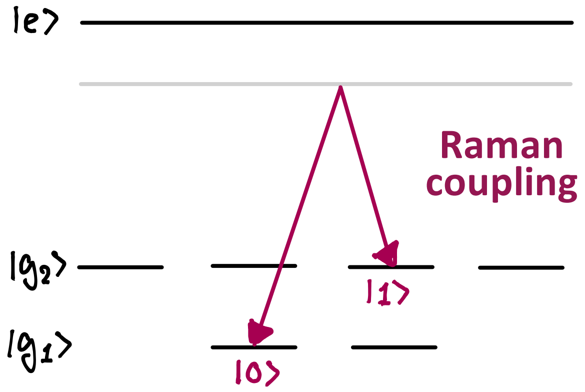

- **Early design with a few ions in large trap**

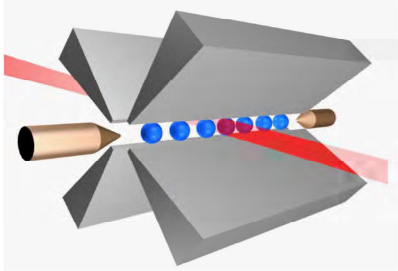

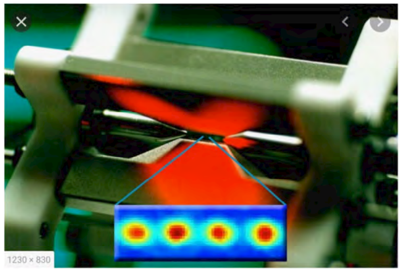

- **Scaling up in Linear Ion Traps**

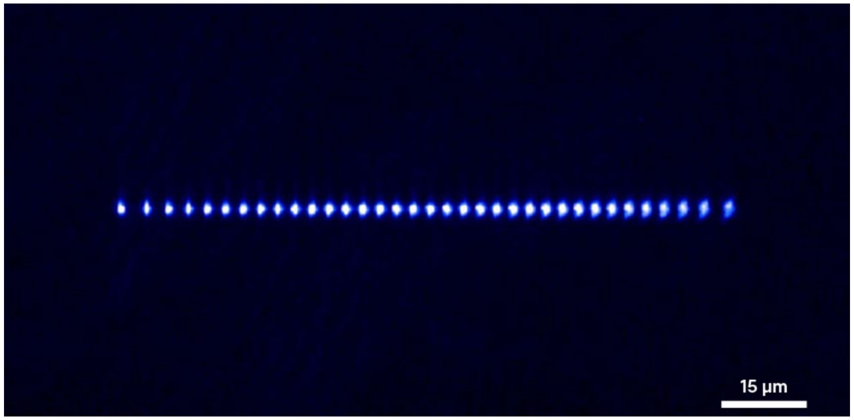

- **Limitations**

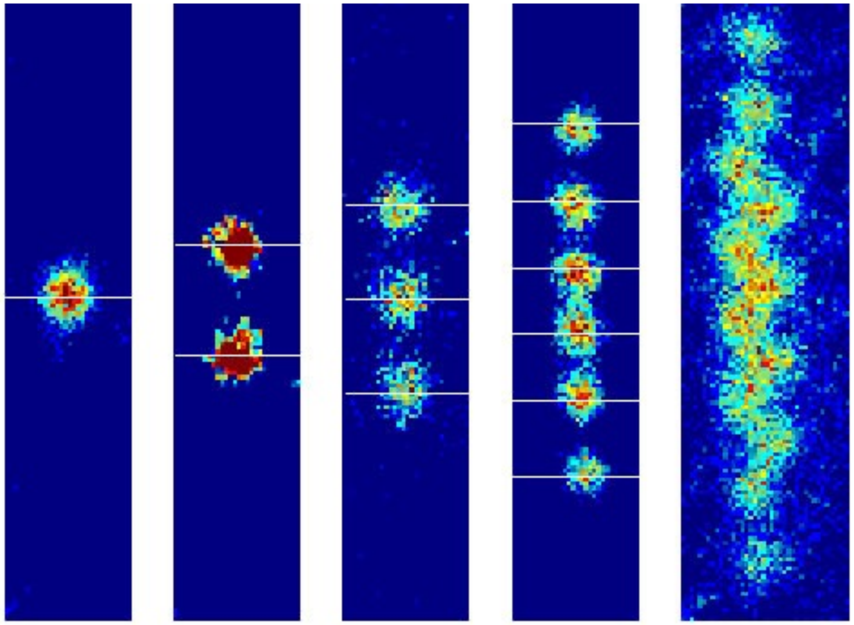

Introduction and Overview (Preskills Notes)

9-10-2024

Status: Many important milestones achieved

- Entanglement of ≥ 20 ions (2018)
- Highest gate & readout fidelities, longest coherence times
- Error Correction, Fault Tolerance proof of principle demonstrations
- Complex algorithms on few ions, quantum simulations with ≥ 50
- Research groups in academia, National Labs, Industry

Some early leaders

NIST	Innsbruck	Quantinuum
Sandia NL	Duke U	IonQ

Many others these days

- Major challenges – same as late 2000's!
- "Clock speed" set by vibrational freqs microfabricated traps do better
- More ions -> harder to cool motion, harder to individually address ions in linear trap.
- Scaling up to 1000's of ions is an enormous challenge

Scalable Ion Trap Quantum Processor – one vision

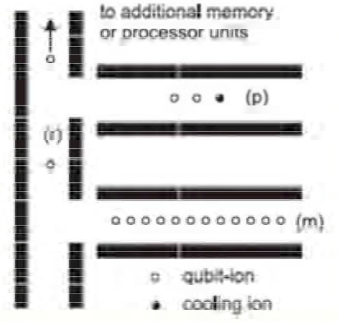

D. Kielpinski, C. Monroe, and D. J. Wineland, Nature 417, 709 (2002).

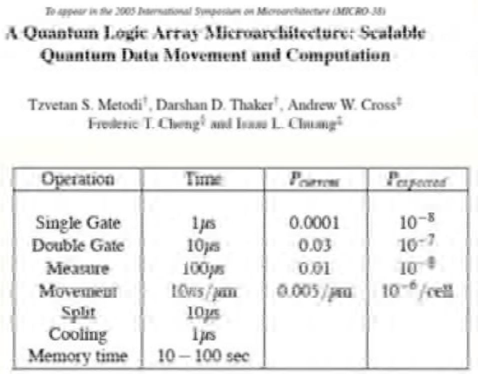

To appear in the 2005 International Symposium on Microarchitecture (MICRO-38)

A Quantum Logic Array Microarchitecture: Scalable Quantum Data Movement and Computation

Tzvetan S. Metodi†, Darshan D. Thaker†, Andrew W. Cross‡
Frederic T. Chong† and Isaac L. Chuang‡

Operation	Time	$P_{current}$	$P_{expected}$
Single Gate	$1\mu s$	0.0001	10^{-8}
Double Gate	$10\mu s$	0.03	10^{-7}
Measure	$100\mu s$	0.01	10^{-8}
Movement	$10ns/\mu m$	$0.005/\mu m$	10^{-6}/cell
Split	$10\mu s$		
Cooling	$1\mu s$		
Memory time	10 – 100 sec		

Introduction and Overview (Preskills Notes)

NIST Group, Current as of 2023

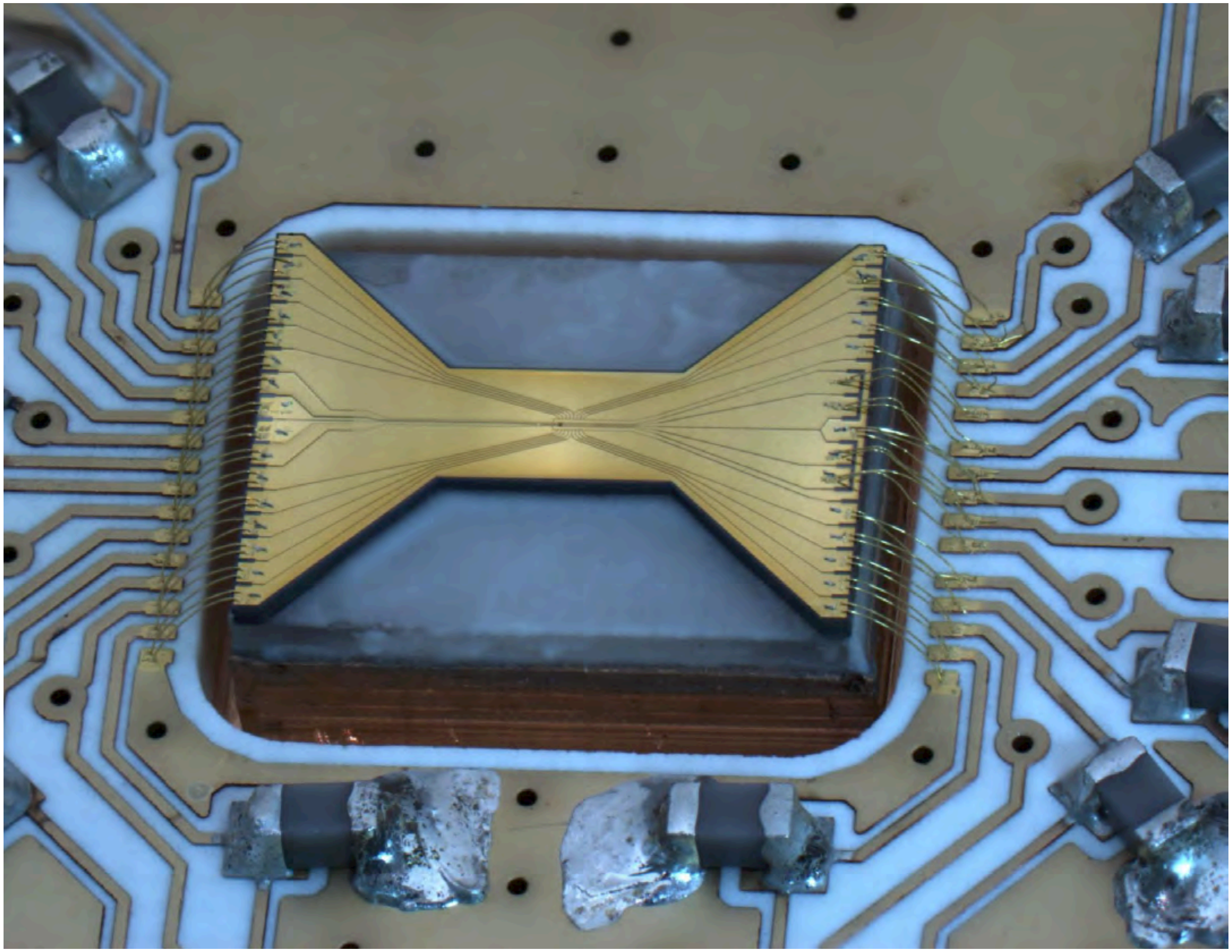

Introduction and Overview (Preskills Notes)

9-10-2024

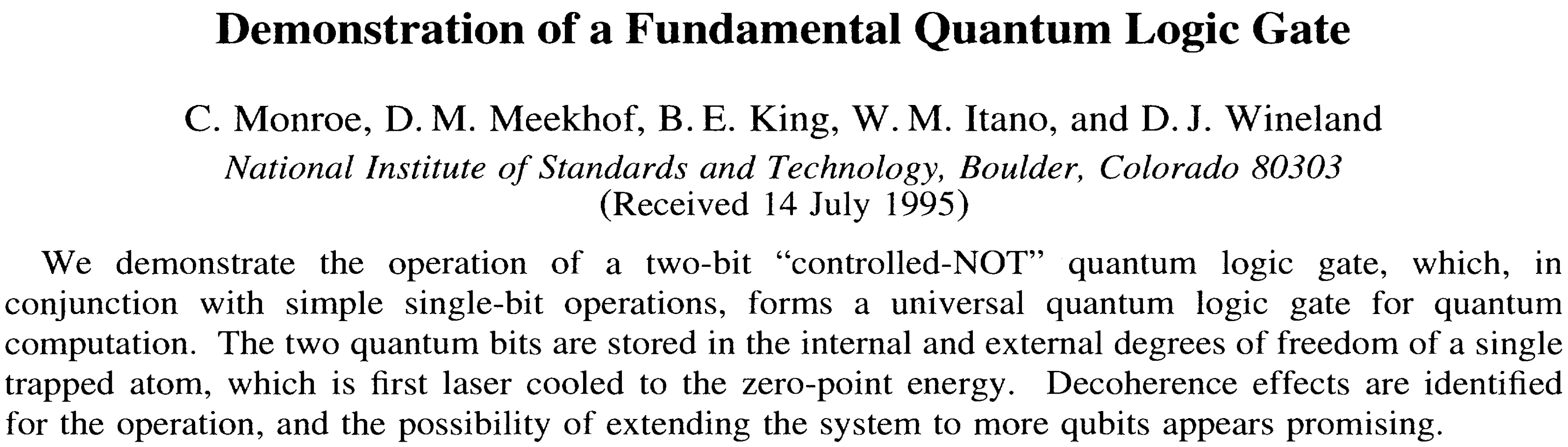

Demonstration of a Fundamental Quantum Logic Gate

C. Monroe, D. M. Meekhof, B. E. King, W. M. Itano, and D. J. Wineland
National Institute of Standards and Technology, Boulder, Colorado 80303

(Received 14 July 1995)

We demonstrate the operation of a two-bit "controlled-NOT" quantum logic gate, which, in conjunction with simple single-bit operations, forms a universal quantum logic gate for quantum computation. The two quantum bits are stored in the internal and external degrees of freedom of a single trapped atom, which is first laser cooled to the zero-point energy. Decoherence effects are identified for the operation, and the possibility of extending the system to more qubits appears promising.

Introduction and Overview (Preskills Notes)

9-10-2024

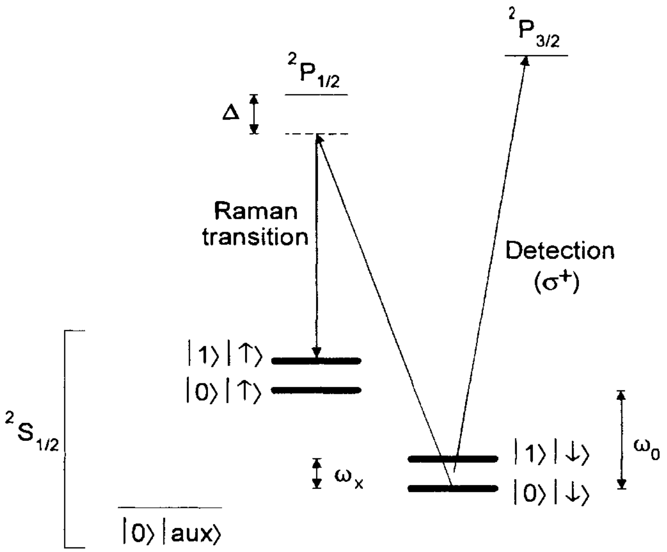

FIG. 1. $^9\text{Be}^+$ energy levels. The levels indicated with thick lines form the basis of the quantum register: internal levels are $|S\rangle = |\downarrow\rangle$ and $|\uparrow\rangle$ ($^2S_{1/2}|F = 2, m_F = 2\rangle$ and $^2S_{1/2}|F = 1, m_F = 1\rangle$ levels, respectively, separated by $\omega_0/2\pi \simeq 1.250$ GHz), and $|\text{aux}\rangle = {}^2S_{1/2}|F = 2, m_F = 0\rangle$ (separated from $|\downarrow\rangle$ by $\simeq$2.5 MHz); external vibrational levels are $|n\rangle = |0\rangle$ and $|1\rangle$ (separated by $\omega_x/2\pi \simeq 11.2$ MHz). Stimulated Raman transitions between $^2S_{1/2}$ hyperfine states are driven through the virtual $^2P_{1/2}$ level ($\Delta \simeq 50$ GHz) with a pair of $\simeq$313 nm laser beams. Measurement of S is accomplished by driving the cycling $|\downarrow\rangle \rightarrow {}^2P_{3/2}|F = 3, m_F = 3\rangle$ transition with σ^+-polarized light and detecting the resulting ion fluorescence.

according to the following format:

(a) A $\pi/2$ pulse is applied on the carrier transition. The effect is described by the operator $V^{1/2}(\pi/2)$ in the notation of Ref. [1].

(b) A 2π pulse is applied on the blue sideband transition between $|\uparrow\rangle$ and an auxiliary atomic level $|\text{aux}\rangle$ (see Fig. 1). (1)

(c) A $\pi/2$ pulse is applied on the carrier transition, with a π phase shift relative to (a), leading to the operator $V^{1/2}(-\pi/2)$ of Ref. [1].

is as follows:

$$\begin{array}{rcl} \text{Input state} & \rightarrow & \text{Output state} \\ |0\rangle|\downarrow\rangle & \rightarrow & |0\rangle|\downarrow\rangle \\ |0\rangle|\uparrow\rangle & \rightarrow & |0\rangle|\uparrow\rangle \\ |1\rangle|\downarrow\rangle & \rightarrow & |1\rangle|\uparrow\rangle \\ |1\rangle|\uparrow\rangle & \rightarrow & |1\rangle|\downarrow\rangle . \end{array} \tag{2}$$

The experiment apparatus is described elsewhere [16,17]. A single $^9\text{Be}^+$ ion is stored in a coaxial-resonator rf-ion trap [17], which provides pseudopotential oscillation frequencies of $(\omega_x, \omega_y, \omega_z)/2\pi \simeq (11.2, 18.2, 29.8)$ MHz along the principal axes of the trap. We cool the ion so that the $n_x = 0$ vibrational ground state is occupied $\simeq$95% of the time by employing resolved-sideband stimulated Raman cooling in the x dimension, exactly as in Ref. [16]. The two Raman beams each contain $\simeq$1 mW of power at $\simeq$313 nm and are detuned $\simeq$50 GHz red of the $^2P_{1/2}$ excited state. The Raman beams are applied to the ion in directions such that their wave-vector difference $\boldsymbol{\delta k}$ points nearly along the x axis of the trap; thus the Raman transitions are highly insensitive to motion in the other two dimensions. The Lamb-Dicke parameter is $\eta_x = \delta k\, x_0 \simeq 0.2$, where $x_0 \simeq 7$ nm is the spread of the $n_x = 0$ wave function. The carrier ($|n\rangle|\downarrow\rangle \rightarrow |n\rangle|\uparrow\rangle$) Rabi frequency is $\Omega_0 2\pi \simeq 140$ kHz, the red ($|1\rangle|\downarrow\rangle \rightarrow |0\rangle|\uparrow\rangle$) and blue ($|0\rangle|\downarrow\rangle \rightarrow |1\rangle|\uparrow\rangle$) sideband Rabi frequencies are $\eta_x\Omega_0/2\pi \simeq 30$ kHz, and the auxiliary transition ($|1\rangle|\uparrow\rangle \rightarrow |0\rangle|\downarrow\rangle$) Rabi frequency is $\eta_x\Omega_{\text{aux}}/2\pi \simeq 12$ kHz. The difference frequency of the Raman beams is tunable from 1200 to 1300 MHz with the use of a double pass acousto-optic modulator (AOM), and the Raman pulse durations are controlled with additional switching AOMs. Since the Raman beams are generated from a single laser and an AOM, broadening of the Raman transitions due to a finite laser linewidth is negligible [18].

Following Raman cooling to the $|0\rangle|\downarrow\rangle$ state, but before application of the CN operation, we apply appropriately

Introduction and Overview (Preskills Notes)

9-10-2024

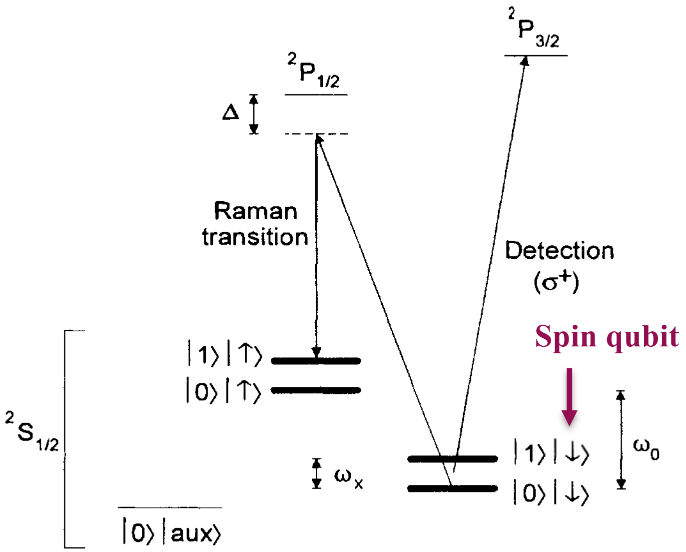

FIG. 1. $^9\text{Be}^+$ energy levels. The levels indicated with thick lines form the basis of the quantum register: internal levels are $|S\rangle = |\downarrow\rangle$ and $|\uparrow\rangle$ ($^2S_{1/2}|F = 2, m_F = 2\rangle$ and $^2S_{1/2}|F = 1, m_F = 1\rangle$ levels, respectively, separated by $\omega_0/2\pi \simeq 1.250$ GHz), and $|\text{aux}\rangle = {}^2S_{1/2}|F = 2, m_F = 0\rangle$ (separated from $|\downarrow\rangle$ by $\simeq$2.5 MHz); external vibrational levels are $|n\rangle = |0\rangle$ and $|1\rangle$ (separated by $\omega_x/2\pi \simeq 11.2$ MHz). Stimulated Raman transitions between $^2S_{1/2}$ hyperfine states are driven through the virtual $^2P_{1/2}$ level ($\Delta \simeq 50$ GHz) with a pair of $\simeq$313 nm laser beams. Measurement of S is accomplished by driving the cycling $|\downarrow\rangle \rightarrow {}^2P_{3/2}|F = 3, m_F = 3\rangle$ transition with σ^+-polarized light and detecting the resulting ion fluorescence.

according to the following format:

(a) A $\pi/2$ pulse is applied on the carrier transition. The effect is described by the operator $V^{1/2}(\pi/2)$ in the notation of Ref. [1].

(b) A 2π pulse is applied on the blue sideband transition between $|\uparrow\rangle$ and an auxiliary atomic level $|\text{aux}\rangle$ (see Fig. 1). (1)

(c) A $\pi/2$ pulse is applied on the carrier transition, with a π phase shift relative to (a), leading to the operator $V^{1/2}(-\pi/2)$ of Ref. [1].

is as follows:

$$\begin{array}{c} \text{Input state} \rightarrow \text{Output state} \\ |0\rangle|\downarrow\rangle \rightarrow |0\rangle|\downarrow\rangle \\ |0\rangle|\uparrow\rangle \rightarrow |0\rangle|\uparrow\rangle \\ |1\rangle|\downarrow\rangle \rightarrow |1\rangle|\uparrow\rangle \\ |1\rangle|\uparrow\rangle \rightarrow |1\rangle|\downarrow\rangle . \end{array} \qquad (2)$$

The experiment apparatus is described elsewhere [16,17]. A single $^9\text{Be}^+$ ion is stored in a coaxial-resonator rf-ion trap [17], which provides pseudopotential oscillation frequencies of $(\omega_x, \omega_y, \omega_z)/2\pi \simeq (11.2, 18.2, 29.8)$ MHz along the principal axes of the trap. We cool the ion so that the $n_x = 0$ vibrational ground state is occupied $\simeq$95% of the time by employing resolved-sideband stimulated Raman cooling in the x dimension, exactly as in Ref. [16]. The two Raman beams each contain $\simeq$1 mW of power at $\simeq$313 nm and are detuned $\simeq$50 GHz red of the $^2P_{1/2}$ excited state. The Raman beams are applied to the ion in directions such that their wave-vector difference $\boldsymbol{\delta}\mathbf{k}$ points nearly along the x axis of the trap; thus the Raman transitions are highly insensitive to motion in the other two dimensions. The Lamb-Dicke parameter is $\eta_x = \delta k\, x_0 \simeq 0.2$, where $x_0 \simeq 7\,\text{nm}$ is the spread of the $n_x = 0$ wave function. The carrier $(|n\rangle|\downarrow\rangle \rightarrow |n\rangle|\uparrow\rangle)$ Rabi frequency is $\Omega_0 2\pi \simeq 140$ kHz, the red $(|1\rangle|\downarrow\rangle \rightarrow |0\rangle|\uparrow\rangle)$ and blue $(|0\rangle|\downarrow\rangle \rightarrow |1\rangle|\uparrow\rangle)$ sideband Rabi frequencies are $\eta_x\Omega_0/2\pi \simeq 30$ kHz, and the auxiliary transition $(|1\rangle|\uparrow\rangle \rightarrow |0\rangle|\downarrow\rangle)$ Rabi frequency is $\eta_x\Omega_{\text{aux}}/2\pi \simeq 12$ kHz. The difference frequency of the Raman beams is tunable from 1200 to 1300 MHz with the use of a double pass acousto-optic modulator (AOM), and the Raman pulse durations are controlled with additional switching AOMs. Since the Raman beams are generated from a single laser and an AOM, broadening of the Raman transitions due to a finite laser linewidth is negligible [18].

Following Raman cooling to the $|0\rangle|\downarrow\rangle$ state, but before application of the CN operation, we apply appropriately

Introduction and Overview (Preskills Notes)

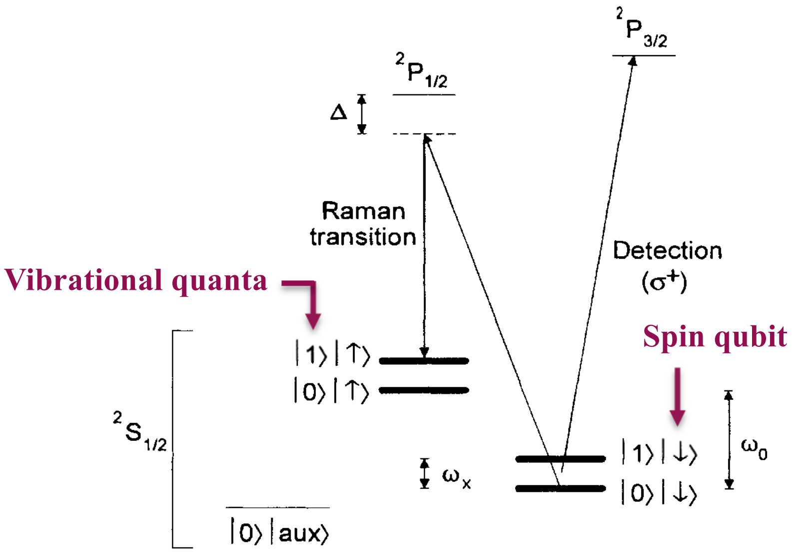

FIG. 1. ^{9}Be$^+$ energy levels. The levels indicated with thick lines form the basis of the quantum register: internal levels are $|S\rangle = |\downarrow\rangle$ and $|\uparrow\rangle$ ($^2S_{1/2}|F=2, m_F=2\rangle$ and $^2S_{1/2}|F=1, m_F=1\rangle$ levels, respectively, separated by $\omega_0/2\pi \simeq 1.250$ GHz), and $|\text{aux}\rangle = {}^2S_{1/2}|F=2, m_F=0\rangle$ (separated from $|\downarrow\rangle$ by $\simeq$2.5 MHz); external vibrational levels are $|n\rangle = |0\rangle$ and $|1\rangle$ (separated by $\omega_x/2\pi \simeq 11.2$ MHz). Stimulated Raman transitions between $^2S_{1/2}$ hyperfine states are driven through the virtual $^2P_{1/2}$ level ($\Delta \simeq 50$ GHz) with a pair of $\simeq$313 nm laser beams. Measurement of S is accomplished by driving the cycling $|\downarrow\rangle \rightarrow {}^2P_{3/2}|F=3, m_F=3\rangle$ transition with σ^+-polarized light and detecting the resulting ion fluorescence.

according to the following format:

(a) A $\pi/2$ pulse is applied on the carrier transition. The effect is described by the operator $V^{1/2}(\pi/2)$ in the notation of Ref. [1].

(b) A 2π pulse is applied on the blue sideband transition between $|\uparrow\rangle$ and an auxiliary atomic level $|\text{aux}\rangle$ (see Fig. 1). (1)

(c) A $\pi/2$ pulse is applied on the carrier transition, with a π phase shift relative to (a), leading to the operator $V^{1/2}(-\pi/2)$ of Ref. [1].

is as follows:

$$\begin{array}{ccc} \text{Input state} & \longrightarrow & \text{Output state} \\ |0\rangle|\downarrow\rangle & \longrightarrow & |0\rangle|\downarrow\rangle \\ |0\rangle|\uparrow\rangle & \longrightarrow & |0\rangle|\uparrow\rangle \\ |1\rangle|\downarrow\rangle & \longrightarrow & |1\rangle|\uparrow\rangle \\ |1\rangle|\uparrow\rangle & \longrightarrow & |1\rangle|\downarrow\rangle . \end{array} \tag{2}$$

The experiment apparatus is described elsewhere [16,17]. A single ^{9}Be$^+$ ion is stored in a coaxial-resonator rf-ion trap [17], which provides pseudopotential oscillation frequencies of $(\omega_x, \omega_y, \omega_z)/2\pi \simeq (11.2, 18.2, 29.8)$ MHz along the principal axes of the trap. We cool the ion so that the $n_x = 0$ vibrational ground state is occupied $\simeq$95% of the time by employing resolved-sideband stimulated Raman cooling in the x dimension, exactly as in Ref. [16]. The two Raman beams each contain $\simeq$1 mW of power at $\simeq$313 nm and are detuned $\simeq$50 GHz red of the $^2P_{1/2}$ excited state. The Raman beams are applied to the ion in directions such that their wave-vector difference $\boldsymbol{\delta}\mathbf{k}$ points nearly along the x axis of the trap; thus the Raman transitions are highly insensitive to motion in the other two dimensions. The Lamb-Dicke parameter is $\eta_x = \delta k\, x_0 \simeq 0.2$, where $x_0 \simeq 7$ nm is the spread of the $n_x = 0$ wave function. The carrier ($|n\rangle|\downarrow\rangle \rightarrow |n\rangle|\uparrow\rangle$) Rabi frequency is $\Omega_0 2\pi \simeq 140$ kHz, the red ($|1\rangle|\downarrow\rangle \rightarrow |0\rangle|\uparrow\rangle$) and blue ($|0\rangle|\downarrow\rangle \rightarrow |1\rangle|\uparrow\rangle$) sideband Rabi frequencies are $\eta_x\Omega_0/2\pi \simeq 30$ kHz, and the auxiliary transition ($|1\rangle|\uparrow\rangle \rightarrow |0\rangle|\downarrow\rangle$) Rabi frequency is $\eta_x\Omega_{\text{aux}}/2\pi \simeq 12$ kHz. The difference frequency of the Raman beams is tunable from 1200 to 1300 MHz with the use of a double pass acousto-optic modulator (AOM), and the Raman pulse durations are controlled with additional switching AOMs. Since the Raman beams are generated from a single laser and an AOM, broadening of the Raman transitions due to a finite laser linewidth is negligible [18].

Following Raman cooling to the $|0\rangle|\downarrow\rangle$ state, but before application of the CN operation, we apply appropriately

Introduction and Overview (Preskills Notes)

9-10-2024

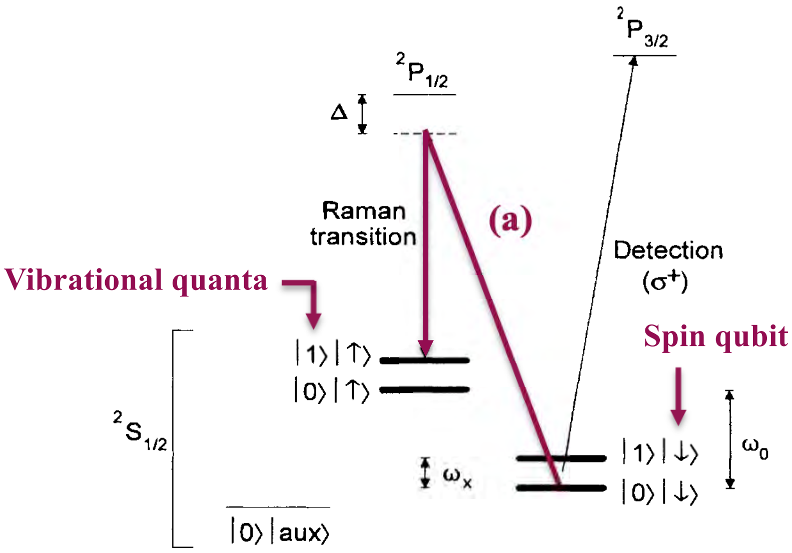

FIG. 1. $^9\text{Be}^+$ energy levels. The levels indicated with thick lines form the basis of the quantum register: internal levels are $|S\rangle = |\downarrow\rangle$ and $|\uparrow\rangle$ ($^2S_{1/2}|F = 2, m_F = 2\rangle$ and $^2S_{1/2}|F = 1, m_F = 1\rangle$ levels, respectively, separated by $\omega_0/2\pi \simeq 1.250$ GHz), and $|\text{aux}\rangle = {}^2S_{1/2}|F = 2, m_F = 0\rangle$ (separated from $|\downarrow\rangle$ by $\simeq$2.5 MHz); external vibrational levels are $|n\rangle = |0\rangle$ and $|1\rangle$ (separated by $\omega_x/2\pi \simeq 11.2$ MHz). Stimulated Raman transitions between $^2S_{1/2}$ hyperfine states are driven through the virtual $^2P_{1/2}$ level ($\Delta \simeq 50$ GHz) with a pair of $\simeq$313 nm laser beams. Measurement of S is accomplished by driving the cycling $|\downarrow\rangle \rightarrow {}^2P_{3/2}|F = 3, m_F = 3\rangle$ transition with σ^+-polarized light and detecting the resulting ion fluorescence.

according to the following format:

(a) A $\pi/2$ pulse is applied on the carrier transition. The effect is described by the operator $V^{1/2}(\pi/2)$ in the notation of Ref. [1].

(b) A 2π pulse is applied on the blue sideband transition between $|\uparrow\rangle$ and an auxiliary atomic level $|\text{aux}\rangle$ (see Fig. 1). (1)

(c) A $\pi/2$ pulse is applied on the carrier transition, with a π phase shift relative to (a), leading to the operator $V^{1/2}(-\pi/2)$ of Ref. [1].

is as follows:

$$\begin{array}{rcl} \text{Input state} & \longrightarrow & \text{Output state} \\ |0\rangle|\downarrow\rangle & \longrightarrow & |0\rangle|\downarrow\rangle \\ |0\rangle|\uparrow\rangle & \longrightarrow & |0\rangle|\uparrow\rangle \\ |1\rangle|\downarrow\rangle & \longrightarrow & |1\rangle|\uparrow\rangle \\ |1\rangle|\uparrow\rangle & \longrightarrow & |1\rangle|\downarrow\rangle . \end{array} \tag{2}$$

The experiment apparatus is described elsewhere [16,17]. A single $^9\text{Be}^+$ ion is stored in a coaxial-resonator rf-ion trap [17], which provides pseudopotential oscillation frequencies of $(\omega_x, \omega_y, \omega_z)/2\pi \simeq (11.2, 18.2, 29.8)$ MHz along the principal axes of the trap. We cool the ion so that the $n_x = 0$ vibrational ground state is occupied $\simeq$95% of the time by employing resolved-sideband stimulated Raman cooling in the x dimension, exactly as in Ref. [16]. The two Raman beams each contain $\simeq$1 mW of power at $\simeq$313 nm and are detuned $\simeq$50 GHz red of the $^2P_{1/2}$ excited state. The Raman beams are applied to the ion in directions such that their wave-vector difference $\boldsymbol{\delta}\mathbf{k}$ points nearly along the x axis of the trap; thus the Raman transitions are highly insensitive to motion in the other two dimensions. The Lamb-Dicke parameter is $\eta_x = \delta k\, x_0 \simeq 0.2$, where $x_0 \simeq 7$ nm is the spread of the $n_x = 0$ wave function. The carrier ($|n\rangle|\downarrow\rangle \longrightarrow |n\rangle|\uparrow\rangle$) Rabi frequency is $\Omega_0 2\pi \simeq 140$ kHz, the red ($|1\rangle|\downarrow\rangle \longrightarrow |0\rangle|\uparrow\rangle$) and blue ($|0\rangle|\downarrow\rangle \longrightarrow |1\rangle|\uparrow\rangle$) sideband Rabi frequencies are $\eta_x\Omega_0/2\pi \simeq 30$ kHz, and the auxiliary transition ($|1\rangle|\uparrow\rangle \longrightarrow |0\rangle|\downarrow\rangle$) Rabi frequency is $\eta_x\Omega_{\text{aux}}/2\pi \simeq 12$ kHz. The difference frequency of the Raman beams is tunable from 1200 to 1300 MHz with the use of a double pass acousto-optic modulator (AOM), and the Raman pulse durations are controlled with additional switching AOMs. Since the Raman beams are generated from a single laser and an AOM, broadening of the Raman transitions due to a finite laser linewidth is negligible [18].

Following Raman cooling to the $|0\rangle|\downarrow\rangle$ state, but before application of the CN operation, we apply appropriately

Introduction and Overview (Preskills Notes)

9-10-2024

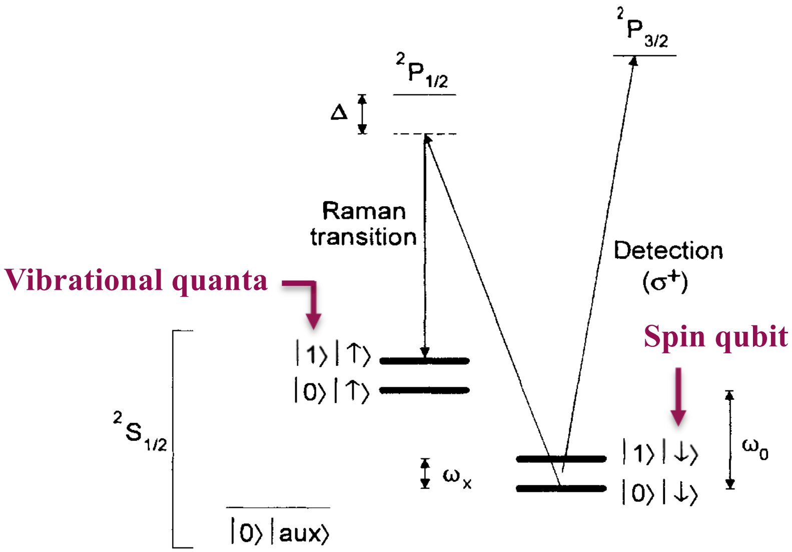

FIG. 1. ^{9}Be$^+$ energy levels. The levels indicated with thick lines form the basis of the quantum register: internal levels are $|S\rangle = |\downarrow\rangle$ and $|\uparrow\rangle$ ($^2S_{1/2}|F=2, m_F=2\rangle$ and $^2S_{1/2}|F=1, m_F=1\rangle$ levels, respectively, separated by $\omega_0/2\pi \simeq 1.250$ GHz), and $|\text{aux}\rangle = {}^2S_{1/2}|F=2, m_F=0\rangle$ (separated from $|\downarrow\rangle$ by $\simeq$2.5 MHz); external vibrational levels are $|n\rangle = |0\rangle$ and $|1\rangle$ (separated by $\omega_x/2\pi \simeq 11.2$ MHz). Stimulated Raman transitions between $^2S_{1/2}$ hyperfine states are driven through the virtual $^2P_{1/2}$ level ($\Delta \simeq 50$ GHz) with a pair of $\simeq$313 nm laser beams. Measurement of S is accomplished by driving the cycling $|\downarrow\rangle \to {}^2P_{3/2}|F=3, m_F=3\rangle$ transition with σ^+-polarized light and detecting the resulting ion fluorescence.

according to the following format:

(a) A $\pi/2$ pulse is applied on the carrier transition. The effect is described by the operator $V^{1/2}(\pi/2)$ in the notation of Ref. [1].

(b) A 2π pulse is applied on the blue sideband transition between $|\uparrow\rangle$ and an auxiliary atomic level $|\text{aux}\rangle$ (see Fig. 1). (1)

(c) A $\pi/2$ pulse is applied on the carrier transition, with a π phase shift relative to (a), leading to the operator $V^{1/2}(-\pi/2)$ of Ref. [1].

is as follows:

$$\begin{array}{rcl} \text{Input state} & \longrightarrow & \text{Output state} \\ |0\rangle|\downarrow\rangle & \longrightarrow & |0\rangle|\downarrow\rangle \\ |0\rangle|\uparrow\rangle & \longrightarrow & |0\rangle|\uparrow\rangle \\ |1\rangle|\downarrow\rangle & \longrightarrow & |1\rangle|\uparrow\rangle \\ |1\rangle|\uparrow\rangle & \longrightarrow & |1\rangle|\downarrow\rangle . \end{array} \qquad (2)$$

The experiment apparatus is described elsewhere [16,17]. A single ^{9}Be$^+$ ion is stored in a coaxial-resonator rf-ion trap [17], which provides pseudopotential oscillation frequencies of $(\omega_x, \omega_y, \omega_z)/2\pi \simeq (11.2, 18.2, 29.8)$ MHz along the principal axes of the trap. We cool the ion so that the $n_x = 0$ vibrational ground state is occupied $\simeq$95% of the time by employing resolved-sideband stimulated Raman cooling in the x dimension, exactly as in Ref. [16]. The two Raman beams each contain $\simeq$1 mW of power at $\simeq$313 nm and are detuned $\simeq$50 GHz red of the $^2P_{1/2}$ excited state. The Raman beams are applied to the ion in directions such that their wave-vector difference $\boldsymbol{\delta}\mathbf{k}$ points nearly along the x axis of the trap; thus the Raman transitions are highly insensitive to motion in the other two dimensions. The Lamb-Dicke parameter is $\eta_x = \delta k\, x_0 \simeq 0.2$, where $x_0 \simeq 7$ nm is the spread of the $n_x = 0$ wave function. The carrier ($|n\rangle|\downarrow\rangle \to |n\rangle|\uparrow\rangle$) Rabi frequency is $\Omega_0 2\pi \simeq 140$ kHz, the red ($|1\rangle|\downarrow\rangle \to |0\rangle|\uparrow\rangle$) and blue ($|0\rangle|\downarrow\rangle \to |1\rangle|\uparrow\rangle$) sideband Rabi frequencies are $\eta_x\Omega_0/2\pi \simeq 30$ kHz, and the auxiliary transition ($|1\rangle|\uparrow\rangle \to |0\rangle|\downarrow\rangle$) Rabi frequency is $\eta_x\Omega_{\text{aux}}/2\pi \simeq 12$ kHz. The difference frequency of the Raman beams is tunable from 1200 to 1300 MHz with the use of a double pass acousto-optic modulator (AOM), and the Raman pulse durations are controlled with additional switching AOMs. Since the Raman beams are generated from a single laser and an AOM, broadening of the Raman transitions due to a finite laser linewidth is negligible [18].

Following Raman cooling to the $|0\rangle|\downarrow\rangle$ state, but before application of the CN operation, we apply appropriately

Introduction and Overview (Preskills Notes)

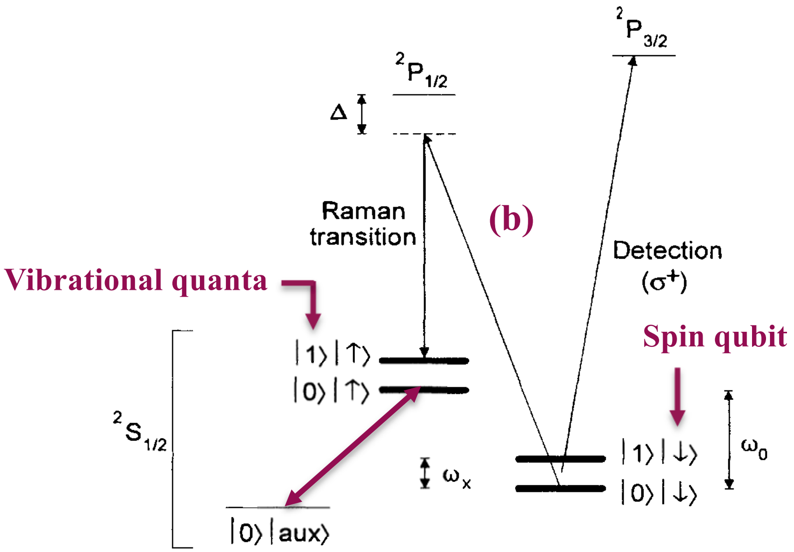

FIG. 1. $^9\text{Be}^+$ energy levels. The levels indicated with thick lines form the basis of the quantum register: internal levels are $|S\rangle = |\downarrow\rangle$ and $|\uparrow\rangle$ ($^2S_{1/2}|F=2, m_F=2\rangle$ and $^2S_{1/2}|F=1, m_F=1\rangle$ levels, respectively, separated by $\omega_0/2\pi \simeq 1.250$ GHz), and $|\text{aux}\rangle = {}^2S_{1/2}|F=2, m_F=0\rangle$ (separated from $|\downarrow\rangle$ by $\simeq 2.5$ MHz); external vibrational levels are $|n\rangle = |0\rangle$ and $|1\rangle$ (separated by $\omega_x/2\pi \simeq 11.2$ MHz). Stimulated Raman transitions between $^2S_{1/2}$ hyperfine states are driven through the virtual $^2P_{1/2}$ level ($\Delta \simeq 50$ GHz) with a pair of $\simeq 313$ nm laser beams. Measurement of S is accomplished by driving the cycling $|\downarrow\rangle \rightarrow {}^2P_{3/2}|F=3, m_F=3\rangle$ transition with σ^+-polarized light and detecting the resulting ion fluorescence.

according to the following format:

(a) A $\pi/2$ pulse is applied on the carrier transition. The effect is described by the operator $V^{1/2}(\pi/2)$ in the notation of Ref. [1].

(b) A 2π pulse is applied on the blue sideband transition between $|\uparrow\rangle$ and an auxiliary atomic level $|\text{aux}\rangle$ (see Fig. 1). (1)

(c) A $\pi/2$ pulse is applied on the carrier transition, with a π phase shift relative to (a), leading to the operator $V^{1/2}(-\pi/2)$ of Ref. [1].

is as follows:

$$\begin{array}{rcl} \text{Input state} & \longrightarrow & \text{Output state} \\ |0\rangle|\downarrow\rangle & \longrightarrow & |0\rangle|\downarrow\rangle \\ |0\rangle|\uparrow\rangle & \longrightarrow & |0\rangle|\uparrow\rangle \\ |1\rangle|\downarrow\rangle & \longrightarrow & |1\rangle|\uparrow\rangle \\ |1\rangle|\uparrow\rangle & \longrightarrow & |1\rangle|\downarrow\rangle . \end{array} \tag{2}$$

The experiment apparatus is described elsewhere [16,17]. A single $^9\text{Be}^+$ ion is stored in a coaxial-resonator rf-ion trap [17], which provides pseudopotential oscillation frequencies of $(\omega_x, \omega_y, \omega_z)/2\pi \simeq (11.2, 18.2, 29.8)$ MHz along the principal axes of the trap. We cool the ion so that the $n_x = 0$ vibrational ground state is occupied $\simeq 95\%$ of the time by employing resolved-sideband stimulated Raman cooling in the x dimension, exactly as in Ref. [16]. The two Raman beams each contain $\simeq 1$ mW of power at $\simeq 313$ nm and are detuned $\simeq 50$ GHz red of the $^2P_{1/2}$ excited state. The Raman beams are applied to the ion in directions such that their wave-vector difference $\boldsymbol{\delta k}$ points nearly along the x axis of the trap; thus the Raman transitions are highly insensitive to motion in the other two dimensions. The Lamb-Dicke parameter is $\eta_x = \delta k\, x_0 \simeq 0.2$, where $x_0 \simeq 7\,\text{nm}$ is the spread of the $n_x = 0$ wave function. The carrier ($|n\rangle|\downarrow\rangle \rightarrow |n\rangle|\uparrow\rangle$) Rabi frequency is $\Omega_0 2\pi \simeq 140$ kHz, the red ($|1\rangle|\downarrow\rangle \rightarrow |0\rangle|\uparrow\rangle$) and blue ($|0\rangle|\downarrow\rangle \rightarrow |1\rangle|\uparrow\rangle$) sideband Rabi frequencies are $\eta_x\Omega_0/2\pi \simeq 30$ kHz, and the auxiliary transition ($|1\rangle|\uparrow\rangle \rightarrow |0\rangle|\downarrow\rangle$) Rabi frequency is $\eta_x\Omega_{\text{aux}}/2\pi \simeq 12$ kHz. The difference frequency of the Raman beams is tunable from 1200 to 1300 MHz with the use of a double pass acousto-optic modulator (AOM), and the Raman pulse durations are controlled with additional switching AOMs. Since the Raman beams are generated from a single laser and an AOM, broadening of the Raman transitions due to a finite laser linewidth is negligible [18].

Following Raman cooling to the $|0\rangle|\downarrow\rangle$ state, but before application of the CN operation, we apply appropriately

Introduction and Overview (Preskills Notes)

9-10-2024

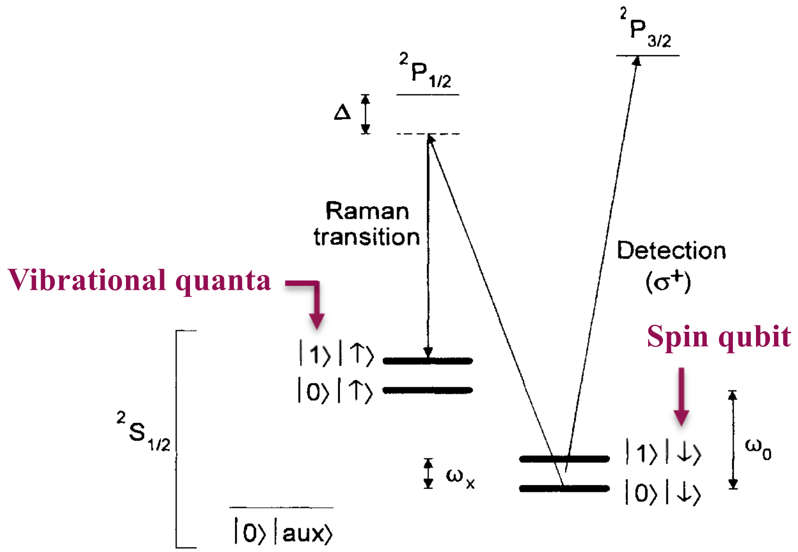

Vibrational quanta

Spin qubit

FIG. 1. ^{9}Be$^+$ energy levels. The levels indicated with thick lines form the basis of the quantum register: internal levels are $|S\rangle = |\downarrow\rangle$ and $|\uparrow\rangle$ ($^2S_{1/2}|F=2, m_F=2\rangle$ and $^2S_{1/2}|F=1, m_F=1\rangle$ levels, respectively, separated by $\omega_0/2\pi \simeq 1.250$ GHz), and $|\mathrm{aux}\rangle = {}^2S_{1/2}|F=2, m_F=0\rangle$ (separated from $|\downarrow\rangle$ by $\simeq$2.5 MHz); external vibrational levels are $|n\rangle = |0\rangle$ and $|1\rangle$ (separated by $\omega_x/2\pi \simeq 11.2$ MHz). Stimulated Raman transitions between $^2S_{1/2}$ hyperfine states are driven through the virtual $^2P_{1/2}$ level ($\Delta \simeq 50$ GHz) with a pair of $\simeq$313 nm laser beams. Measurement of S is accomplished by driving the cycling $|\downarrow\rangle \rightarrow {}^2P_{3/2}|F=3, m_F=3\rangle$ transition with σ^+-polarized light and detecting the resulting ion fluorescence.

according to the following format:

(a) A $\pi/2$ pulse is applied on the carrier transition. The effect is described by the operator $V^{1/2}(\pi/2)$ in the notation of Ref. [1].

(b) A 2π pulse is applied on the blue sideband transition between $|\uparrow\rangle$ and an auxiliary atomic level $|\mathrm{aux}\rangle$ (see Fig. 1). (1)

(c) A $\pi/2$ pulse is applied on the carrier transition, with a π phase shift relative to (a), leading to the operator $V^{1/2}(-\pi/2)$ of Ref. [1].

is as follows:

$$\begin{array}{rcl} \text{Input state} & \longrightarrow & \text{Output state} \\ |0\rangle|\downarrow\rangle & \longrightarrow & |0\rangle|\downarrow\rangle \\ |0\rangle|\uparrow\rangle & \longrightarrow & |0\rangle|\uparrow\rangle \\ |1\rangle|\downarrow\rangle & \longrightarrow & |1\rangle|\uparrow\rangle \\ |1\rangle|\uparrow\rangle & \longrightarrow & |1\rangle|\downarrow\rangle . \end{array} \tag{2}$$

The experiment apparatus is described elsewhere [16,17]. A single ^{9}Be$^+$ ion is stored in a coaxial-resonator rf-ion trap [17], which provides pseudopotential oscillation frequencies of $(\omega_x, \omega_y, \omega_z)/2\pi \simeq (11.2, 18.2, 29.8)$ MHz along the principal axes of the trap. We cool the ion so that the $n_x = 0$ vibrational ground state is occupied $\simeq$95% of the time by employing resolved-sideband stimulated Raman cooling in the x dimension, exactly as in Ref. [16]. The two Raman beams each contain $\simeq$1 mW of power at $\simeq$313 nm and are detuned $\simeq$50 GHz red of the $^2P_{1/2}$ excited state. The Raman beams are applied to the ion in directions such that their wave-vector difference $\boldsymbol{\delta}\mathbf{k}$ points nearly along the x axis of the trap; thus the Raman transitions are highly insensitive to motion in the other two dimensions. The Lamb-Dicke parameter is $\eta_x = \delta k\, x_0 \simeq 0.2$, where $x_0 \simeq 7\,\mathrm{nm}$ is the spread of the $n_x = 0$ wave function. The carrier ($|n\rangle|\downarrow\rangle \rightarrow |n\rangle|\uparrow\rangle$) Rabi frequency is $\Omega_0 2\pi \simeq 140$ kHz, the red ($|1\rangle|\downarrow\rangle \rightarrow |0\rangle|\uparrow\rangle$) and blue ($|0\rangle|\downarrow\rangle \rightarrow |1\rangle|\uparrow\rangle$) sideband Rabi frequencies are $\eta_x\Omega_0/2\pi \simeq 30$ kHz, and the auxiliary transition ($|1\rangle|\uparrow\rangle \rightarrow |0\rangle|\downarrow\rangle$) Rabi frequency is $\eta_x\Omega_{\mathrm{aux}}/2\pi \simeq 12$ kHz. The difference frequency of the Raman beams is tunable from 1200 to 1300 MHz with the use of a double pass acousto-optic modulator (AOM), and the Raman pulse durations are controlled with additional switching AOMs. Since the Raman beams are generated from a single laser and an AOM, broadening of the Raman transitions due to a finite laser linewidth is negligible [18].

Following Raman cooling to the $|0\rangle|\downarrow\rangle$ state, but before application of the CN operation, we apply appropriately

Introduction and Overview (Preskills Notes)

9-10-2024

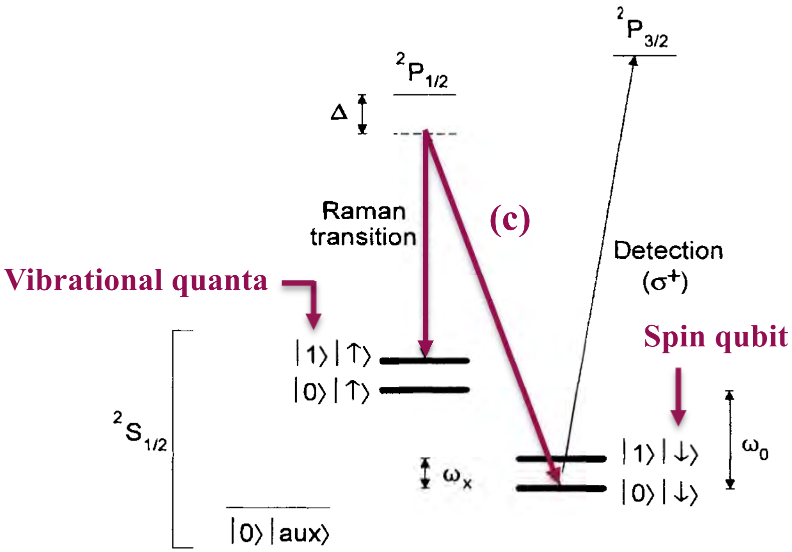

FIG. 1. $^9\text{Be}^+$ energy levels. The levels indicated with thick lines form the basis of the quantum register: internal levels are $|S\rangle = |\downarrow\rangle$ and $|\uparrow\rangle$ ($^2S_{1/2}|F=2, m_F=2\rangle$ and $^2S_{1/2}|F=1, m_F=1\rangle$ levels, respectively, separated by $\omega_0/2\pi \simeq 1.250$ GHz), and $|\text{aux}\rangle = {}^2S_{1/2}|F=2, m_F=0\rangle$ (separated from $|\downarrow\rangle$ by $\simeq$2.5 MHz); external vibrational levels are $|n\rangle = |0\rangle$ and $|1\rangle$ (separated by $\omega_x/2\pi \simeq 11.2$ MHz). Stimulated Raman transitions between $^2S_{1/2}$ hyperfine states are driven through the virtual $^2P_{1/2}$ level ($\Delta \simeq 50$ GHz) with a pair of $\simeq$313 nm laser beams. Measurement of S is accomplished by driving the cycling $|\downarrow\rangle \rightarrow {}^2P_{3/2}|F=3, m_F=3\rangle$ transition with σ^+-polarized light and detecting the resulting ion fluorescence.

according to the following format:

(a) A $\pi/2$ pulse is applied on the carrier transition. The effect is described by the operator $V^{1/2}(\pi/2)$ in the notation of Ref. [1].

(b) A 2π pulse is applied on the blue sideband transition between $|\uparrow\rangle$ and an auxiliary atomic level $|\text{aux}\rangle$ (see Fig. 1). (1)

(c) A $\pi/2$ pulse is applied on the carrier transition, with a π phase shift relative to (a), leading to the operator $V^{1/2}(-\pi/2)$ of Ref. [1].

is as follows:

$$\begin{array}{rcl} \text{Input state} & \longrightarrow & \text{Output state} \\ |0\rangle|\downarrow\rangle & \longrightarrow & |0\rangle|\downarrow\rangle \\ |0\rangle|\uparrow\rangle & \longrightarrow & |0\rangle|\uparrow\rangle \\ |1\rangle|\downarrow\rangle & \longrightarrow & |1\rangle|\uparrow\rangle \\ |1\rangle|\uparrow\rangle & \longrightarrow & |1\rangle|\downarrow\rangle . \end{array} \qquad (2)$$

The experiment apparatus is described elsewhere [16,17]. A single $^9\text{Be}^+$ ion is stored in a coaxial-resonator rf-ion trap [17], which provides pseudopotential oscillation frequencies of $(\omega_x, \omega_y, \omega_z)/2\pi \simeq (11.2, 18.2, 29.8)$ MHz along the principal axes of the trap. We cool the ion so that the $n_x = 0$ vibrational ground state is occupied $\simeq$95% of the time by employing resolved-sideband stimulated Raman cooling in the x dimension, exactly as in Ref. [16]. The two Raman beams each contain $\simeq$1 mW of power at $\simeq$313 nm and are detuned $\simeq$50 GHz red of the $^2P_{1/2}$ excited state. The Raman beams are applied to the ion in directions such that their wave-vector difference $\boldsymbol{\delta}\mathbf{k}$ points nearly along the x axis of the trap; thus the Raman transitions are highly insensitive to motion in the other two dimensions. The Lamb-Dicke parameter is $\eta_x = \delta k\, x_0 \simeq 0.2$, where $x_0 \simeq 7\,\text{nm}$ is the spread of the $n_x = 0$ wave function. The carrier $(|n\rangle|\downarrow\rangle \longrightarrow |n\rangle|\uparrow\rangle)$ Rabi frequency is $\Omega_0 2\pi \simeq 140$ kHz, the red $(|1\rangle|\downarrow\rangle \longrightarrow |0\rangle|\uparrow\rangle)$ and blue $(|0\rangle|\downarrow\rangle \longrightarrow |1\rangle|\uparrow\rangle)$ sideband Rabi frequencies are $\eta_x\Omega_0/2\pi \simeq 30$ kHz, and the auxiliary transition $(|1\rangle|\uparrow\rangle \longrightarrow |0\rangle|\downarrow\rangle)$ Rabi frequency is $\eta_x\Omega_{\text{aux}}/2\pi \simeq 12$ kHz. The difference frequency of the Raman beams is tunable from 1200 to 1300 MHz with the use of a double pass acousto-optic modulator (AOM), and the Raman pulse durations are controlled with additional switching AOMs. Since the Raman beams are generated from a single laser and an AOM, broadening of the Raman transitions due to a finite laser linewidth is negligible [18].

Following Raman cooling to the $|0\rangle|\downarrow\rangle$ state, but before application of the CN operation, we apply appropriately

Introduction and Overview (Preskills Notes)

9-10-2024

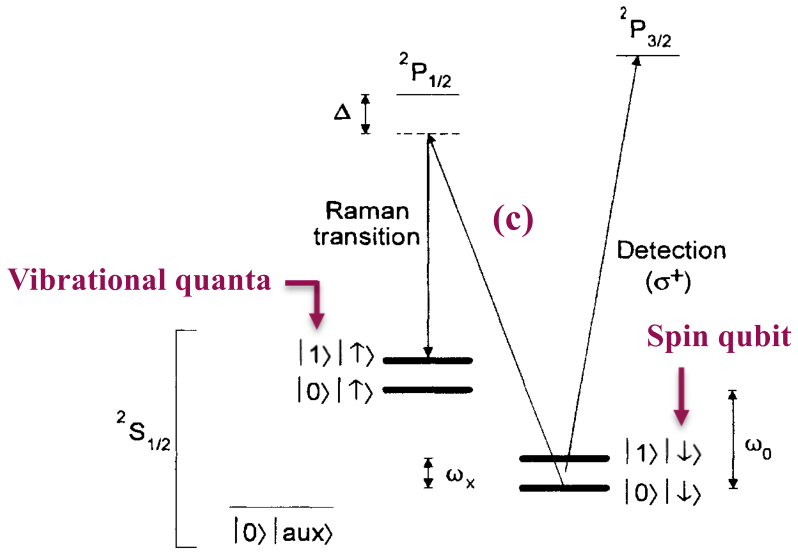

FIG. 1. $^9\mathrm{Be}^+$ energy levels. The levels indicated with thick lines form the basis of the quantum register: internal levels are $|S\rangle = |\downarrow\rangle$ and $|\uparrow\rangle$ ($^2S_{1/2}|F = 2, m_F = 2\rangle$ and $^2S_{1/2}|F = 1, m_F = 1\rangle$ levels, respectively, separated by $\omega_0/2\pi \simeq 1.250$ GHz), and $|\mathrm{aux}\rangle = {}^2S_{1/2}|F = 2, m_F = 0\rangle$ (separated from $|\downarrow\rangle$ by $\simeq$2.5 MHz); external vibrational levels are $|n\rangle = |0\rangle$ and $|1\rangle$ (separated by $\omega_x/2\pi \simeq 11.2$ MHz). Stimulated Raman transitions between $^2S_{1/2}$ hyperfine states are driven through the virtual $^2P_{1/2}$ level ($\Delta \simeq 50$ GHz) with a pair of $\simeq$313 nm laser beams. Measurement of S is accomplished by driving the cycling $|\downarrow\rangle \rightarrow {}^2P_{3/2}|F = 3, m_F = 3\rangle$ transition with σ^+-polarized light and detecting the resulting ion fluorescence.

according to the following format:

(a) A $\pi/2$ pulse is applied on the carrier transition. The effect is described by the operator $V^{1/2}(\pi/2)$ in the notation of Ref. [1].

(b) A 2π pulse is applied on the blue sideband transition between $|\uparrow\rangle$ and an auxiliary atomic level $|\mathrm{aux}\rangle$ (see Fig. 1). (1)

(c) A $\pi/2$ pulse is applied on the carrier transition, with a π phase shift relative to (a), leading to the operator $V^{1/2}(-\pi/2)$ of Ref. [1].

is as follows:

$$\begin{array}{rcl} \text{Input state} & \longrightarrow & \text{Output state} \\ |0\rangle|\downarrow\rangle & \longrightarrow & |0\rangle|\downarrow\rangle \\ |0\rangle|\uparrow\rangle & \longrightarrow & |0\rangle|\uparrow\rangle \\ |1\rangle|\downarrow\rangle & \longrightarrow & |1\rangle|\uparrow\rangle \\ |1\rangle|\uparrow\rangle & \longrightarrow & |1\rangle|\downarrow\rangle . \end{array} \tag{2}$$

The experiment apparatus is described elsewhere [16,17]. A single $^9\mathrm{Be}^+$ ion is stored in a coaxial-resonator rf-ion trap [17], which provides pseudopotential oscillation frequencies of $(\omega_x, \omega_y, \omega_z)/2\pi \simeq (11.2, 18.2, 29.8)$ MHz along the principal axes of the trap. We cool the ion so that the $n_x = 0$ vibrational ground state is occupied $\simeq$95% of the time by employing resolved-sideband stimulated Raman cooling in the x dimension, exactly as in Ref. [16]. The two Raman beams each contain $\simeq$1 mW of power at $\simeq$313 nm and are detuned $\simeq$50 GHz red of the $^2P_{1/2}$ excited state. The Raman beams are applied to the ion in directions such that their wave-vector difference $\boldsymbol{\delta}\mathbf{k}$ points nearly along the x axis of the trap; thus the Raman transitions are highly insensitive to motion in the other two dimensions. The Lamb-Dicke parameter is $\eta_x = \delta k\, x_0 \simeq 0.2$, where $x_0 \simeq 7$ nm is the spread of the $n_x = 0$ wave function. The carrier ($|n\rangle|\downarrow\rangle \rightarrow |n\rangle|\uparrow\rangle$) Rabi frequency is $\Omega_0 2\pi \simeq 140$ kHz, the red ($|1\rangle|\downarrow\rangle \rightarrow |0\rangle|\uparrow\rangle$) and blue ($|0\rangle|\downarrow\rangle \rightarrow |1\rangle|\uparrow\rangle$) sideband Rabi frequencies are $\eta_x\Omega_0/2\pi \simeq 30$ kHz, and the auxiliary transition ($|1\rangle|\uparrow\rangle \rightarrow |0\rangle|\downarrow\rangle$) Rabi frequency is $\eta_x\Omega_{\mathrm{aux}}/2\pi \simeq 12$ kHz. The difference frequency of the Raman beams is tunable from 1200 to 1300 MHz with the use of a double pass acousto-optic modulator (AOM), and the Raman pulse durations are controlled with additional switching AOMs. Since the Raman beams are generated from a single laser and an AOM, broadening of the Raman transitions due to a finite laser linewidth is negligible [18].

Following Raman cooling to the $|0\rangle|\downarrow\rangle$ state, but before application of the CN operation, we apply appropriately

Introduction and Overview (Preskills Notes)

9-10-2024

Some Benchmarks for Ion Traps

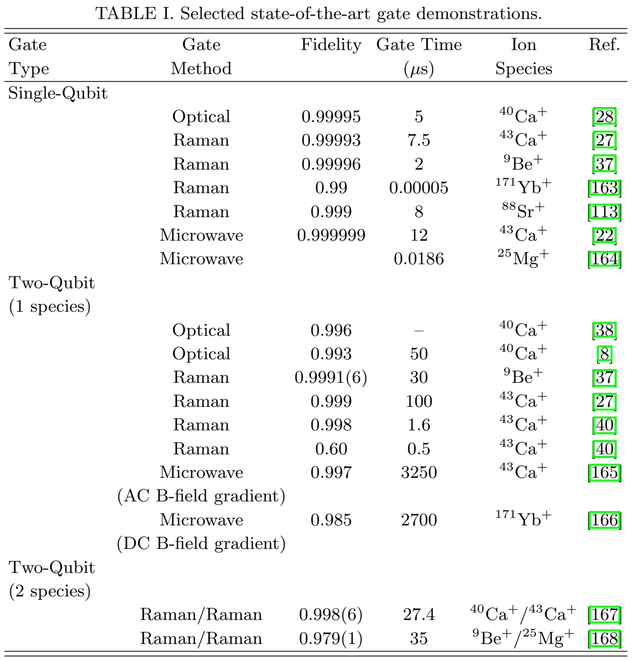

TABLE I. Selected state-of-the-art gate demonstrations.

Gate Type	Gate Method	Fidelity	Gate Time (μs)	Ion Species	Ref.
Single-Qubit					
	Optical	0.99995	5	^{40}Ca$^+$	[28]
	Raman	0.99993	7.5	^{43}Ca$^+$	[27]
	Raman	0.99996	2	^{9}Be$^+$	[37]
	Raman	0.99	0.00005	^{171}Yb$^+$	[163]
	Raman	0.999	8	^{88}Sr$^+$	[113]
	Microwave	0.999999	12	^{43}Ca$^+$	[22]
	Microwave		0.0186	^{25}Mg$^+$	[164]
Two-Qubit (1 species)					
	Optical	0.996	–	^{40}Ca$^+$	[38]
	Optical	0.993	50	^{40}Ca$^+$	[8]
	Raman	0.9991(6)	30	^{9}Be$^+$	[37]
	Raman	0.999	100	^{43}Ca$^+$	[27]
	Raman	0.998	1.6	^{43}Ca$^+$	[40]
	Raman	0.60	0.5	^{43}Ca$^+$	[40]
	Microwave (AC B-field gradient)	0.997	3250	^{43}Ca$^+$	[165]
	Microwave (DC B-field gradient)	0.985	2700	^{171}Yb$^+$	[166]
Two-Qubit (2 species)					
	Raman/Raman	0.998(6)	27.4	^{40}Ca$^+$/^{43}Ca$^+$	[167]
	Raman/Raman	0.979(1)	35	^{9}Be$^+$/^{25}Mg$^+$	[168]

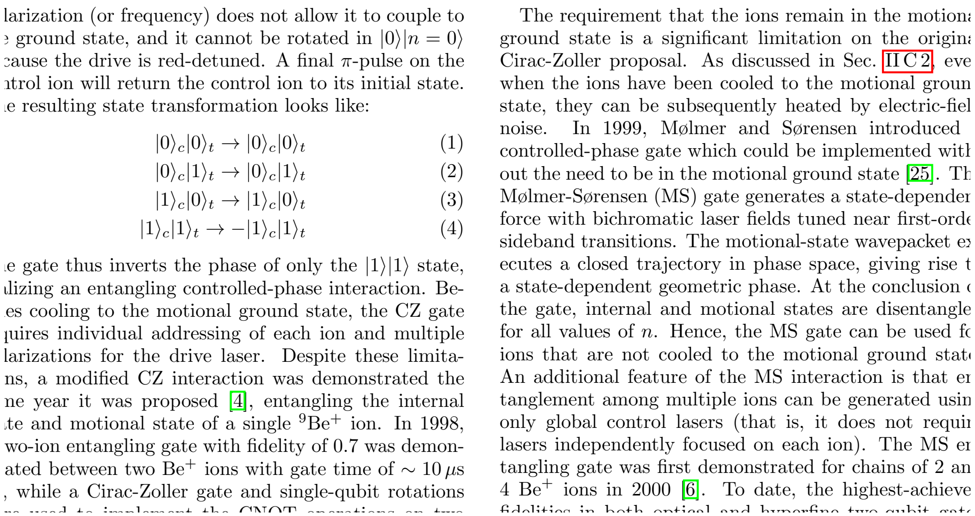

larization (or frequency) does not allow it to couple to
ground state, and it cannot be rotated in $|0\rangle|n=0\rangle$
cause the drive is red-detuned. A final π-pulse on the
ntrol ion will return the control ion to its initial state.
e resulting state transformation looks like:

$$|0\rangle_c|0\rangle_t \rightarrow |0\rangle_c|0\rangle_t \quad (1)$$

$$|0\rangle_c|1\rangle_t \rightarrow |0\rangle_c|1\rangle_t \quad (2)$$

$$|1\rangle_c|0\rangle_t \rightarrow |1\rangle_c|0\rangle_t \quad (3)$$

$$|1\rangle_c|1\rangle_t \rightarrow -|1\rangle_c|1\rangle_t \quad (4)$$

e gate thus inverts the phase of only the $|1\rangle|1\rangle$ state,
lizing an entangling controlled-phase interaction. Be-
es cooling to the motional ground state, the CZ gate
quires individual addressing of each ion and multiple
larizations for the drive laser. Despite these limita-
ns, a modified CZ interaction was demonstrated the
ne year it was proposed [4], entangling the internal
te and motional state of a single ^{9}Be$^+$ ion. In 1998,
wo-ion entangling gate with fidelity of 0.7 was demon-
ated between two Be$^+$ ions with gate time of $\sim 10\,\mu s$
, while a Cirac-Zoller gate and single-qubit rotations

The requirement that the ions remain in the motiona
ground state is a significant limitation on the origina
Cirac-Zoller proposal. As discussed in Sec. II C 2, eve
when the ions have been cooled to the motional groun
state, they can be subsequently heated by electric-fiel
noise. In 1999, Mølmer and Sørensen introduced
controlled-phase gate which could be implemented witl
out the need to be in the motional ground state [25]. Tl
Mølmer-Sørensen (MS) gate generates a state-depender
force with bichromatic laser fields tuned near first-ord
sideband transitions. The motional-state wavepacket e
ecutes a closed trajectory in phase space, giving rise t
a state-dependent geometric phase. At the conclusion
the gate, internal and motional states are disentangle
for all values of n. Hence, the MS gate can be used f
ions that are not cooled to the motional ground stat
An additional feature of the MS interaction is that e
tanglement among multiple ions can be generated usin
only global control lasers (that is, it does not requi
lasers independently focused on each ion). The MS e
tangling gate was first demonstrated for chains of 2 an
4 Be$^+$ ions in 2000 [6]. To date, the highest-achieve

Some links to get started

Amazon Braket (IonQ, other Technologies)
https://aws.amazon.com/braket/

Quantinuum (Ion Trap Quantum Computing
https://www.quantinuum.com

IonQ https://ionq.com

NIST https://www.nist.gov/pml/time-and-frequency-division/ion-storage

Challenge: Do a web search and look for the largest GHZ state made in the lab

$$|GHZ\rangle = \frac{1}{\sqrt{N}}\left(|00\ldots00\rangle + |11\ldots11\rangle\right)$$

Note: What is the fidelity of the state ?

Introduction and Overview (Preskills Notes)

9-10-2024

Neutral Atom based Quantum Processors

Optical tweezer array

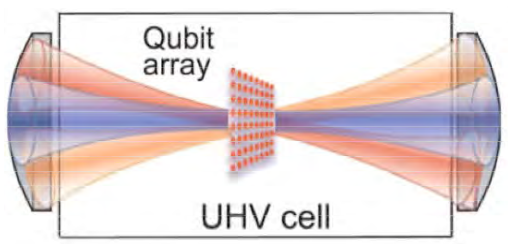

Fluorescing atoms

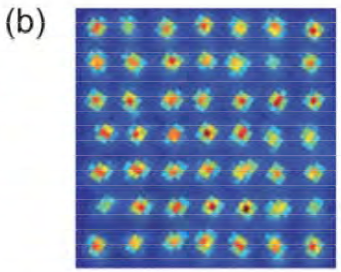

- Large numbers of non-interacting qubits, (~ 256) trapped in 2D or 3D arrays.
- Qubits interact when excited into Rydberg states with large dipole moments
- Major advantage: Weak coupling to the environment when not doing gates
  ⇨ excellent quantum memory
- Favorite platform for quantum simulation of quantum manybody physics
- BEC's in optical lattices as analog simulators of superconductivity, quantum magnetism and more

2-photon transition to a Rydberg state

Linear Trap Array

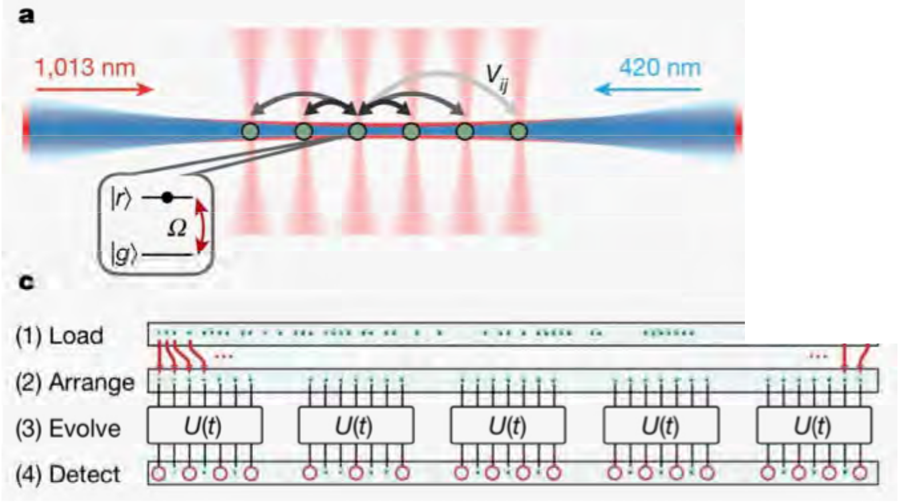

Sorted into groups of *n*

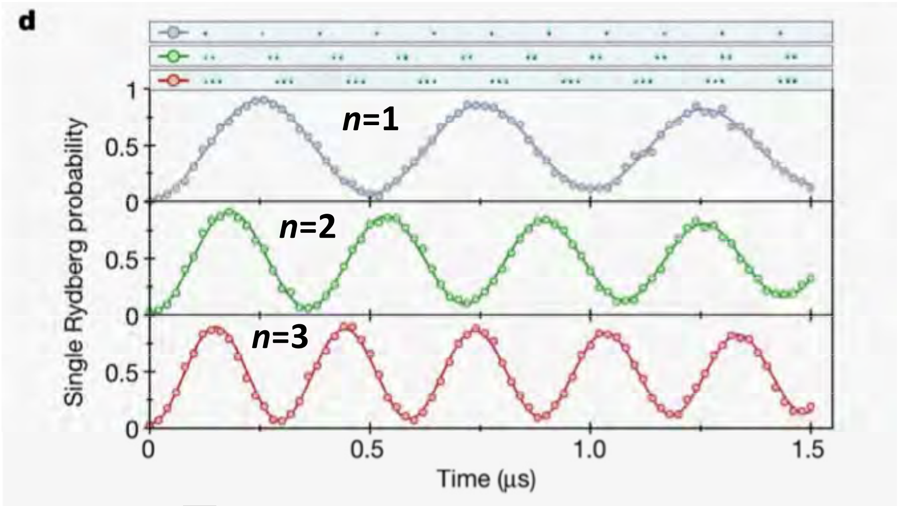

$\sqrt{n}$ enhancement of Rabi frequency

Introduction and Overview (Preskills Notes)

9-10-2024

Linear Trap Array

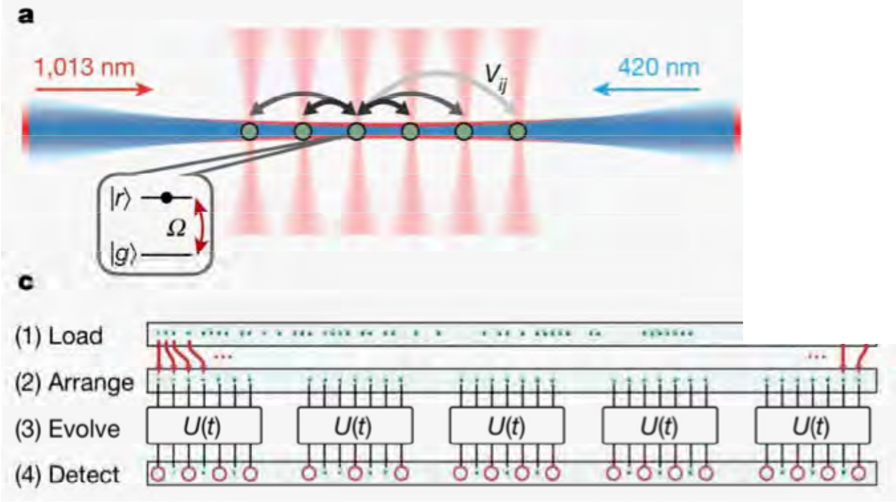

Sorted into groups of *n*

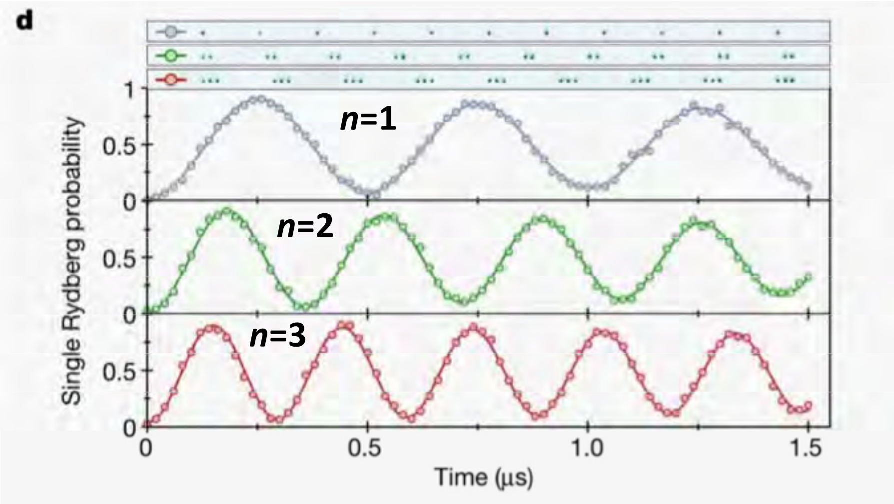

$\sqrt{n}$ enhancement of Rabi frequency

Rydberg Blockade

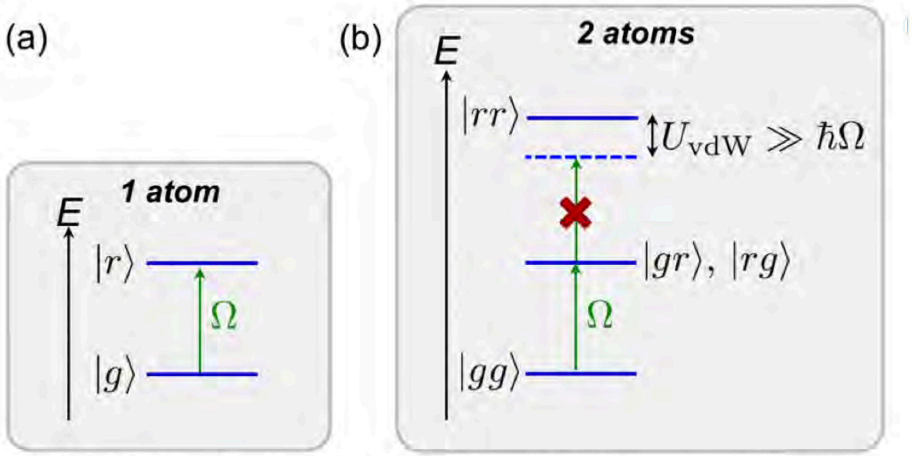

Principle of the Rydberg blockade. (a) A resonant laser couples, with strength Ω, the Rydberg state |r and the ground state |g of an atom. (b) For two nearby atoms, interactions U vdW shift the doubly excited state |rr, preventing the double excitation of the atom pair when U vdW Ω.

Controlled-Phase Gate

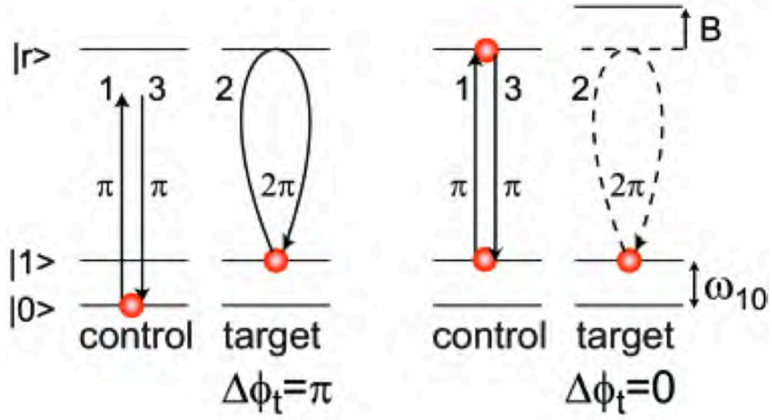

π phase shift of Target conditioned on Control

Introduction and Overview (Preskills Notes)

Rydberg Blockade

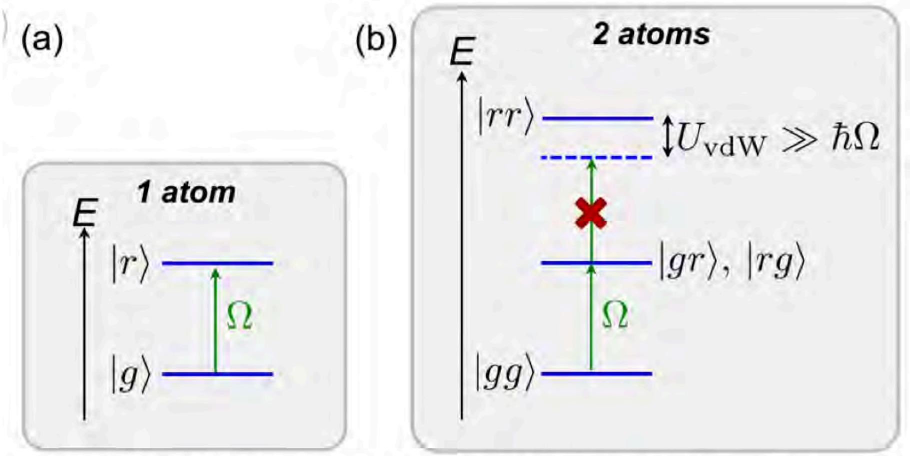

Principle of the Rydberg blockade. (a) A resonant laser couples, with strength Ω, the Rydberg state |r and the ground state |g of an atom. (b) For two nearby atoms, interactions U vdW shift the doubly excited state |rr, preventing the double excitation of the atom pair when U vdW Ω.

Controlled-Phase Gate

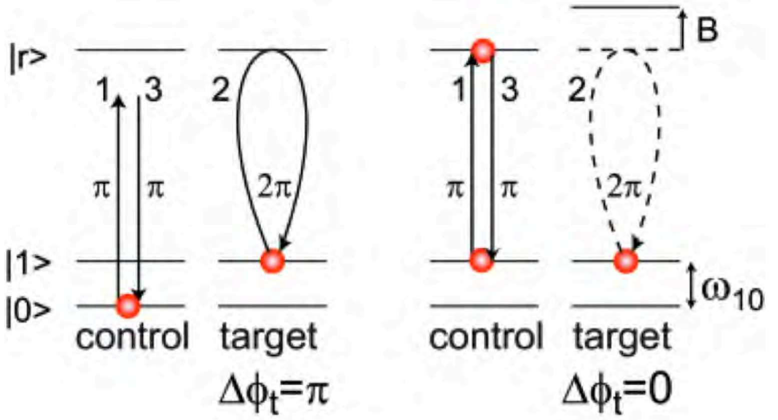

π phase shift of Target conditioned on Control

Some links to get started

QuEra https://www.quera.com/aquila

Cold Quanta https://coldquanta.com

Sandia, Los Alamos National Labs

Individual PI's – Quantum Simulation

Lukin, Vuletic, Greiner, Endres, Bloch, Saffman, Biederman, Browaeys, Weiss, and many, many others…

9-10-2024

Introduction and Overview (Preskills Notes)

Superconducting Qubits

- The basic building block is the so-called Transmon Qubit
- A Transmon is a nonlinear oscillator made from a Josephson Junction and other circuit elements

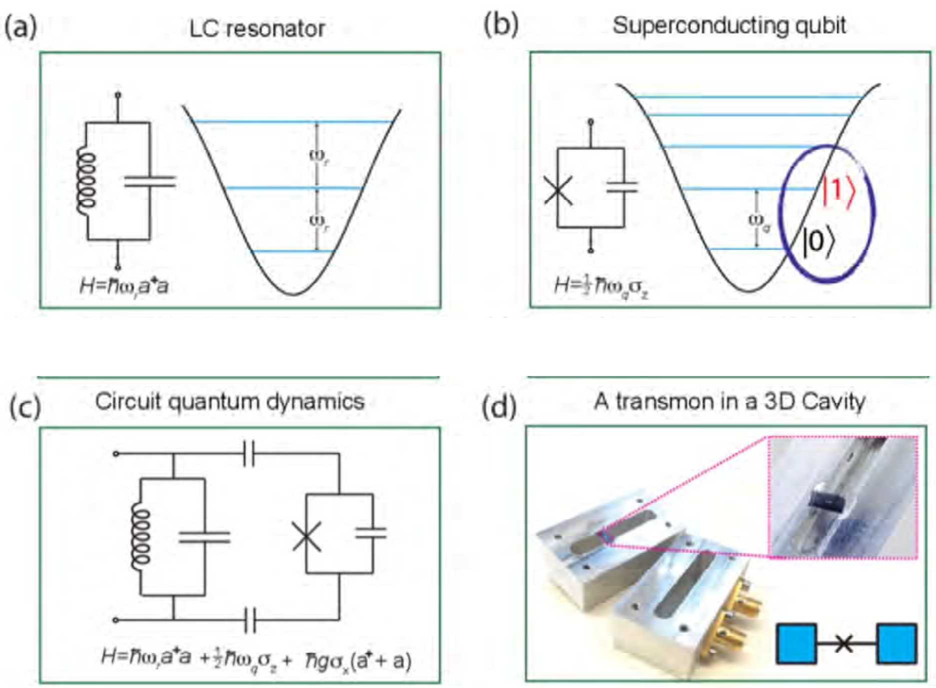

Jaynes-Cummings Hamiltonian

Superconducting Qubits

IBM 4–Transmon device (2017)

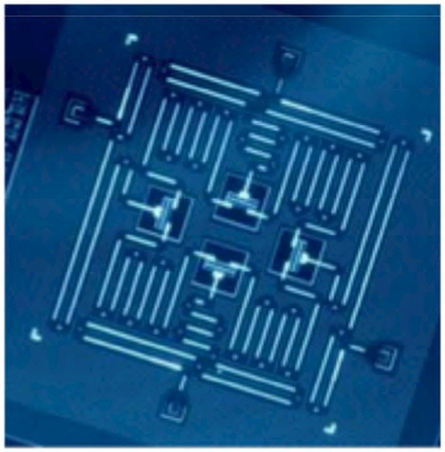

A device consisting of four transmon qubits, four quantum busses, and four readout resonators fabricated by IBM and published in npj Quantum Information in January 2017.[4]

Google 54–Transmon device (2019)

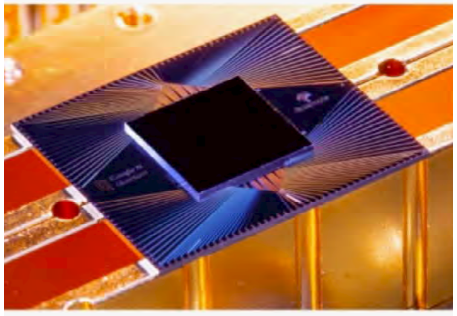

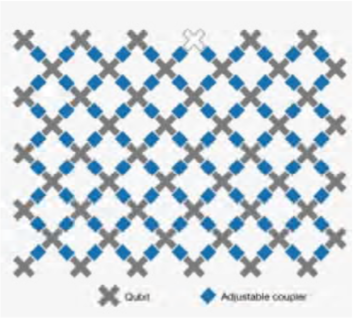

Introduction and Overview (Preskills Notes)

Superconducting Qubits

IBM 4–Transmon device (2017)

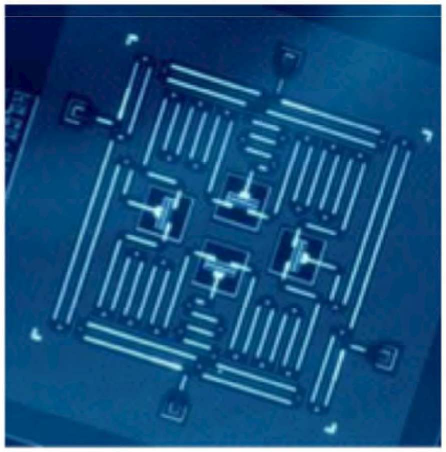

A device consisting of four transmon qubits, four quantum busses, and four readout resonators fabricated by IBM and published in npj Quantum Information in January 2017.[4]

Google 54–Transmon device (2019)

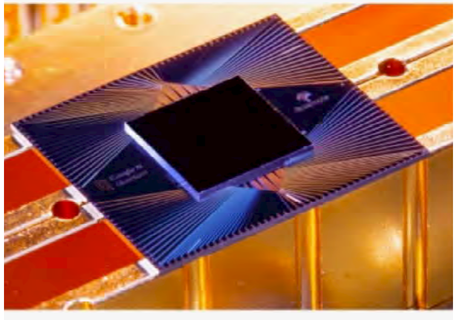

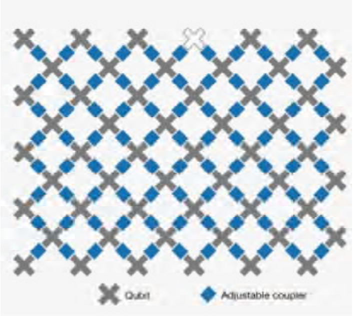

Advantages

- Solid State platform, looks like electronics
- Clearer path to scale up to many qubits?

Challenges

- Gates, coherence times not as good as atomic platforms, but gap is closing
- Requires dilution refrigerator

Industry Favorite

- Large efforts at IBM, Google, Rigetti

  ↑

  Cloud Quantum Computing

- **Amazon Braket** (IonQ, other Technology)

  https://aws.amazon.com/braket/

Introduction and Overview (Preskills Notes)

9-12-2024

Spins in Silicon Quantum Dots

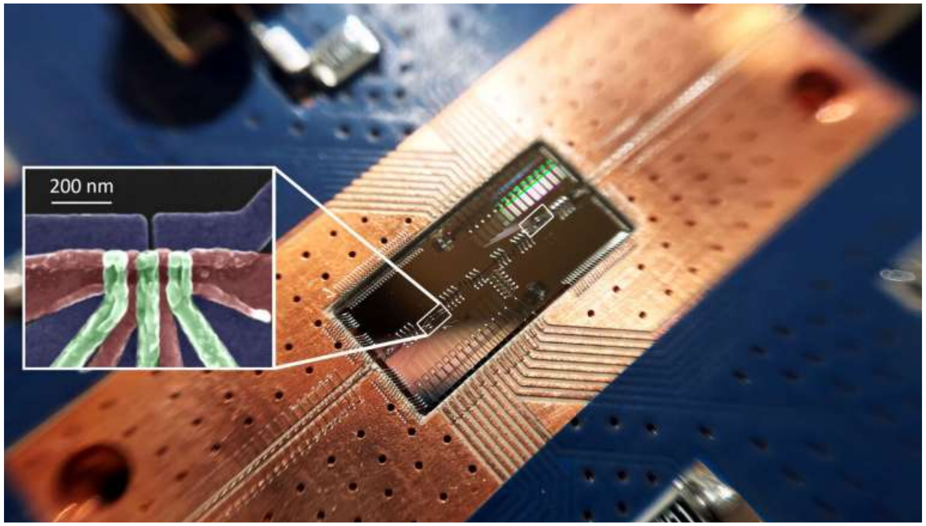

Introduction and Overview (Preskills Notes)

Spins in Silicon Quantum Dots

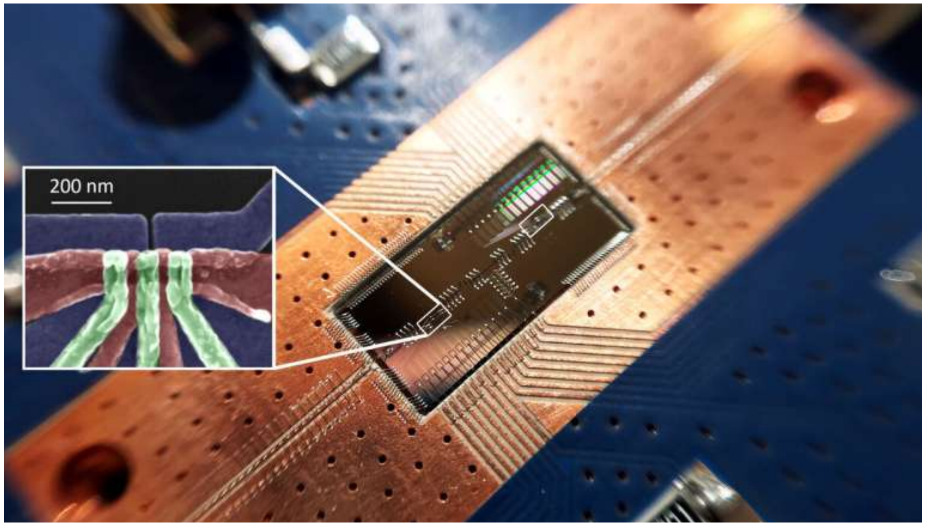

- Si is highly scalable

Introduction and Overview (Preskills Notes)

9-12-2024

Spins in Silicon Quantum Dots

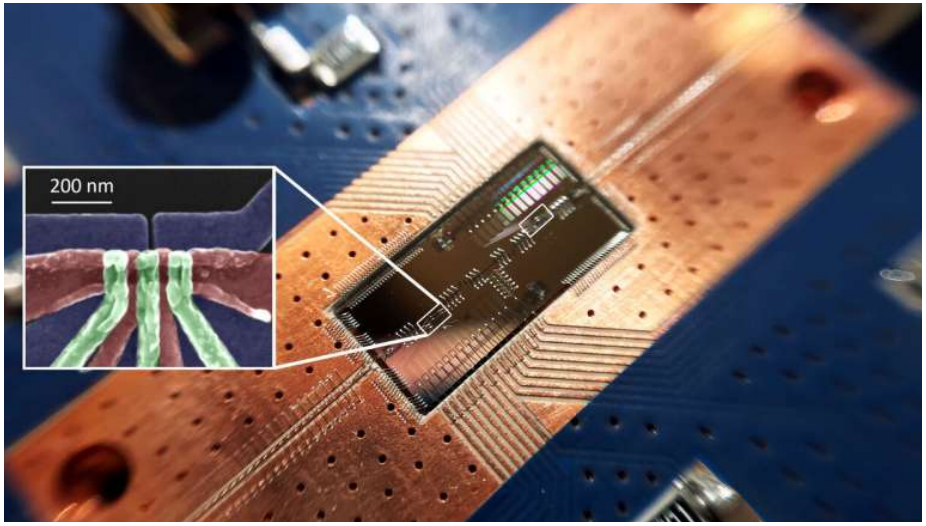

- Si is highly scalable
- Qubits and Quantum Gates demonstrated

Introduction and Overview (Preskills Notes)

Spins in Silicon Quantum Dots

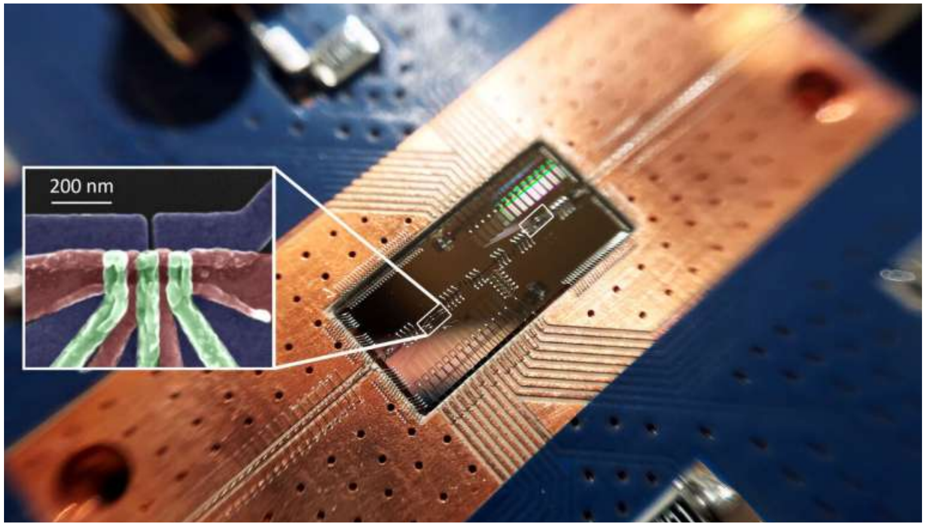

- Si is highly scalable
- Qubits and Quantum Gates demonstrated
- Fidelities below State-of-the-Art

Introduction and Overview (Preskills Notes)

9-12-2024

Spins in Silicon Quantum Dots

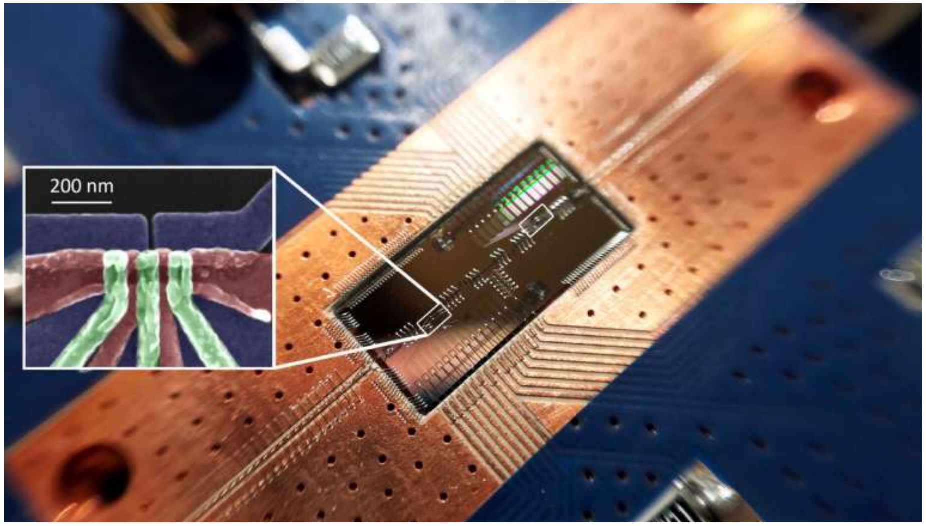

- Si is highly scalable
- Qubits and Quantum Gates demonstrated
- Fidelities below State-of-the-Art
- HRL Laboratories, UNSW (Australia) group, Princeton Group, many others…

Introduction and Overview (Preskills Notes)

Spins in Silicon Quantum Dots

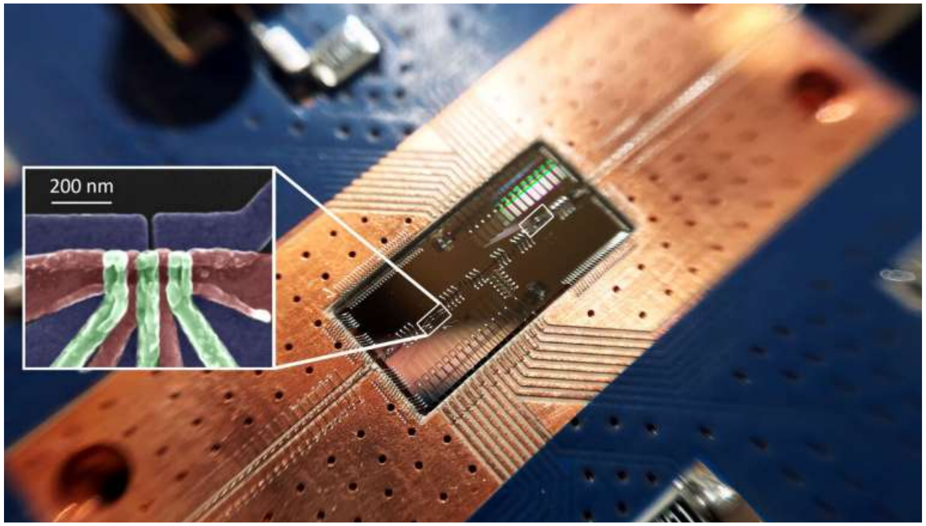

- Si is highly scalable
- Qubits and Quantum Gates demonstrated
- Fidelities below State-of-the-Art
- HRL Laboratories, UNSW (Australia) group, Princeton Group, many others…

Introduction and Overview (Preskills Notes)

9-12-2024

Comparing Physical Platforms: Status as of 2022

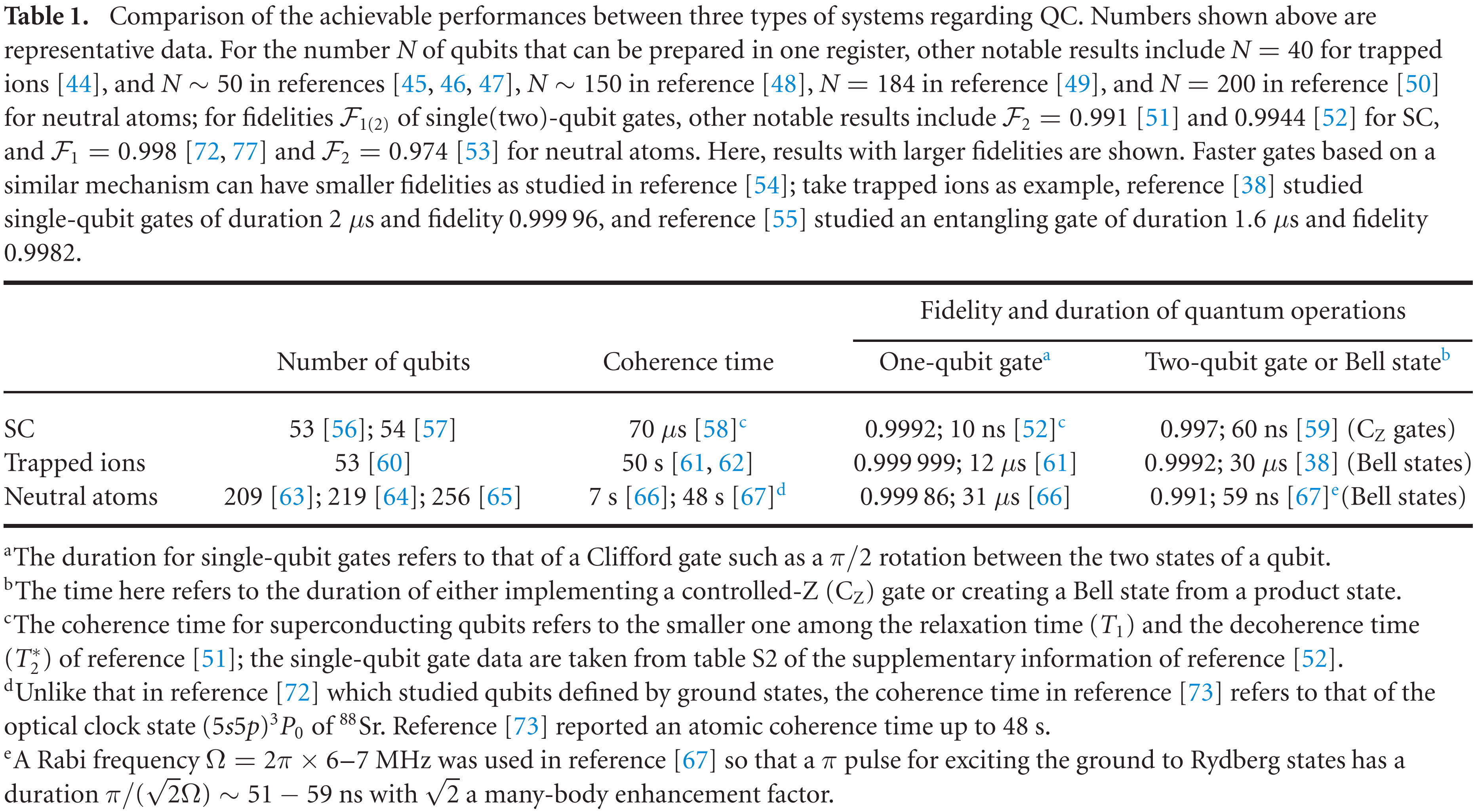

Table 1. Comparison of the achievable performances between three types of systems regarding QC. Numbers shown above are representative data. For the number N of qubits that can be prepared in one register, other notable results include $N = 40$ for trapped ions [44], and $N \sim 50$ in references [45, 46, 47], $N \sim 150$ in reference [48], $N = 184$ in reference [49], and $N = 200$ in reference [50] for neutral atoms; for fidelities $\mathcal{F}_{1(2)}$ of single(two)-qubit gates, other notable results include $\mathcal{F}_2 = 0.991$ [51] and 0.9944 [52] for SC, and $\mathcal{F}_1 = 0.998$ [72, 77] and $\mathcal{F}_2 = 0.974$ [53] for neutral atoms. Here, results with larger fidelities are shown. Faster gates based on a similar mechanism can have smaller fidelities as studied in reference [54]; take trapped ions as example, reference [38] studied single-qubit gates of duration 2 μs and fidelity 0.999 96, and reference [55] studied an entangling gate of duration 1.6 μs and fidelity 0.9982.

			Fidelity and duration of quantum operations	
	Number of qubits	Coherence time	One-qubit gate[a]	Two-qubit gate or Bell state[b]
SC	53 [56]; 54 [57]	70 μs [58][c]	0.9992; 10 ns [52][c]	0.997; 60 ns [59] (C_Z gates)
Trapped ions	53 [60]	50 s [61, 62]	0.999 999; 12 μs [61]	0.9992; 30 μs [38] (Bell states)
Neutral atoms	209 [63]; 219 [64]; 256 [65]	7 s [66]; 48 s [67][d]	0.999 86; 31 μs [66]	0.991; 59 ns [67][e](Bell states)

[a] The duration for single-qubit gates refers to that of a Clifford gate such as a $\pi/2$ rotation between the two states of a qubit.

[b] The time here refers to the duration of either implementing a controlled-Z (C_Z) gate or creating a Bell state from a product state.

[c] The coherence time for superconducting qubits refers to the smaller one among the relaxation time (T_1) and the decoherence time (T_2^*) of reference [51]; the single-qubit gate data are taken from table S2 of the supplementary information of reference [52].

[d] Unlike that in reference [72] which studied qubits defined by ground states, the coherence time in reference [73] refers to that of the optical clock state $(5s5p)^3P_0$ of ^{88}Sr. Reference [73] reported an atomic coherence time up to 48 s.

[e] A Rabi frequency $\Omega = 2\pi \times 6$–7 MHz was used in reference [67] so that a π pulse for exciting the ground to Rydberg states has a duration $\pi/(\sqrt{2}\Omega) \sim 51 - 59$ ns with $\sqrt{2}$ a many-body enhancement factor.

Introduction and Overview (Preskills Notes)

Other Platforms

Nuclear Magnetic Resonance

- ∗ Qubits encoded in spin-1/2 nuclei in a single molecule.
- ∗ Mature technology, many early proof of principle demonstrations
- ∗ Fundamentally not scalable, many early demonstrations, largely abandoned

Photonics

- ∗ Photons can carry QI in, e. g., their polarization state.
- ∗ Great for transmitting quantum info
- ∗ Easy to make, transmit and detect
- ∗ Difficult to store ⇨ work on photon Quantum Memories
- ∗ Photon-photon gates in cavities, mediated By Rydberg polaritons, One-Way Q.C., Measurement based Quantum Computing
- ∗ **PsiQuantum,** https://www.psiquantum.com

Other Platforms

- ∗ NV Centers in Diamond – Good for Quantum Sensing
- ∗ Electrons floating on liquid Helium

⋮

Introduction and Overview (Preskills Notes)

9-12-2024

ARTICLE

https://doi.org/10.1038/s41467-019-13335-7

OPEN

Coupling a single electron on superfluid helium to a superconducting resonator

Gerwin Koolstra[1], Ge Yang[1] & David I. Schuster[1]*

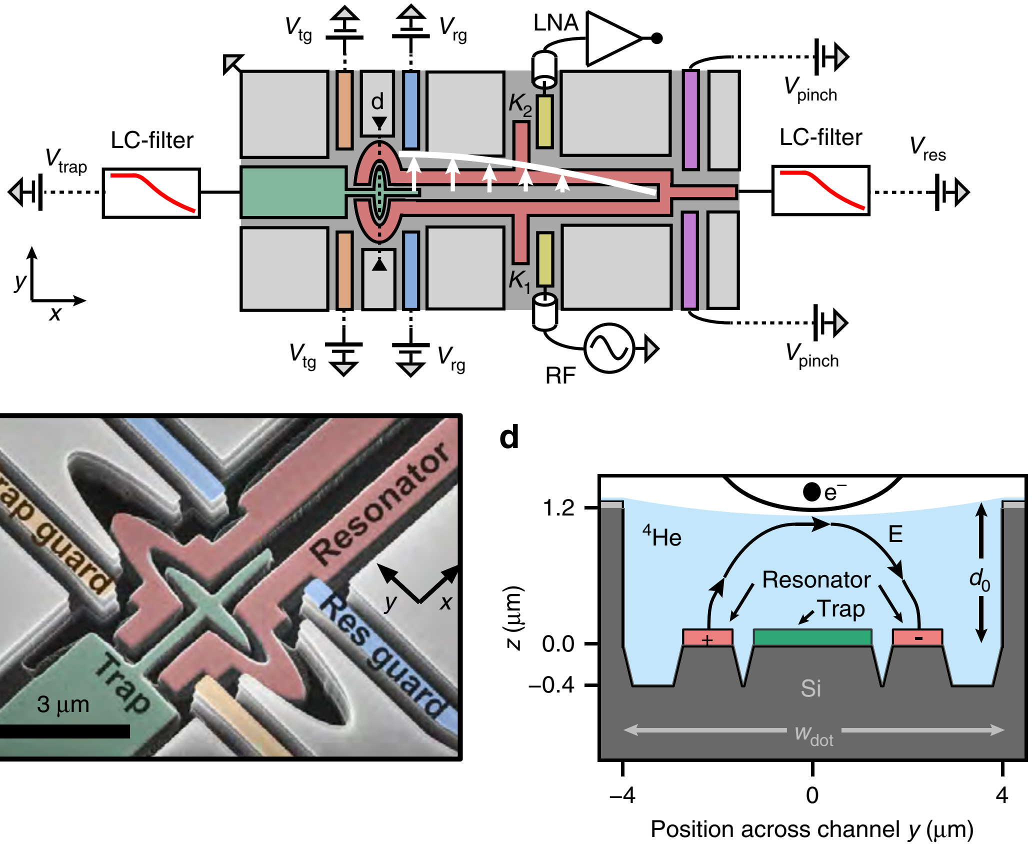

Fig. 1 An electron-on-helium dot **a** Optical micrograph and **b** schematic of the device. The resonator (red) can be probed with microwaves via coplanar waveguides

Introduction and Overview (Preskills Notes)

9-12-2024

Let’s go look at some websites…

Introduction and Overview (Preskills Notes)

9-12-2024

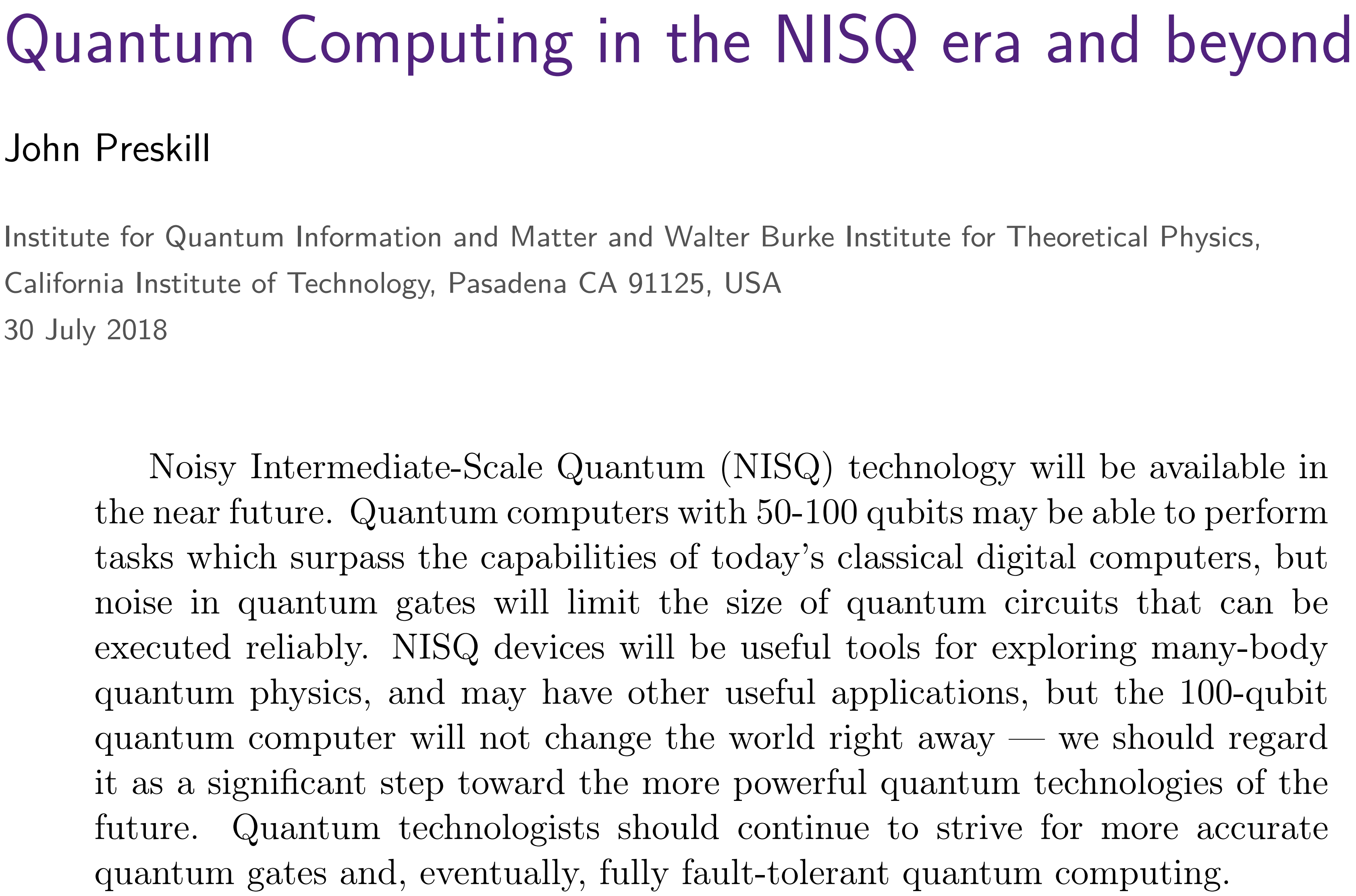

Quantum Computing in the NISQ era and beyond

John Preskill

Institute for Quantum Information and Matter and Walter Burke Institute for Theoretical Physics,
California Institute of Technology, Pasadena CA 91125, USA

30 July 2018

Noisy Intermediate-Scale Quantum (NISQ) technology will be available in the near future. Quantum computers with 50-100 qubits may be able to perform tasks which surpass the capabilities of today's classical digital computers, but noise in quantum gates will limit the size of quantum circuits that can be executed reliably. NISQ devices will be useful tools for exploring many-body quantum physics, and may have other useful applications, but the 100-qubit quantum computer will not change the world right away — we should regard it as a significant step toward the more powerful quantum technologies of the future. Quantum technologists should continue to strive for more accurate quantum gates and, eventually, fully fault-tolerant quantum computing.